NATIONAL TRANSPORTATION SAFETY BOARD

Office of Research and Engineering
Washington, D.C. 20594

May 4, 2000

Aircraft Performance

Group Chairman's Aircraft Performance Study
by John O'Callaghan

A. ACCIDENT

Location:	Sixty miles South of Nantucket, MA
Date:	October 31, 1999
Time:	0150 Eastern Standard Time (EST)
Flight:	EgyptAir Flight 990
Aircraft:	Boeing 767-366ER, Registration SU-GAP
NTSB#:	DCA00MA006

B. GROUP

Chairman: John O'Callaghan
Senior Aerospace Engineer
NTSB

Members: Mohamed A. Hamid Hamdy
Engineer - General Manager Training
EgyptAir

Maher Ismaiel Mohamed
Head of Airworthiness - Central Administration
Egyptian Civil Aviation Authority

Dennis D. Chandler
Engineer - PW4000 Operability/ Propulsion System Analysis
Pratt & Whitney

John Hed
Flight Test Engineer
Federal Aviation Administration

Timothy Mazzitelli
Lead Engineer - Aerodynamics, Stability & Control
The Boeing Company

C. SUMMARY

At about 0150 Eastern Standard Time (EST) on October 31, 1999, a Boeing 767-366ER, registration SU-GAP, operated by EgyptAir as Flight 990, crashed into the Atlantic Ocean about 60 miles South of Nantucket, MA. EgyptAir Flight 990 (MSR990) was being operated under the provisions of Egyptian Civil Aviation Regulations Part 121 and United States Title 14 Code of Federal Regulations Part 129 as a scheduled, international flight from John F. Kennedy Airport (JFK), New York, New York, to Cairo International Airport in Cairo, Egypt. The flight departed JFK about 0122 EST, with 4 flightcrew members, 10 flight attendants, and 203 passengers on board. There were no survivors. The airplane was destroyed by impact forces. Floating debris from the aircraft was recovered on the morning of October 31, 1999.

The purpose of the Aircraft Performance Group (ACPG) is to determine and analyze the motion of the aircraft and the physical forces that produce that motion. In particular, the Group attempts to define the aircraft position and orientation throughout the flight, and determine its response to control inputs, system failures, external disturbances, or other factors that could affect its trajectory. The data the ACPG uses to obtain this information includes but is not limited to the following:

- Wreckage location and condition.
- Air route (ARSR) and airport surveillance (ASR) radar data.
- Digital Flight Data Recorder (DFDR) data.
- Cockpit Voice Recorder (CVR) information.
- Weather information.
- Engineering simulator studies.
- Ground and flight tests.

This aircraft performance study describes the results of using the data listed above in defining, as far as possible, the motion of EgyptAir Flight 990. The study introduces the aircraft motion data collected during the investigation, describes the methods used to extract additional aircraft motion information from DFDR, radar, CVR, and weather data, and presents the results of these calculations.

D. DETAILS OF THE INVESTIGATION

I. Wreckage Location and Condition

The wreckage of MSR990 was found in two debris fields about 1,200 feet apart. The main debris field, centered at 40° 20' 51" N, 69° 45' 24" W, contained the bulk of the airplane fuselage, wings, empennage, right engine, and flight recorders. A smaller debris field, centered at 40° 20' 57" N, 69° 45' 40" W, consisted mainly of parts associated with the left engine. The small size of the aircraft parts found in both debris fields and the radar data presented below are consistent with the airplane fragmenting upon impact with the water at a high speed and steep impact angle.

II. Radar Data

Description of Radar Sites That Tracked MSR990

In general, two types of radar are used in order to provide position and track information, both for aircraft cruising at high altitudes between airport terminal airspaces, and those operating at low altitude and speeds within terminal airspaces.

Air Route Surveillance Radars (ARSRs) are long range (250 NM) radars used to track aircraft cruising between terminal airspaces. ARSR antennas rotate at 5 to 6 RPM, resulting in a radar return every 10 to 12 seconds. A block of airspace may be covered by more than one ARSR antenna, in which case the data from these antennas are fed to an FAA central computer where the returns are sorted and the data converted to latitude, longitude, and altitude information. The converted data is displayed to the FAA Air Route Traffic Control Center (ARTCC) controller, and recorded electronically in National Track Analysis Program (NTAP) text format. While an aircraft may be detected by several ARSRs, the ARTCC controller will only see one radar return on his display for that aircraft, and only one set of position data will be recorded in NTAP format for that aircraft. The raw data generated by each ARSR is not recorded in the NTAP file; rather, the position information computed by sorting through the returns from all the ARSRs sending data is recorded.

Along the East and West coasts of the United States, ARSRs used by the FAA to provide air traffic control services are also used by the United States Air Force (USAF) for air sovereignty mission purposes. The USAF 84th Radar Evaluation Squadron (84 RADES) monitors the returns from these ARSRs and records the raw data generated by each. Thus, where the FAA and USAF share ARSR sites, the raw data from each ARSR that is used to compute the position information recorded in the FAA NTAP file is available from the records kept by the 84 RADES. For a given aircraft, the position information recorded in the FAA NTAP file is reflected in the data recorded for one or more of the ARSR sites by the 84 RADES.

According to data recorded by the 84 RADES, four ARSR sites detected returns from MSR 990. These sites are located at North Truro, Massachusetts (NOR); Riverhead, New York (RIV); Gibbsboro, New Jersey (GIB); and Oceana, Virginia (OCA). The OCA site is about 260 NM Southwest of JFK and only recorded a handful of transponder returns from

MSR990, the last of which was received while the airplane was level at 23,000 ft., about 17 minutes before the last radar return from the RIV site. The data from OCA is included with the other radar data in the electronic records for this performance study, but because the data from the other sites is more abundant and relevant to the time just before the accident, no OCA data will be plotted or discussed further in this study.

FAA Airport Surveillance Radars (ASRs) are short range (60 NM) radars used to provide air traffic control services in terminal areas. The FAA records the data received by each site in Continuous Data Recording (CDR) text format. The FAA ASR-9 radar at Nantucket, Massachusetts (ACK) received and recorded returns from MSR990 during the time of the accident.

Another FAA ASR-9, at Islip, New York (ISP), may have received returns from MSR990 during the time of the accident, but because the aircraft was over 57 NM from the antenna at the time, the computer software used to process the data would have filtered these returns out and so no radar returns identified as MSR990 were recorded in the ISP CDR file. However, some returns from the Islip radar during the period of interest were made available to the NTSB by the MEGADATA company, which has a passive radar sensor near ISP. The MEGADATA system senses the signals output from the ISP radar and the responses to these signals broadcast by aircraft transponders, and determines the aircraft position from this information. The ISP data provided by MEGADATA is consistent with the radar returns from the ACK ASR-9, and since the ACK data is more complete than the ISP data, it is used for the plots and discussions in this study. However, the ISP data is included in the electronic records.

Primary and Secondary Radar Returns

A radar detects the position of an object by broadcasting an electronic signal that is reflected by the object and returned to the radar antenna. These reflected signals are called *primary returns.* Knowing the speed of the radar signal and the time interval between when the signal was broadcast and when it was returned, the distance, or range, from the radar antenna to the reflecting object can be determined. Knowing the direction the radar antenna was pointing when the signal was broadcast, the direction (or bearing, or azimuth) from the radar to the object can be determined. Range and azimuth from the radar to the object define the object's position. In general, primary returns are not used to measure the altitude of sensed objects, though the ARSRs do have altitude estimation capability (see below). The 84 RADES records this estimated altitude, but the FAA does not (the information is not used by ARTCCs).

The strength or quality of the return signal from the object depends on many factors, including the range to the object, the object's size and shape, and atmospheric conditions. In addition, any object in the path of the radar beam can potentially return a signal, and a reflected signal contains no information about the identity of the object that reflected it. These difficulties make distinguishing individual aircraft from each other and other objects (e.g., flocks of birds) based on primary returns alone unreliable and uncertain.

To improve the consistency and reliability of radar returns, aircraft are equipped with transponders that sense the beacon interrogator signals broadcast from radar sites, and in turn broadcast a response signal. Thus, even if the radar site is unable to sense a weak reflected signal (primary return), it will sense the response signal broadcast by the transponder and be able to determine the aircraft position. The response signal can also contain additional information, such as the identifying "Beacon Code" for the aircraft, and the aircraft's pressure altitude (also called "Mode C" altitude). The Beacon Code identifier for MSR990 was 1712. Transponder signals received by the radar site are called *secondary returns*.

Recorded Radar Data

Each FAA ARTCC records the radar data used by that Center and displayed to its controllers. Both the Boston and New York ARTCCs tracked MSR990 and saved long range ARSR data in NTAP format. The parameters of interest in these files are:

- Universal Coordinated Time (UTC) of the radar return, in hours, minutes, and seconds.
- Transponder beacon code associated with the return (secondary returns only).
- Transponder reported altitude in hundreds of feet associated with the return (secondary returns only). The transponder reports pressure altitude, but the FAA computers adjust this altitude for the current altimeter setting for the area in which the airplane is flying. This adjusted altitude is recorded in the NTAP file.
- Latitude and Longitude of the radar return as calculated by the ARTCC.

The 84 RADES records the raw data from each ARSR site, including the following parameters:

- UTC time of the radar return, in hours, minutes, and seconds.
- Transponder beacon code associated with the return (secondary returns only).
- Transponder reported altitude in hundreds of feet associated with the return (secondary returns only). The transponder reports pressure altitude, and unlike the FAA, the 84 RADES records this altitude directly. No adjustment for altimeter setting is made. The resolution of this data is ± 50 ft.
- Radar sensed altitude in hundreds of feet. This is the altitude estimate made by the ARSR based on the reflected signal from the radar target. The root-mean-square accuracy of this data is ± 3000 ft. However, this accuracy can be affected by the altitude of the target and atmospheric conditions (see discussion below).
- Slant Range from the radar antenna to the return, in NM. The accuracy of this data is ± 1/16 NM or about ± 380 ft.
- Azimuth relative to True North from the radar antenna to the return, in degrees. The accuracy of this data is ± 0.176 degrees.
- Latitude and Longitude of the radar return as calculated by 84 RADES software.

The data recorded by the Nantucket ASR-9 (ACK) in CDR format includes the following parameters:

- UTC time of the radar return, in hours, minutes, and seconds.
- Transponder beacon code associated with the return (secondary returns only).
- Transponder reported altitude in hundreds of feet associated with the return (secondary returns only). The transponder reports pressure altitude. The altitude recorded in the CDR file depends on the site recording the data; some sites record both pressure altitude, and pressure altitude adjusted for altimeter setting. Others record just the adjusted altitude. The ACK CDR file includes both altitudes. The resolution of this data is ± 50 ft.
- Slant Range from the radar antenna to the return, in NM. The accuracy of this data is ± 1/16 NM or about ± 380 ft.
- Azimuth relative to Magnetic North from the radar antenna to the return, in Azimuth Change Pulses (ACPs). ACP values range from 0 to 4096, where 0 = 0° magnetic and 4096 = 360° magnetic. Thus, the azimuth to the target in degrees would be:

  (Azimuth in degrees) = (360/4096) x (Azimuth in ACPs) = (0.08789) x (Azimuth in ACPs)

  The accuracy of this data is ± 2 ACP or ± 0.176 degrees. The ACK ASR-9 uses a magnetic variation of 16° W to compute magnetic azimuth.

The data listed above is stored in the electronic records for this performance study. The files, time periods, and other details of these records are listed in Table 1.

Presentation of the Radar Data

To calculate performance parameters from the radar data (such as ground speed, track angle, rate of climb, etc.), it is convenient to express the position of the airplane in rectangular Cartesian coordinates. The Cartesian coordinate system used in this study is centered at the ACK ASR-9 radar antenna and its axes extend East, North, and up from the center of the Earth. The data from the New York and Boston ARTCCs, the 84 RADES, and the ACK ASR-9 are all converted into this coordinate system for plotting and performance calculations. Latitude and longitude coordinates are transformed into this coordinate system using the WGS84 ellipsoid model of the Earth.

Performance calculations are also made easier if time is expressed in total seconds elapsed from some reference time, rather than in the hours : minutes : seconds format recorded by the radar sites. For this performance study, an Elapsed Time (ET) parameter is created for this purpose. The ET is chosen arbitrarily to be related to the UTC time recorded by the ACK ASR-9 as follows:

0.0 ET = 06:50:00 UTC ACK ASR-9 Time

The local time at the site of the accident is United States Eastern Standard Time (EST). EST is five hours behind UTC (EST = UTC - 5 hours).

The UTC times recorded for all the ARSR-4 sites and the ASR-9 sites are coordinated to the same satellite based Global Positioning System (GPS) clock. Message time stamps initiate within the receiving/recording equipment.

Selected primary and secondary returns from the Boston ARTCC and the ACK, RIV, NOR, and GIB ARSR-4 radar sites are tabulated in Tables 2-6 and plotted graphically in Figures 2-7. The tables list all the secondary returns for MSR990 (Beacon Code 1712) and selected primary returns received by the radar sites for a period from 200 seconds before the accident until the time the aircraft disappeared from radar. Where necessary, the raw data recorded by the sites has been converted into Latitude/Longitude coordinates, and Nautical Miles North and East of the ACK ASR-9 radar site.

Not all the primary returns that were recorded by the radar sites during this period are listed in Tables 2-6 or plotted in Figures 2-7. Those that are not listed or plotted are not in the neighborhood of the flight path of MSR990 and therefore are not likely to be returns from the airplane itself or from parts that may have separated from the airplane. The complete record of *all* the primary returns from the radar sites is contained in the electronic records listed in Table 1, within the limits described in that Table.

Figure 1 shows the location of the GIB, ISP, RIV, ACK, and NOR radar sites, together with the flight track of the airplane from JFK to the accident site as recorded by secondary returns from RIV and primary returns from ACK.

Figures 2-7 show plan views and time history views of the following information derived from the ACK, Boston ARTCC, RIV, GIB, and NOR radar returns:

- Latitude/Longitude coordinates
- Distances North and East of the ACK ASR-9 (Cartesian coordinates)
- Altitude
- Rate of climb derived from altitude data

These plots collectively show an expanded view of the crash site area, and a detailed view showing the last radar returns received from MSR990 on a larger scale. The location of the wreckage debris fields are also shown.

Various salient features of these plots are discussed below. Following these discussions, some aircraft performance calculations based on the radar data are presented.

"False Primaries" and "Frequency Interference" From Riverhead ARSR-4 (RIV)

Figures 2a and 4a show a multitude of primary returns recorded by the Boston ARTCC in the neighborhood of the flight path of MSR990. It is of interest to determine if these returns are real, and if so, what object or objects may have produced them; or if they are not real, why they appear in the Boston ARTCC NTAP file.

If the primary returns are real, meaning that they correspond to a radar signal that has been reflected from an object in the path of the signal, then similar returns should be received by other radar sites whose range is sufficient to cover the area in question. Figures 2a and 2b show that while the ACK ASR-9 picked up primary returns that are consistent with the flight path of MSR990, it did not pick up any primary returns away from the flight path of MSR990 similar to those recorded by the Boston ARTCC. The Boston primary returns to the South of MSR990's flight path may be out of range of the ACK ASR-9, but those to the North of the flight path are not (since the ASR-9 is receiving the primaries from MSR990 and the antenna is North of the flight path). These facts suggest that many of the Boston primaries, which do not appear in the ACK data, may not be real.

Looking at a larger area of primary returns over an extended period from the GIB, NOR, and RIV ARSR-4 sites casts further doubt upon the validity of the Boston primary returns. Figures 8a-8c plot the primary returns from each of these sites over the area covering the flight path of MSR990 for the period from 06:30:00 UTC to 07:00:00 UTC. The flight path itself is also shown in these Figures. Notice in Figure 8c that the RIV ARSR-4 recorded a pie-shaped "fan" of primaries extending to the East, with the RIV radar site lying on the extended centerline of the fan. This fan of primaries is not recorded by the NOR or GIB radar sites. Indeed, it is unlikely that there really were objects in the atmosphere arranged in such a way as to produce the fan pattern recorded by the RIV site.

The fan of primaries recorded by the RIV site is evidence of frequency interference. This problem, first identified in June 1997 and under study since, is the result of the mutual interference of radar signals from two neighboring sites that are transmitting at frequencies that are close to one another, and that cause the radars to "detect" false signals. The 84 RADES confirms that the fan of primaries at RIV is the result of interference from an ARSR-4 at Buck Harbor, Maine. The USAF and the FAA have identified a solution and continue to coordinate its implementation. This activity also affects radar sites in Canada, and must be coordinated with the Canadian government. This effort is in progress, but in the meantime the interference and its effects at RIV persist.

Figure 8c shows that the accident site is near the Northern edge of the fan of false RIV primaries. It is therefore likely that the numerous Boston ARTCC primaries plotted in Figures 2a and 4a that are not confirmed by similar returns from the ACK, GIB, or NOR sites are false signals resulting from the frequency interference at RIV.

Radar Sensed Altitude Data

Figures 3 and 7 indicate that at about ET = -10 seconds, the airplane started a rapid descent from cruise at 33,000 ft., reaching 16,700 feet at about ET = 33 seconds. At this point, no more secondary returns were received from the aircraft by any of the radar sites, though the sites continued to receive primary returns consistent with the airplane. Information from the airplane's DFDR (discussed in Section D-III) indicates that at about this time the engines started to shut down. The end of the secondary radar data is likely due to the interruption of power to the airplane's transponder resulting from the engine shutdown.

As described above, the airplane transponder transmits the pressure altitude sensed by the airplane's air data system to the radar site in response to an interrogation signal from the site. Without transponder information, the radar can not associate an accurate and reliable altitude with a return. However, the ARSR-4 long range radars have the ability to estimate the altitude of primary returns based on the properties of the reflected primary signal. The ASR-9 radar does not have this ability, and so can not record any altitude information at all without a secondary return.

The ARSR-4 uses a "stacked beam" arrangement when receiving primary radar returns in order to measure aircraft altitude. The receive beams consist of nine narrow layers stacked in elevation, of which five beams are used at a given time for either "low stack" receptions or "high stack" receptions. Radar returns are detected in two or more beams simultaneously, and by sensing the relative signal strength between adjacent beams, the ARSR-4 data processor can compute the elevation angle to the aircraft. This computation, when combined with the site elevation and atmospheric refractivity index (computed dynamically by built-in ARSR-4 weather station information), is used to estimate an aircraft's altitude based on primary radar returns. When signal strength differences between adjacent beams are not distinguishable (e.g., if a target is very weak or appears very low in the lowest stacked beam), the primary radar may not be able to resolve an altitude. In this case, the radar will report the altitude as 102,000 feet as a flag that a valid altitude estimate was not possible.

Figure 7 plots the altitude sensed by the ARSR-4s at RIV, GIB, and NOR. Even when a secondary return containing altitude information is received by these radars and associated with a corresponding primary return, the radar will still estimate the altitude of the primary return. Thus, in Figure 7a we can compare the altitudes estimated from primary returns with the transponder altitudes from the corresponding secondary returns. The Figure shows that when the airplane is relatively close to the radar site, the altitude estimated from the primary returns is close to the altitude reported by the airplane transponder. The sensed altitude from RIV agrees well with the secondary data throughout the flight. At the beginning of the flight, the airplane is much closer to GIB than NOR, and here the GIB sensed altitudes are closer to the transponder altitudes than those from NOR. At the end of the flight, the airplane is much closer to NOR than GIB, and here the NOR sensed altitudes are more accurate than the GIB sensed altitudes.

Note that even in the areas where the sensed altitudes compare well with the transponder altitudes, they are still consistently 1000 feet or so above the transponder altitudes. This difference results from the fact that the sensed altitude is measuring the actual height of the radar targets above mean sea level (MSL), whereas the transponder altitude is reporting the pressure altitude of the airplane above sea level. These two altitudes will only be identical under standard atmospheric conditions. To correct the transponder altitude to actual altitude above MSL, it is not sufficient to simply adjust the altitude for the altimeter setting (sea level pressure) for the area in question, because the *lapse* of pressure with altitude in the actual atmosphere will differ from that of the standard atmosphere. Instead, the transponder altitude should be considered an accurate measure of atmospheric pressure, but only an approximation of actual altitude. An estimate of the actual pressure lapse with altitude can be obtained from weather balloons (radiosondes) launched near the time and place of the

accident. Comparing the pressure implied by the transponder altitude data with the pressure measured by the radiosondes, the actual MSL altitude of the airplane can be estimated.

Tables 7a and 7b show data for radiosonde balloons launched from Upton, NY, and Chatham, MA, at 12:00 UTC (07:00 EST) on 10/31/1999, or about five hours after the accident. Upton has an elevation of 20 feet and is located at 40° 52' N Latitude, 72° 52' W Longitude, which is about 9.5 NM West of the RIV radar site. Chatham has an elevation of 16 feet and is located at 41° 40' N Latitude, 69° 58' W Longitude, which is about 21 NM South - Southeast of the NOR radar site. The measurements taken by the radiosondes include static pressure and temperature, dew point, wind direction and speed. The radiosondes calculate and record their height above the surface by solving the hydrostatic equation using the measured temperature and pressure (the hydrostatic equation is described in Section D-IV). The pressure altitude listed in the tables is not recorded by the radiosonde, but is calculated based on the static pressure measurement and the equations of the standard atmosphere. The difference between the pressure altitude and radar measured altitude indicates that at 33,000 feet pressure altitude, the actual altitude is about 1000 feet higher. This difference decreases as pressure altitude decreases, and is consistent with the difference between the radar sensed altitudes from the RIV, NOR, and GIB ARSR-4 radars and the altitude reported by the airplane's transponder.

These results indicate that when the airplane is relatively close to the radar site and at a sufficient altitude, the primary radar sensed altitude is often very accurate, with errors much less than the 3000 feet root-mean-squared (RMS) accuracy specification reported for the ARSR-4 system. However, Figure 7a shows that when the airplane gets far from the radar site, the accuracy of the radar estimation deteriorates rapidly, and the errors can easily exceed 3000 feet. This is consistent with design specification, which only requires the ARSR-4 to maintain a 3000 ft RMS height error between 5 and 175 NM. It is typical for the height accuracy of long-range, three-dimensional radar systems to quickly degrade beyond specified ranges due to wide variances in atmospheric conditions and magnification of errors that accumulate as a function of range. In particular, if the airplane is at low altitude, under certain atmospheric conditions the altitude measurement can be distorted significantly (this "ducting" effect is discussed below). The behavior of altitude data from other sources, and the known performance capabilities of the airplane, must be considered when evaluating the credibility of the radar sensed altitude data.

The area of the flight where the radar reported altitudes are of particular interest is the time after ET = 33 seconds, when the last secondary radar return is received by the ACK ASR-9. In this region, the radar sensed altitude data from the GIB, RIV, and NOR ARSR-4s are the only altitude information available.

Figure 7b is a close up of the altitude data during the last minutes of the accident flight. Returns from both NOR and RIV, the sites closest to the airplane at the time, suggest that the airplane recovered from its initial dive at about 17,000 feet, and climbed back to about 24,000 feet before diving once more and disappearing from radar. A recovery from the initial dive is consistent with secondary altitude data from the ACK ASR-9 shown in Figure 3a and 5a, which show the rate of descent decreasing starting at ET = 15 seconds. At ET = 99 seconds, single returns from both NOR and RIV show radar targets at about 18,000 feet in

the second dive; at about ET = 123 seconds, NOR shows a target at about 8000 feet, while RIV shows a target at about 13,000 feet. No further returns are received from NOR, but at ET = 134 and 146 seconds RIV shows additional targets at 12,400 and 10,800 feet, respectively.

These last few returns from NOR and RIV may be reflected off of separate targets (which would be consistent with parts separating from the airplane), but this is not necessarily the case. According to the 84 RADES[1], analysis of radiosonde data for the night of the accident indicates that multiple refractive layers were present in the atmosphere, which caused abnormal bending of the radar beams. This "ducting" phenomenon, which is not uncommon for the time of year of the accident, can cause significant errors in the radar altitude estimates when the target is at low altitudes. Table 8 shows the possible magnitude of the errors produced by this effect, as determined by a statistical analysis of returns from the NOR and RIV sites conducted by the 84 RADES. In this analysis, the transponder reported altitude from continuous sampling of returns from the two sites was corrected to true MSL based on radiosonde data and compared with the radar sensed altitude from the corresponding primary returns. The criteria used for selecting radar returns to include in this statistical analysis were as follows:

- Returns received between 00:00 UTC 10/29/1999 and 00:00 UTC 11/2/1999 (radiosonde data indicated that the atmospheric conditions throughout this period were similar to those on 10/31/1999, the night of the accident)
- Reinforced Beacon data with valid Mode C at altitudes between 100 ft and 35,000 ft MSL and valid primary return sensed altitudes between 0 ft and 100,000 ft MSL
- Only targets over the water
- NOR targets in a range band from 90 NM to 110 NM
- RIV targets in a range band from 120 NM to 140 NM

Table 8 shows that for targets below 5,000 feet, RIV would on average erroneously sense the altitude of the target 9,000 feet above the target's actual altitude. The altitudes sensed by NOR would be high by about 4,000 feet. Therefore, during the second dive of the accident flight, the primary returns sensed at 13,000 feet by RIV and at 8,000 feet by NOR could actually both be at 4,000 feet. The RIV returns at 12,400 and 10,800 feet could actually be closer to 3,000 and 2,000 feet, respectively.

These lower altitudes are more consistent with an airplane in a dive, and with the performance of the Boeing 767. Figures 3b and 5b show that during these last seconds of flight, the airplane's East/North and Latitude/Longitude coordinates were not changing significantly (i.e., the ground speed was low). Therefore, to maintain flying speed, the vertical velocity component of the airplane must have been large. If the airplane were actually at the 13,000 and 10,800 foot altitudes recorded by the RIV radar, the rate of descent would have been small, and when combined with the small ground speed, the total speed of the airplane would have been too low to be consistent with its performance

[1] The following discussion about the effect of the atmosphere on the altitudes sensed by the ARSR-4 radars is a summary of an electronic mail message from 84 RADES to the Airplane Performance Group Chairman sent on December 12, 1999.

capabilities. If the airplane were at the lower, 5,000 and 2,000 foot altitudes, the rate of descent would have been higher, and the total speed more consistent with the airplane's abilities.

The RIV primary return sensed altitudes at the beginning of the flight shown in Figure 7a do not appear to be erroneously high by 9,000 feet at altitudes below 5,000 feet. However, these returns are well within 120 NM of the RIV radar site and so do not meet the criteria listed above for inclusion in the statistical analysis. This indicates that the error due to the "ducting" effect becomes more pronounced as the range from the radar site increases.

Slant Range Correction for East/North and Latitude/Longitude Calculations

The range sensed and recorded by the ACK ASR-9 is the *slant range*, or straight line distance, from the radar antenna to the target. To calculate the East/North and Latitude/Longitude coordinates of the target, the altitude of the target above the radar antenna must be known, as well as the slant range and azimuth. If the altitude data is missing, then the transformation can not be done correctly and will be in error. The magnitude of the error is greater for high altitudes and short ranges, and decreases at lower altitudes and with distance from the radar antenna.

The ASR-9, unlike the ARSR-4 radars, does not have the capability to estimate the altitudes of primary returns. Therefore, the correct Latitude/Longitude and East/North coordinates of primary returns from the ASR-9 can not be calculated unless altitude information from another source is available. In Figures 3 and 5, the altitude of primary returns from the ACK ASR-9 have been estimated based on the sensed primary altitudes from the RIV and NOR ARSR-4 radars. The ACK primary data altitude trace in Figure 3 and its derivative in Figure 5 represent a smooth curve through the measured ARSR-4 data. The altitude fit is used in the conversion of the ACK primary range and azimuth data to East/North and Latitude/Longitude coordinates. This altitude is tabulated as "Assumed Altitude" in Table 2b.

Performance Calculations Based on Radar Data

Airplanes generally fly nose first, i.e., their motion is primarily along the longitudinal axis. When this is the case, the angles of attack and sideslip are usually small enough that the equations of motion can be simplified to the point that the aircraft orientation (heading, pitch and roll angles) as well as velocities can be determined from the 3 dimensional position of the aircraft as a function of time. Radar data can provide this position information, within limits. The velocity and angle calculations are very sensitive to the first and second time derivatives of the radar position data; consequently, any noise, or random uncertainty or error, in the radar data will contaminate the derivatives significantly and produce very noisy and questionable velocity and orientation angle results. In general, the radar data must first be smoothed to obtain usable results. Even then, the results of the calculations should be treated as qualitative estimates rather than exact, quantitative measurements of the airplane performance. Radar data is no substitute for DFDR data in performance calculations.

The ground track of the aircraft is affected by winds. To compute airspeed and heading from the ground speed and track angle obtained from the radar data, an estimate of the winds is required.

During the first dive on the accident flight, the DFDR stopped recording at about the same time as the radar sites stopped receiving transponder signals from MSR990. Therefore, the estimates of airplane performance based on primary radar data are the only source of performance information available during the final 100 seconds of flight. Curve fits of the radar data and wind data from Table 7 were used to estimate performance parameters of MSR990 from cruise at 33,000 feet, through the end of the radar data. The curve fits of the radar data are presented in Figure 9. The results of the performance calculations are discussed in Section D-VI. The results include comparisons with the DFDR data during the time that the DFDR was operating.

III. Digital Flight Data Recorder (DFDR) and Cockpit Voice Recorder (CVR) Data

DFDR and CVR Data Description

The aircraft cockpit voice recorder (CVR) and digital flight data recorder (DFDR) were recovered from the ocean floor and sent to Washington, DC for readout.

Descriptions of the DFDR and CVR and the recorder readout processes can be found in the Factual Reports of the Flight Data Recorder and Cockpit Voice Recorder Groups, respectively. The DFDR readout results in tabulated and plotted values of the recorded flight parameters versus time. The CVR readout results in a transcript of the CVR events, a partial list of which is shown in Table 9. Selected CVR events listed in Table 9 are also depicted in Figures 10-22, which plot DFDR and other data as described in Section IV.

Coordination of Radar, DFDR, and CVR Times

The ACK ASR9 radar, the DFDR, and the CVR record their information with respect to time, but these recorded times are not synchronized. To use these data sources together, their times must be synchronized to a single reference time. This reference time is the Elapsed Time (ET) introduced in Section D-II and used throughout this study.

As described in Section D-II, the reference time ET is arbitrarily chosen to equal 0.0 seconds when the ACK ASR-9 clock reads 06:50:00 UTC. The relationship between the ET reference and the DFDR time is established by comparing the altitude recorded by the DFDR with the Mode C altitude recorded by the ACK ASR-9. Both altitudes are based on the static pressure sensed at the airplane's static pressure ports, and on a sea level pressure of 29.92 "Hg (i.e., both altitudes are Pressure Altitude). By adjusting the DFDR times so that the DFDR altitude aligns with the ACK Mode C altitude during the first dive, the offset between DFDR time and ACK time (and hence, ET) can be determined.

Figure 10b shows the results of this process. The DFDR altitude line in the Figure is a very good fit of the ACK ASR-9 Mode C altitude returns, indicating that the DFDR and radar

returns have been synchronized to the same time. The conversion from DFDR time to ET established by the alignment of the altitudes is

ET = (DFDR subframe number) - 6181.02 seconds

The DFDR subframe number increments every second and is the time base for the DFDR data.

The relationship between the times of events recorded on the CVR and the ET reference is established by first establishing the conversion from CVR to DFDR time, and then using the DFDR to ET time conversion described above.

The CVR to DFDR time conversion is accomplished by comparing the times of events recorded on both the DFDR and CVR. These common events include the start and end of radio transmissions (both recorders detect microphone keying activity), and the activation of the Master Warning alarm (a discrete changes value on the DFDR, and the aural alarm is heard on the CVR).

The time alignment of these common DFDR and CVR events is complicated by two factors:

- The DFDR Microphone Keying and Master Warning discretes are only sampled once every second, and so the times of these events have an uncertainty of $\pm$ 0.5 seconds.

- The CVR tape does not record a time parameter, and so the timing of CVR events must be determined at the time the tape is replayed. If the tape is not replayed at the same speed at which it was recorded, the CVR times established during the process will be in error. Furthermore, the speed of the CVR tape during recording can vary, so the appropriate playback speed depends on the portion of tape being read.

The correct playback speed of the CVR tape can be approximated by adjusting it so that, upon playback, the AC electrical noise signal that bleeds into the CVR system and is recorded on the CVR produces a signal whose frequency matches that of the AC generator that produced the noise. The frequency of this generator is assumed to be exactly 400 Hz. If the CVR tape is played too quickly, the AC noise signal frequency will be greater than 400 Hz, and if it is played too slowly, the frequency will be less than 400 Hz. The actual AC generator on the airplane may not have been operating at exactly 400 Hz, and the tape speed itself can vary during recording, so this method only gives a first approximation of the timing of CVR events. The times from this approximation are then adjusted so that the Microphone Keying and Master Warning events recorded on the CVR fall within corresponding one second intervals on the DFDR. These time intervals equal the difference in the DFDR subframe numbers between the data samples that indicate a change in state of the Keying or Warning discretes.

The adjustments in the CVR times necessary to match the Microphone Keying events with their corresponding DFDR time intervals define a conversion from CVR time to DFDR time at each of the Keying events. Nineteen such Keying events exist for the MSR990 CVR.

CVR times falling between Microphone Keying events are converted to DFDR time by linearly interpolating the time conversions from the surrounding Keying events.

The last Microphone Keying event occurred about three minutes before the end of the CVR recording. With no adjustment to the first approximation of the CVR timing during this period, the time of the start of the aural Master Warning alarm heard on the CVR falls between the times of the DFDR samples indicating a change in state of the Master Warning discrete. Therefore, the CVR tape playback speed during this period is correct to within the limits inherent in the one second sample rate available to align the CVR and DFDR timing.

In Table 9, the time of CVR events is expressed both in ACK ASR-9 UTC time, and in the reference Elapsed Time.

IV. Radar and DFDR Data Performance Calculations

Overview

As mentioned in Section D-II, after the DFDR data ends at ET = 37 seconds, the only source of aircraft performance information is radar data. The radar data describes the airplane's position with time, but not other parameters of interest, such as speed, orientation, flight path angle, and rate of climb or descent. However, these parameters can be estimated from the position of the airplane by assuming coordinated flight.

The DFDR records many, but not all, performance parameters of interest. Many additional parameters can be derived from the DFDR parameters; however, the DFDR parameters can suffer from inherent measurement errors, and must be corrected before being used in these calculations.

This section describes the corrections applied to the DFDR data, and the calculations used to derive additional performance parameters from the corrected data. The DFDR corrections discussed here attempt to remove the following errors:

- Static pressure source errors
- Accelerometer location and bias errors
- Angle of attack measurement errors due to rotational motion

The performance parameters derived from the corrected DFDR data include:

- True airspeed
- Mach number
- Dynamic and static pressure
- Static temperature and speed of sound
- True altitude and integrated altitude
- Rate of Climb/Descent
- Flight path angle
- Wind speed and direction

The results of these corrections and derivations are presented in Figures 10-23. The Figures also present the results of performance calculations based on the curve fits through the radar data, as discussed in Section D-II.

Mach Number, Static Temperature, Sound Speed, and True Airspeed Calculations

True airspeed equals the Mach number multiplied by the speed of sound; the speed of sound is a function of the static temperature, and the static temperature can be derived from total temperature and Mach number. Mach number can be found from calibrated airspeed and static pressure. Total temperature and calibrated airspeed are recorded directly by the DFDR, and the static pressure can be determined from the DFDR pressure altitude and known reference pressure of 29.92" Hg.

For the calculations based on radar data, the position of the airplane with time is used to calculate ground speed. True airspeed can then be calculated using the ground speed and radiosonde wind data. For MSR990, the wind data from the Upton, NY radio listed in Table 7a was used for this calculation. This data is also plotted in Figure 22. The radiosonde temperature data can be used to calculate the speed of sound. True airspeed and speed of sound determine the Mach number. The static pressure implied by the altitude data can be used with Mach number to obtain total pressure, and then total and static pressures can be used to calculate calibrated airspeed.

Figures 11, 12, 13 and 21 show the results of both the DFDR and radar based calculations. Note that some of the lines in Figures 11 and 13 are labeled as "Corrected" or "Uncorrected." The "Uncorrected" lines are the results of the DFDR calculations described above without correcting the static pressure based on the DFDR pressure altitude for measurement errors. The "Corrected" lines are the results of the calculations with these errors removed (to the extent possible). The details of how the pressure data corrections are made are discussed below.

Pressure Based True Altitude Calculation

The altitude recorded by the DFDR is pressure altitude; i.e., it is the altitude in the standard atmosphere corresponding to the static pressure sensed at the airplane's static port. As discussed in Section D-II, the altitude in the actual atmosphere corresponding to the local

static pressure generally does not equal the pressure altitude, and it is insufficient to simply adjust the pressure altitude for the local sea level pressure because, in general, the lapse rate of pressure with altitude does not match the lapse rate in the standard atmosphere.

To estimate the actual altitude of MSR990, the cruising altitude of 33,000 feet is adjusted upward so that the new altitude matches the radiosonde altitude with a static pressure corresponding to a pressure altitude of 33,000 feet. During the dive, the change in altitude corresponding to a change in static pressure is calculated by solving the hydrostatic equation continuously. The hydrostatic equation describes the pressure increment across a differential element of air required to balance the weight of the element. With static pressure and the static temperature values from the speed calculations, the density and weight of the air element can be calculated throughout the dive.

The results of this calculation are shown in Figure 10 as the line labeled “Corrected for Actual Atmosphere.” Note that there is another line on this plot labeled “Accelerometer Integration.” This is the altitude that results from integrating the DFDR load factor data twice to derive aircraft position. It is a better estimate of the actual path of the airplane since it does not suffer from the static pressure sensing errors inherent in the DFDR altitude data; the difference between the “Accelerometer Integration” and “Corrected for Actual Atmosphere” lines indicate that the effects of these sensing errors can be significant.

Accelerometer Data Corrections and Integration

An accurate estimate of the flight path of the airplane during relatively short intervals (about 30 to 60 seconds) can be obtained by integrating accelerometer data. However, the accelerometers are in general not located coincident with the center of gravity (CG) of the airplane, and so before integrating the load factors at the CG must be calculated from the accelerometer data and the rotational velocity of the airplane described by the time history of the yaw, pitch and roll angles. Furthermore, accelerometers generally contain small offsets, or “biases,” that produce large errors in speed and position if not removed prior to integration. The values of the biases can be determined by trial and error, selecting them so that the aircraft position that results from integrating the accelerations agrees with known positions determined from another source.

In this study, accelerometer biases were chosen so that the integrated position and altitude during level flight between ET = -44 seconds and ET = -14 seconds agree well with the North and East positions calculated by integrating DFDR track angle and ground speed, and with the (constant) altitude data during the period. These biases were then used to integrate the accelerometer data from ET = -19 seconds to the end of the DFDR data at ET = 37 seconds. The values of the biases (in g’s) are as follows:

$\Delta n_x = 0.00426847$
$\Delta n_y = 0.01000000$
$\Delta n_z = -0.02701800$

The magnitude of these offsets is illustrated graphically in Figure 16. The Figure shows the DFDR load factors together with the “Corrected” load factors, which have been adjusted to reflect values at the CG and shifted by the bias values.

The altitude resulting from the accelerometer integration is plotted in Figure 10; the initial altitude for the integration has been set equal to the initial “Corrected for Actual Atmosphere” altitude. The flight path angle based on the integrated altitude is shown in Figure 14, along with flight path angles calculated from altitudes based on the previously mentioned “Corrected” and “Uncorrected” pressure measurements.

Figure 10 shows that there is a significant difference between the integrated altitude and the “Corrected for Actual Atmosphere” altitude. This difference increases towards the bottom of the dive where the Mach number is well beyond the M_D and V_D speed limits of the airplane. This suggests that at these Mach numbers the pressure sensed at the static ports differs from the actual freestream static pressure. An incorrect static pressure measurement will introduce error into the DFDR altitude and airspeed measurements, and into parameters derived from these measurements. However, assuming the integrated altitude more closely matches the actual altitude, the difference between the integrated and pressure based altitudes can be used to calculate the error in the static pressure measurements.

Static Pressure Measurement Error Correction

The static pressure measurement error used in this study is defined as

$$\Delta P = P_{TRUE} - P_{MEASURED}$$

where P_{TRUE} is the actual freestream static pressure, and $P_{MEASURED}$ is the static pressure sensed at the airplane static ports, as determined from the DFDR pressure altitude data.

To calculate P_{TRUE}, the integrated altitude is shifted so that it matches the DFDR pressure altitude at 33,000 feet. This shifted altitude is the altitude the DFDR would have recorded if there were no static pressure error (assuming that the shifted integrated altitude matches the actual altitude). Then, the static pressure corresponding to a pressure altitude equal to the shifted integrated altitude is determined; this is the actual freestream pressure, i.e., P_{TRUE}.

The error in the total pressure (P_{TOTAL}) sensed by the airplane pitot tubes is assumed to be small at all subsonic Mach numbers. The total pressure can be calculated correctly from the uncorrected static pressure measurement and DFDR calibrated airspeed.

Once P_{TRUE} and P_{TOTAL} have been calculated, the Mach number, static temperature, speed of sound, and true airspeed calculations can be redone. The results of these calculations are shown in Figures 11, 13 and 20 as the “Corrected” data.

The magnitude of ΔP is shown in Figure 23. The top graph in the Figure shows the absolute value of the pressure error. The middle graph shows the pressure coefficient error (ΔC_P);

ΔC_P is ΔP divided by dynamic pressure, and non-dimensionalizes the error. The bottom graph in Figure 23 plots ΔC_P against Mach number. This graph shows that the pressure error is very small through the range normal operating speeds, but starts to grow once the speed exceeds the M_{MO} of 0.86. The graph further shows that the error is not solely dependent upon Mach number; as the Mach number decreases as the airplane starts to recover from the dive, the ΔC_Ps are slightly different than they were when Mach number was increasing during the dive. The difference may be due to the different angles of attack in the two regions; during the dive the angle of attack is about -2°, and during the recovery the angle of attack increases steadily to about 5°, as shown in Figure 14.

Angle of Attack Calculations

The angle of attack vane angle recorded by the DFDR is plotted in Figure 14.[2] The angle of attack vane is located near the nose of the airplane, and is hinged so that it remains aligned with the local airflow. The angle recorded by the vane varies with the body angle of attack but is not equal to it. The body angle of attack corresponding to the vane angle can be determined from the calibration of the vane; Figure 14 shows the result as the "Angle of Attack at Vane" line.

The local angle of attack sensed by the vane is affected by the pitch rate of the airplane, because the vane is near the nose and pitching motion will move the vane up and down, changing the relative motion between the vane and the oncoming air. The angle of attack at the wing, which is closer to the CG, will therefore be different from the angle of attack at the vane when the pitch rate is not zero. Figure 14 shows the result of removing the pitch rate effects from the angle of attack measurement as the line labeled "Angle of Attack at CG."

The angle of attack from the radar data is estimated from a calculation of the normal load factor and an estimate of the weight and lift characteristics of the airplane. The result is shown in Figure 14. In this calculation, the angle of attack for zero lift was assumed to be -1°; the actual angle of attack for zero lift is closer to -2°. Consequently, the calculated angle of attack required to achieve a given lift coefficient will be high by about a degree. Oscillations in the curve fits of the radar data also introduce some error into the calculations. However, given the overall uncertainty in the performance parameters derived from radar data, these effects are relatively small and the radar based calculations provide a good sense of the motion of the airplane.

[2] All angles of attack in this study are referred to the fuselage reference line (body angle of attack).

Note on Plotted DFDR Data

To perform the various calculations described in this section, the recorded DFDR parameters must be combined mathematically in computer programs. This requires that all the data be defined at common time points. However, the data is recorded at different times and at different rates. To define the data at common time points, the parameters need to be interpolated to the common time standard. The interpolated DFDR data is plotted in the Figures in this study; to see plots and tables of the original, non-interpolated data, see the DFDR Group Chairman's Factual Report.

The interpolations used in this study always preserve the values of the original, recorded data points. A smooth curve (as opposed to a straight line) is used to determine the value of points that lie between data samples. This should be kept in mind when considering plots such as those shown in Figure 19, which contains engine parameters. The sudden jumps in the right engine parameters at about ET = 23 seconds appear to be defined by smooth curves, but each is in fact defined by a single (seemingly errant) point. The interpolation gives the (erroneous) impression of multiple points defining the jumps. The errant points in the original data are likely due to discontinuities in the engine monitoring software after the right engine cutoff switch goes to the "CUTOFF" position sometime between ET = 21 and 22 seconds.

E. CONCLUSIONS

This study presents the radar and DFDR data available for EgyptAir Flight 990, and describes additional airplane performance information derived from these sources. The radar, DFDR, and derived data indicate that the following sequence of events occurred during the final minutes of the flight:

The airplane was initially cruising at 33,000 feet and Mach 0.79 on a magnetic heading of about 80 degrees. At about ET = -15 seconds (06:49:45 UTC), the autopilot disconnected, but aside from starting a slow, 0.5 degrees/second roll to the left, the airplane remained straight and level for approximately 8 seconds. At about ET = -7 seconds, the left and right throttles were retarded to minimum idle at a rate of about 25 degrees/second. The maximum rate of throttle movement that can be commanded by the autothrottle system is 10.5 degrees/second. About one second after the start of the throttle movement, the left and right elevator panels moved about 3.5 degrees in the trailing edge down (TED) direction. At ET = -6 seconds, the pitch angle started to decrease at an initial rate of about 4 degrees/second, then settling to an almost constant rate of 2 degrees/second over 19 seconds until reaching 40 degrees nose down at ET = 15 seconds.

During the dive, the wings remained within 10 degrees of level and the heading remained about 80 degrees, increasing to about 85 degrees between ET = 20 and 33 seconds.

At ET = 6 seconds, the left and right elevators moved an additional 1.5 degrees TED. Prior to this point, the normal load factor had been about 0.2 g's; after this point, the load factor decreased to about -0.1 g's. During this time, between ET = 6 and 10 seconds, the "Low Engine Oil Pressure" discretes on both the left and right engines activated. The discretes remained activated until sometime betwen ET = 17 to 21 seconds, when the normal load factor increased above zero.
At about ET = 8 seconds and about 30,800 feet, the Mach number exceeded the maximum operating Mach number (0.86) and the Master Warning alarm sounded. At ET = 23 seconds, the Mach number reached a peak value of 0.99 at an altitude of about 22,200 feet. The maximum rate of descent during the dive was about 39,000 feet/minute at ET = 19 seconds and an altitude of about 24,600 feet.

At ET = 15 seconds and about 27,300 feet, the left and right elevator panels started to move slowly (at about 0.6 degrees/second) trailing edge up (TEU), back towards their neutral position. The pitch angle, angle of attack, and normal load factor also started to increase at this point, so that by the end of the DFDR data at ET = 37 seconds the pitch angle had increased to about 8 degrees nose down, and the airplane was experiencing about 2.4 g's in the recovery.

During this time, at ET = 21 seconds, the left and right elevator panels started to "split," or move asymmetrically. The right elevator panel reversed direction and started to move trailing edge down, while the left elevator panel continued to travel trailing edge up. The split between the left and right elevators continued to the end of the data, varying in magnitude but averaging about 4 degrees difference between the panels.

Between ET = 21 and 23 seconds, the engine start lever switch for both engines moved from the "Run" to the "Cutoff" position. Between ET = 24 and 25 seconds, both throttle handles moved full forward. Between ET = 25 and 26 seconds, the speedbrake handle moved to its fully deployed position. Coincident with this activity, between ET = 24 and 27 seconds, the left elevator panel moved briefly in the trailing edge down direction, from 3 degrees TEU to 1 degree TEU, before moving back up to 3 degrees TEU.

The DFDR data ends at ET = 37 seconds. The last transponder return from the airplane was received at about ET = 34 seconds. Performance calculations based on primary radar returns indicate that the airplane recovered from the dive at about 16,000 feet, climbing back to about 24,000 or 25,000 feet at ET = 75 seconds. During this climb, the airplane turned 60 degrees to the right, changing heading from about 80 degrees to about 140 degrees.

After ET = 75 seconds, the airplane started a second dive that continued until impact with the ocean about 54 NM South and 14 NM East of the Nantucket ASR-9 radar antenna. There are only seven primary returns from the airplane during the second dive, and the altitude estimates from these returns suffer from potentially large errors. These difficulties introduce a significant amount of uncertainty into the performance calculations during the second dive. However, the data appears to indicate impact with the ocean at about ET = 150 seconds. Impact at this time requires an average descent rate during the second dive of about 20,000 feet/minute.

This study describes the motion of EgyptAir Flight 990 during the accident sequence, but does not address the underlying causes of that motion.

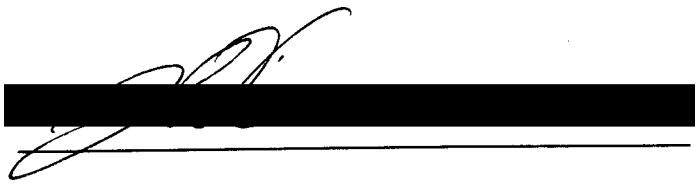

John O'Callaghan
Senior Aerospace Engineer
May 4, 2000

Directory: *Data for Parties\Nantucket (ACK) ASR9*			
File	**Start of Data (EST)**	**End of Data (EST)**	**Description**
TG.zip	01:00:00	03:00:00	All primary and secondary returns received by the FAA ASR-9 Airport Surveillance Radar at Nantucket, MA, at bearings ranging from 90° magnetic through 270° magnetic. The TG.zip file is a compressed ASCII text file that contains the data in FAA Continuous Data Recording (CDR) format.

Directory: *Data for Parties\Boston Center*			
Files	**Start of Data (EST)**	**End of Data (EST)**	**Description**
MSR990A.TXT MSR990E.TXT MSR990N.TXT MSR990N1.TXT MSR990P.TXT MSR990P1.TXT MSR990P2.TXT	01:21:08	02:04:51	Data for Beacon Code 1712 and all primaries recorded by the FAA Boston Center Air Route Traffic Control Center (ARTCC). Radar information received by various long range, Air Route Surveillance Radar (ARSR) antenna sites is collected and processed by FAA computers for display to Center controllers and recording. The data in these files can include data collected by the RIV, NOR, and GIB FAA/Air Force ARSR-4 antenna sites The data files are in National Track Analysis Program (NTAP) ASCII format.

Directory: *Data for Parties\New York Center*			
Files	**Start of Data (EST)**	**End of Data (EST)**	**Description**
MSRNT3.TXT MSRNT7.TXT MSRNT8.TXT MSRNT9.TXT MSRNT10.TXT MSRNT11.TXT	01:21:08	01:56:45	Data for Beacon Code 1712 and all primaries recorded by the FAA New York Center ARTCC. Radar information received by various long range, Air Route Surveillance Radar (ARSR) antenna sites is collected and processed by FAA computers for display to Center controllers and recording. The data in these files can include data collected by the RIV, NOR, and GIB FAA/Air Force ARSR-4 antenna sites. The data files are in National Track Analysis Program (NTAP) ASCII format.

Directory: *Data for Parties\Megadata*			
Files	**Start of Data (EST)**	**End of Data (EST)**	**Description**
RADAR.xls	01:46:03	01:50:31	The MEGADATA system passively senses the responses aircraft transponders transmit upon receiving signals broadcast from an ASR9 radar site neighboring the MEGADATA sensor. The outgoing transmission from the radar site is also sensed, and with this information the MEGADATA system can "piggyback" on the ASR9 and determine aircraft position and transponder information (beacon code and altitude). The file contains data recorded by the MEGADATA system that was passively sensing transmissions and responses to the FAA ASR-9 radar at Islip, NY. The file is in Microsoft Excel format.

Directory: *Data for Parties\Navy Vacapes*			
Files	**Start of Data (EST)**	**End of Data (EST)**	**Description**
Egyptair1712.doc	01:44:59	01:55:57	Data for Beacon Code 1712 and all primaries recorded by the USAF/FAA ARSR-4 radar site at Riverhead, NY (RIV), as processed by the Fleet Area Control and Surveillance Facility, Virginia Capes. The file is in Microsoft Word format.

Directory: *Data for Parties\84th RADES*			
Files	**Start of Data (EST)**	**End of Data (EST)**	**Description**
egypt.ppt egyptall.xls ntsbc~1.doc NTSBfilters990Only.xls NTSBfiltersAll.xls Only_990.xls	01:15:00	02:05:00	Data for all Beacon Codes and primaries as processed by the 84th Radar Evaluation Squadron for a variety of USAF/FAA ARSR-4 radar sites on the East Coast, including the following, which tracked MSR990: Riverhead, NY (RIV); North Truro, MA (NOR); Gibbsboro, NJ (GIB); Oceana, VA (OCA). The .xls files are in Microsoft Excel format; the .ppt file is in Microsoft PowerPoint format; and the .doc file is in Microsoft Word format.

Table 1. Electronic records of radar data for MSR990.

UTC Time HH:MM:SS	Elapsed Time Seconds	Pressure Altitude feet	Range Nautical Miles	Bearing ACPs	Bearing Degrees	Distance N of ACK Nautical Miles	Distance E of ACK Nautical Miles	Latitude DD:MM:SS	Longitude DD:MM:SS
6:49:56.89	-3.11	32800	56.78	2189	192.39	-56.412	3.556	40° 18' 33.42'' N	69° 58' 58.99'' W
6:50:1.51	1.51	32200	56.59	2182	191.78	-56.189	4.149	40° 18' 46.67'' N	69° 58' 12.43'' W
6:50:6.13	6.13	31000	56.38	2175	191.16	-55.949	4.735	40° 19' 0.9'' N	69° 57' 26.27'' W
6:50:10.63	10.63	29000	56.19	2169	190.63	-55.742	5.235	40° 19' 13.12'' N	69° 56' 46.96'' W
6:50:15.13	15.13	26000	55.97	2161	189.93	-55.494	5.900	40° 19' 27.7'' N	69° 55' 54.66'' W
6:50:19.87	19.87	22500	55.78	2154	189.32	-55.279	6.478	40° 19' 40.25'' N	69° 55' 9.13'' W
6:50:24.28	24.28	19900	55.59	2148	188.79	-55.055	6.966	40° 19' 53.44'' N	69° 54' 30.7'' W
6:50:28.99	28.99	17900	55.41	2140	188.09	-54.805	7.619	40° 20' 8.19'' N	69° 53' 39.29'' W
6:50:33.4	33.4	16700	55.28	2131	187.29	-54.576	8.356	40° 20' 21.74'' N	69° 52' 41.22'' W

Table 2a. All (ACK) ASR-9 Secondary Returns for Beacon Code 1712.

UTC Time HH:MM:SS	Elapsed Time Seconds	Slant Range Nautical Miles	Bearing ACPs	Bearing Degrees	Assumed Altitude feet	Distance N of ACK Nautical Miles	Distance E of ACK Nautical Miles	Latitude DD:MM:SS	Longitude DD:MM:SS
6:48:52.42	-67.58	59.88	2280	200.39	32977	-59.460	-4.565	40° 15' 30.67" N	70° 9' 37.03" W
6:48:57.16	-62.84	59.63	2272	199.69	32977	-59.261	-3.819	40° 15' 42.64" N	70° 8' 38.45" W
6:49:1.54	-58.46	59.38	2267	199.25	32977	-59.038	-3.350	40° 15' 56.04" N	70° 8' 1.64" W
6:49:6.28	-53.72	59.13	2258	198.46	32977	-58.828	-2.524	40° 16' 8.67" N	70° 6' 56.77" W
6:49:10.9	-49.1	58.91	2254	198.11	32977	-58.621	-2.155	40° 16' 21.05" N	70° 6' 27.78" W
6:49:15.64	-44.36	58.66	2248	197.58	32977	-58.388	-1.609	40° 16' 35.07" N	70° 5' 44.86" W
6:49:20.14	-39.86	58.44	2241	196.96	32977	-58.181	-0.978	40° 16' 47.49" N	70° 4' 55.32" W
6:49:24.64	-35.36	58.22	2235	196.44	32977	-57.966	-0.441	40° 17' 0.35" N	70° 4' 13.12" W
6:49:29.26	-30.74	58	2229	195.91	32977	-57.747	0.093	40° 17' 13.5" N	70° 3' 31.23" W
6:49:33.88	-26.12	57.78	2222	195.29	32977	-57.522	0.710	40° 17' 26.99" N	70° 2' 42.73" W
6:49:38.62	-21.38	57.56	2216	194.77	32977	-57.292	1.234	40° 17' 40.76" N	70° 2' 1.5" W
6:49:43.12	-16.88	57.38	2208	194.06	32977	-57.092	1.931	40° 17' 52.75" N	70° 1' 6.74" W
6:49:47.74	-12.26	57.19	2203	193.62	32977	-56.884	2.361	40° 18' 5.15" N	70° 0' 32.95" W
6:49:52.36	-7.64	57	2194	192.83	32977	-56.656	3.136	40° 18' 18.82" N	69° 59' 32.07" W
6:50:38.35	38.35	55.13	2123	186.59	16355	-54.324	9.001	40° 20' 36.73" N	69° 51' 50.43" W
6:50:42.97	42.97	54.97	2114	185.80	16828	-54.033	9.721	40° 20' 54.11" N	69° 50' 53.74" W
6:50:47.47	47.47	54.88	2105	185.01	17705	-53.798	10.448	40° 21' 8.16" N	69° 49' 56.56" W
6:50:52.09	52.09	54.84	2097	184.31	19153	-53.614	11.096	40° 21' 19.22" N	69° 49' 5.52" W
6:50:56.71	56.71	54.88	2093	183.96	20939	-53.567	11.430	40° 21' 22.13" N	69° 48' 39.32" W
6:51:1.33	61.33	54.97	2088	183.52	22336	-53.551	11.857	40° 21' 23.1" N	69° 48' 5.77" W
6:51:5.74	65.74	55.13	2085	183.25	23710	-53.637	12.135	40° 21' 17.99" N	69° 47' 43.93" W
6:51:10.57	70.57	55.28	2081	182.90	24537	-53.699	12.496	40° 21' 14.3" N	69° 47' 15.59" W
6:51:15.19	75.19	55.44	2079	182.72	25062	-53.810	12.696	40° 21' 7.63" N	69° 46' 59.89" W
6:51:19.81	79.81	55.59	2077	182.55	24814	-53.920	12.896	40° 21' 0.98" N	69° 46' 44.12" W
6:51:24.43	84.43	55.72	2079	182.72	23710	-54.099	12.764	40° 20' 50.2" N	69° 46' 54.57" W
6:51:28.96	88.96	55.84	2073	182.20	22370	-54.111	13.294	40° 20' 49.3" N	69° 46' 12.88" W
6:51:33.67	93.67	55.91	2075	182.37	20559	-54.237	13.148	40° 20' 41.57" N	69° 46' 24.28" W
6:51:38.29	98.29	55.88	2072	182.11	18561	-54.166	13.395	40° 20' 45.68" N	69° 46' 4.8" W
6:51:42.91	102.91	55.78	2071	182.02	16534	-54.064	13.458	40° 20' 51.57" N	69° 45' 59.77" W
6:51:47.44	107.44	55.78	2069	181.85	14702	-54.036	13.627	40° 20' 53.08" N	69° 45' 46.4" W
6:51:52.06	112.06	55.72	2068	181.76	12895	-53.969	13.698	40° 20' 56.98" N	69° 45' 40.75" W
6:51:56.68	116.68	55.72	2069	181.85	11176	-53.999	13.618	40° 20' 55.02" N	69° 45' 47.04" W
6:52:1.3	121.3	55.69	2065	181.49	9491	-53.894	13.944	40° 21' 1.15" N	69° 45' 21.34" W
6:52:5.8	125.8	55.69	2069	181.85	7833	-53.985	13.615	40° 20' 55.62" N	69° 45' 47.23" W
6:52:10.54	130.54	55.69	2066	181.58	6060	-53.928	13.864	40° 20' 58.88" N	69° 45' 27.52" W
6:52:15.16	135.16	55.69	2067	181.67	4409	-53.953	13.783	40° 20' 57.26" N	69° 45' 33.91" W
6:52:19.78	139.78	55.66	2075	182.37	2947	-54.091	13.113	40° 20' 48.98" N	69° 46' 26.6" W
6:52:38.14	158.14	55.59	2068	181.76	0	-53.881	13.676	40° 21' 1.22" N	69° 45' 42.14" W
6:52:42.88	162.88	55.59	2069	181.85	0	-53.902	13.594	40° 20' 59.99" N	69° 45' 48.66" W
6:52:47.26	167.26	55.59	2069	181.85	0	-53.902	13.594	40° 20' 59.99" N	69° 45' 48.66" W
6:53:1.24	181.24	55.59	2068	181.76	0	-53.881	13.676	40° 21' 1.22" N	69° 45' 42.14" W
6:53:15.09	195.09	55.53	2067	181.67	0	-53.802	13.744	40° 21' 5.96" N	69° 45' 36.79" W
6:53:56.56	236.56	55.47	2060	181.05	0	-53.594	14.306	40° 21' 18.36" N	69° 44' 52.54" W

Table 2b. Selected Nantucket (ACK) ASR-9 Primary Returns.

UTC Time HH:MM:SS	Elapsed Time Seconds	Mode C Altitude feet	Latitude DD:MM:SS	Longitude DD:MM:SS	Distance N of ACK Nautical Miles	Distance E of ACK Nautical Miles
6:45:27	-273	33000	40° 5' 53" N	70° 43' 9" W	-68.987	-30.256
6:45:39	-261	33000	40° 6' 13" N	70° 41' 10" W	-68.664	-28.735
6:45:51	-249	33000	40° 7' 12" N	70° 39' 12" W	-67.690	-27.223
6:46:3	-237	33000	40° 7' 32" N	70° 37' 13" W	-67.367	-25.702
6:46:15	-225	33000	40° 8' 9" N	70° 35' 16" W	-66.759	-24.206
6:46:27	-213	33000	40° 8' 52" N	70° 33' 7" W	-66.051	-22.556
6:46:39	-201	33000	40° 9' 19" N	70° 31' 19" W	-65.608	-21.176
6:46:51	-189	33000	40° 9' 47" N	70° 29' 20" W	-65.148	-19.656
6:47:3	-177	33000	40° 10' 31" N	70° 27' 22" W	-64.421	-18.149
6:47:15	-165	33000	40° 11' 21" N	70° 25' 23" W	-63.594	-16.628
6:47:27	-153	33000	40° 11' 49" N	70° 23' 14" W	-63.133	-14.982
6:47:39	-141	33000	40° 12' 24" N	70° 21' 26" W	-62.554	-13.604
6:47:51	-129	33000	40° 12' 59" N	70° 19' 28" W	-61.975	-12.098
6:48:3	-117	33000	40° 13' 20" N	70° 17' 29" W	-61.629	-10.581
6:48:15	-105	33000	40° 13' 55" N	70° 15' 30" W	-61.048	-9.063
6:48:27	-93	33000	40° 14' 31" N	70° 13' 42" W	-60.451	-7.687
6:48:39	-81	33000	40° 15' 12" N	70° 11' 43" W	-59.769	-6.170
6:48:51	-69	33000	40° 15' 48" N	70° 9' 34" W	-59.171	-4.526
6:49:3	-57	33000	40° 16' 9" N	70° 7' 45" W	-58.822	-3.138
6:49:15	-45	33000	40° 16' 51" N	70° 5' 46" W	-58.122	-1.623
6:49:27	-33	33000	40° 17' 11" N	70° 3' 58" W	-57.789	-0.248
6:49:39	-21	33000	40° 17' 54" N	70° 1' 59" W	-57.071	1.266
6:49:51	-9	33000	40° 18' 43" N	69° 60' 0" W	-56.253	2.780
6:50:3	3	32000	40° 19' 26" N	69° 58' 0" W	-55.532	4.306
6:50:15	15	26800	40° 19' 31" N	69° 56' 12" W	-55.440	5.679
6:50:27	27	19100	40° 20' 21" N	69° 54' 2" W	-54.594	7.330

Table 3a. All Boston ARTCC Secondary Returns starting 300 seconds before accident.

UTC Time HH:MM:SS	Elapsed Time Seconds	Latitude DD:MM:SS	Longitude DD:MM:SS	Distance N of ACK Nautical Miles	Distance E of ACK Nautical Miles
6:45:3	-297	40° 27' 0" N	70° 40' 56" W	-47.822	-28.387
6:45:3	-297	40° 35' 27" N	70° 37' 27" W	-39.388	-25.682
6:45:3	-297	39° 47' 9" N	69° 14' 18" W	-87.606	37.931
6:45:5	-295	40° 2' 19" N	69° 33' 25" W	-72.547	23.149
6:45:27	-273	40° 15' 1" N	69° 50' 19" W	-59.897	10.174
6:45:27	-273	39° 47' 47" N	69° 13' 36" W	-86.967	38.463
6:45:29	-271	40° 2' 11" N	69° 33' 15" W	-72.680	23.278
6:45:39	-261	40° 16' 13" N	69° 53' 33" W	-58.702	7.703
6:45:51	-249	40° 16' 39" N	69° 57' 8" W	-58.273	4.967
6:45:51	-249	40° 16' 39" N	69° 57' 8" W	-58.273	4.967
6:45:51	-249	39° 47' 2" N	69° 13' 59" W	-87.720	38.175
6:46:3	-237	40° 17' 0" N	70° 0' 33" W	-57.926	2.359
6:46:15	-225	40° 14' 42" N	70° 5' 11" W	-60.227	-1.177
6:46:15	-225	40° 22' 25" N	70° 2' 19" W	-52.508	1.010
6:46:15	-225	40° 22' 25" N	70° 2' 19" W	-52.508	1.010
6:46:17	-223	40° 2' 23" N	69° 30' 59" W	-72.469	25.012
6:46:27	-213	40° 8' 51" N	70° 32' 57" W	-66.016	-22.411
6:46:27	-213	40° 23' 5" N	70° 5' 34" W	-51.841	-1.467
6:46:27	-213	39° 47' 16" N	69° 13' 37" W	-87.484	38.455
6:46:39	-201	40° 22' 55" N	70° 9' 19" W	-52.006	-4.324
6:46:51	-189	40° 24' 7" N	70° 12' 33" W	-50.802	-6.786
6:46:51	-189	40° 11' 15" N	69° 50' 58" W	-63.666	9.686
6:46:51	-189	39° 46' 40" N	69° 13' 50" W	-88.086	38.294
6:46:52	-188	39° 48' 48" N	70° 16' 30" W	-86.122	-9.881
6:46:53	-187	39° 59' 20" N	69° 44' 35" W	-75.571	14.607
6:47:3	-177	40° 14' 39" N	70° 21' 51" W	-60.253	-13.903
6:47:3	-177	40° 18' 58" N	70° 18' 17" W	-55.943	-11.168
6:47:3	-177	40° 24' 49" N	70° 15' 58" W	-50.096	-9.387
6:47:3	-177	40° 11' 35" N	69° 54' 32" W	-63.338	6.960
6:47:3	-177	40° 11' 35" N	69° 54' 32" W	-63.338	6.960
6:47:3	-177	40° 19' 2" N	69° 51' 39" W	-55.882	9.147
6:47:15	-165	40° 19' 9" N	70° 21' 42" W	-55.752	-13.773
6:47:15	-165	40° 13' 33" N	69° 57' 24" W	-61.374	4.767
6:47:15	-165	40° 21' 6" N	69° 54' 29" W	-53.819	6.982
6:47:16	-164	39° 47' 26" N	70° 17' 22" W	-87.487	-10.550
6:47:27	-153	40° 21' 51" N	70° 24' 25" W	-53.043	-15.835
6:47:27	-153	40° 14' 36" N	70° 0' 37" W	-60.326	2.310
6:47:27	-153	39° 47' 22" N	69° 13' 9" W	-87.381	38.813
6:47:39	-141	40° 23' 47" N	70° 27' 17" W	-51.100	-18.011
6:47:39	-141	40° 14' 20" N	70° 4' 34" W	-60.594	-0.706
6:47:39	-141	40° 20' 9" N	70° 2' 14" W	-54.775	1.074
6:47:39	-141	40° 20' 9" N	70° 2' 14" W	-54.775	1.074
6:47:51	-129	40° 21' 21" N	70° 31' 57" W	-53.517	-21.579
6:47:51	-129	40° 28' 25" N	70° 29' 17" W	-46.458	-19.512
6:47:51	-129	40° 19' 39" N	70° 20' 24" W	-55.255	-12.780
6:47:51	-129	40° 19' 39" N	70° 20' 24" W	-55.255	-12.780
6:47:51	-129	40° 14' 24" N	70° 8' 9" W	-60.526	-3.443
6:47:51	-129	40° 20' 44" N	70° 5' 28" W	-54.192	-1.391
6:47:52	-128	40° 35' 2" N	69° 11' 38" W	-39.691	39.510
6:47:53	-127	39° 56' 18" N	69° 18' 43" W	-78.484	34.458
6:48:3	-117	40° 23' 32" N	70° 34' 50" W	-51.320	-23.765
6:48:3	-117	40° 19' 38" N	70° 20' 14" W	-55.272	-12.653
6:48:3	-117	40° 15' 42" N	70° 11' 23" W	-59.222	-5.910
6:48:3	-117	40° 22' 33" N	70° 8' 41" W	-52.373	-3.842
6:48:3	-117	39° 47' 58" N	69° 12' 17" W	-86.774	39.473
6:48:4	-116	39° 48' 9" N	70° 16' 21" W	-86.772	-9.767
6:48:4	-116	40° 35' 1" N	69° 11' 47" W	-39.709	39.397
6:48:15	-105	40° 18' 54" N	70° 20' 14" W	-56.006	-12.656
6:48:15	-105	40° 16' 46" N	70° 14' 25" W	-58.151	-8.223
6:48:15	-105	40° 16' 46" N	70° 14' 25" W	-58.151	-8.223

Table 3b. Selected Boston ARTCC Primary Returns (page 1 of 3).

UTC Time HH:MM:SS	Elapsed Time Seconds	Latitude DD:MM:SS	Longitude DD:MM:SS	Distance N of ACK Nautical Miles	Distance E of ACK Nautical Miles
6:48:15	-105	40° 24' 20" N	70° 11' 34" W	-50.586	-6.037
6:48:15	-105	39° 46' 16" N	69° 13' 22" W	-88.483	38.657
6:48:16	-104	39° 47' 54" N	70° 16' 21" W	-87.022	-9.768
6:48:17	-103	40° 2' 18" N	69° 27' 43" W	-72.536	27.515
6:48:27	-93	40° 26' 8" N	70° 41' 8" W	-48.688	-28.546
6:48:27	-93	40° 18' 6" N	70° 17' 39" W	-56.812	-10.687
6:48:27	-93	40° 24' 32" N	70° 15' 9" W	-50.381	-8.766
6:48:27	-93	39° 46' 59" N	69° 12' 51" W	-87.762	39.047
6:48:39	-81	40° 18' 47" N	70° 21' 14" W	-56.120	-13.419
6:48:39	-81	40° 24' 22" N	70° 18' 55" W	-50.540	-11.635
6:48:39	-81	39° 47' 14" N	69° 12' 40" W	-87.511	39.185
6:48:40	-80	39° 46' 56" N	70° 10' 53" W	-87.997	-5.567
6:48:51	-69	40° 22' 11" N	70° 23' 25" W	-52.713	-15.071
6:48:52	-68	39° 46' 26" N	70° 11' 13" W	-88.497	-5.824
6:49:3	-57	40° 20' 23" N	70° 27' 53" W	-54.499	-18.484
6:49:3	-57	40° 25' 22" N	70° 25' 57" W	-49.521	-16.989
6:49:3	-57	40° 25' 22" N	70° 25' 57" W	-49.521	-16.989
6:49:3	-57	39° 46' 23" N	69° 12' 51" W	-88.362	39.053
6:49:15	-45	40° 21' 12" N	70° 31' 7" W	-53.670	-20.945
6:49:15	-45	40° 25' 34" N	70° 29' 21" W	-49.309	-19.577
6:49:27	-33	40° 24' 52" N	70° 33' 29" W	-49.993	-22.728
6:49:39	-21	40° 25' 19" N	70° 36' 55" W	-49.527	-25.341
6:49:39	-21	39° 47' 44" N	69° 11' 50" W	-87.004	39.821
6:49:51	-9	40° 23' 30" N	70° 41' 23" W	-51.321	-28.755
6:49:51	-9	40° 28' 29" N	70° 39' 27" W	-46.346	-27.248
6:49:51	-9	40° 28' 29" N	70° 39' 27" W	-46.346	-27.248
6:50:3	3	40° 28' 55" N	70° 42' 52" W	-45.894	-29.845
6:50:3	3	39° 46' 44" N	69° 12' 12" W	-88.007	39.549
6:50:27	27	39° 47' 27" N	69° 11' 41" W	-87.287	39.939
6:50:39	39	40° 21' 32" N	69° 51' 33" W	-53.381	9.217
6:50:39	39	40° 21' 32" N	69° 51' 33" W	-53.381	9.217
6:50:39	39	40° 21' 32" N	69° 51' 33" W	-53.381	9.217
6:50:39	39	40° 21' 32" N	69° 51' 33" W	-53.381	9.217
6:50:39	39	40° 21' 32" N	69° 51' 33" W	-53.381	9.217
6:50:51	51	39° 46' 14" N	69° 12' 24" W	-88.509	39.400
6:50:53	53	40° 21' 14" N	69° 49' 26" W	-53.677	10.831
6:51:5	65	40° 21' 20" N	69° 47' 27" W	-53.573	12.343
6:51:17	77	40° 21' 3" N	69° 47' 19" W	-53.856	12.446
6:51:29	89	40° 20' 40" N	69° 46' 20" W	-54.237	13.196
6:51:41	101	40° 20' 48" N	69° 46' 10" W	-54.103	13.323
6:51:53	113	40° 20' 54" N	69° 45' 11" W	-54.000	14.072
6:52:5	125	40° 20' 54" N	69° 45' 21" W	-54.001	13.945
6:52:51	171	39° 46' 56" N	69° 10' 54" W	-87.797	40.546
6:53:15	195	39° 45' 57" N	69° 11' 26" W	-88.785	40.146
6:54:3	243	40° 15' 24" N	69° 50' 58" W	-59.515	9.676
6:54:15	255	40° 14' 51" N	69° 54' 45" W	-60.071	6.789
6:54:15	255	40° 16' 43" N	69° 54' 1" W	-58.203	7.346
6:54:27	267	40° 12' 58" N	69° 59' 13" W	-61.959	3.380
6:54:27	267	40° 18' 9" N	69° 57' 14" W	-56.773	4.889
6:54:27	267	40° 18' 9" N	69° 57' 14" W	-56.773	4.889
6:54:27	267	40° 18' 9" N	69° 57' 14" W	-56.773	4.889
6:54:27	267	40° 18' 5" N	69° 54' 8" W	-56.836	7.254
6:54:39	279	40° 11' 48" N	70° 3' 41" W	-63.128	-0.032
6:54:39	279	40° 18' 15" N	70° 0' 49" W	-56.675	2.155
6:54:51	291	40° 27' 7" N	70° 32' 7" W	-47.748	-21.675
6:54:51	291	40° 13' 22" N	70° 6' 34" W	-61.560	-2.234
6:54:51	291	40° 13' 22" N	70° 6' 34" W	-61.560	-2.234
6:54:51	291	40° 13' 22" N	70° 6' 34" W	-61.560	-2.234
6:55:3	303	40° 27' 25" N	70° 35' 41" W	-47.432	-24.389
6:55:3	303	40° 27' 25" N	70° 35' 41" W	-47.432	-24.389

Table 3b (continued). Selected Boston ARTCC Primary Returns (page 2 of 3).

UTC Time HH:MM:SS	Elapsed Time Seconds	Latitude DD:MM:SS	Longitude DD:MM:SS	Distance N of ACK Nautical Miles	Distance E of ACK Nautical Miles
6:55:3	303	40° 27' 25" N	70° 35' 41" W	-47.432	-24.389
6:55:3	303	40° 14' 19" N	70° 9' 57" W	-60.607	-4.817
6:55:3	303	40° 18' 32" N	70° 8' 1" W	-56.391	-3.337
6:55:3	303	40° 20' 45" N	70° 7' 17" W	-54.174	-2.776
6:55:15	315	40° 27' 59" N	70° 39' 8" W	-46.848	-27.011
6:55:15	315	40° 20' 13" N	70° 11' 3" W	-54.705	-5.649
6:55:27	327	40° 28' 54" N	70° 42' 33" W	-45.913	-29.604
6:55:27	327	40° 28' 54" N	70° 42' 33" W	-45.913	-29.604
6:55:27	327	40° 28' 54" N	70° 42' 33" W	-45.913	-29.604
6:55:27	327	40° 20' 40" N	70° 14' 38" W	-54.250	-8.380
6:55:39	339	40° 20' 37" N	70° 18' 24" W	-54.293	-11.252
6:55:51	351	40° 22' 3" N	70° 21' 28" W	-52.852	-13.586
6:56:3	363	40° 23' 20" N	70° 24' 32" W	-51.559	-15.918
6:56:15	375	40° 22' 54" N	70° 28' 28" W	-51.980	-18.917
6:56:15	375	40° 22' 54" N	70° 28' 28" W	-51.980	-18.917
6:56:15	375	40° 22' 54" N	70° 28' 28" W	-51.980	-18.917
6:57:3	423	40° 13' 19" N	70° 16' 11" W	-61.599	-9.580
6:57:3	423	40° 13' 19" N	70° 16' 11" W	-61.599	-9.580
6:58:4	484	40° 3' 5" N	69° 10' 54" W	-71.644	40.386
6:58:27	507	40° 16' 20" N	69° 53' 12" W	-58.585	7.970
6:58:27	507	40° 16' 22" N	69° 50' 6" W	-58.546	10.336
6:58:27	507	40° 16' 22" N	69° 50' 6" W	-58.546	10.336
6:58:39	519	40° 15' 17" N	69° 57' 30" W	-59.641	4.689
6:58:39	519	39° 49' 54" N	69° 42' 4" W	-84.999	16.575
6:58:51	531	39° 50' 17" N	69° 41' 43" W	-84.615	16.842
6:58:51	531	39° 50' 17" N	69° 41' 43" W	-84.615	16.842
6:58:51	531	39° 50' 17" N	69° 41' 43" W	-84.615	16.842
6:58:51	531	39° 50' 17" N	69° 41' 43" W	-84.615	16.842
6:59:3	543	40° 17' 48" N	70° 3' 46" W	-57.126	-0.095
6:59:3	543	40° 17' 48" N	70° 3' 46" W	-57.126	-0.095
6:59:3	543	39° 50' 16" N	69° 41' 44" W	-84.632	16.829
6:59:15	555	40° 18' 53" N	70° 7' 1" W	-56.042	-2.574
6:59:27	567	40° 19' 11" N	70° 10' 36" W	-55.739	-5.307
6:59:27	567	39° 49' 9" N	69° 42' 5" W	-85.750	16.565
6:59:29	569	39° 57' 55" N	69° 31' 49" W	-76.941	24.401
6:59:39	579	40° 19' 24" N	70° 14' 1" W	-55.518	-7.913
6:59:39	579	39° 49' 9" N	69° 41' 55" W	-85.749	16.693
6:59:41	581	39° 57' 55" N	69° 31' 49" W	-76.941	24.401
6:59:51	591	40° 21' 49" N	70° 16' 52" W	-53.095	-10.080
6:59:51	591	40° 21' 49" N	70° 16' 52" W	-53.095	-10.080
6:59:51	591	40° 21' 49" N	70° 16' 52" W	-53.095	-10.080
6:59:51	591	40° 16' 3" N	69° 51' 45" W	-58.866	9.077
6:59:51	591	39° 49' 39" N	69° 41' 25" W	-85.247	17.075

Table 3b (concluded). Selected Boston ARTCC Primary Returns (page 3 of 3).

UTC Time HH:MM:SS	Elapsed Time Seconds	Mode C Altitude feet	ARSR4 Measured Altitude feet	Latitude DD:MM:SS	Longitude DD:MM:SS	Distance N of ACK Nautical Miles	Distance E of ACK Nautical Miles
6:46:50.02	-189.98	33000	N/A	40° 9' 59.12" N	70° 29' 37.76" W	-64.945	-19.882
6:47:2.04	-177.96	33000	N/A	40° 10' 44.57" N	70° 27' 34.69" W	-64.194	-18.309
6:47:14.045	-165.955	33000	42000	40° 11' 29.98" N	70° 25' 41.54" W	-63.443	-16.864
6:47:26.04	-153.96	33000	N/A	40° 11' 56.51" N	70° 23' 46.49" W	-63.006	-15.396
6:47:38.045	-141.955	33000	45200	40° 12' 23.9" N	70° 21' 41.73" W	-62.555	-13.804
6:47:49.985	-130.015	33000	39600	40° 12' 50.92" N	70° 19' 46.77" W	-62.109	-12.338
6:48:2.04	-117.96	33000	39600	40° 13' 18.18" N	70° 17' 51.85" W	-61.658	-10.872
6:48:13.99	-106.01	33000	40800	40° 14' 6.27" N	70° 15' 49.47" W	-60.860	-9.311
6:48:25.91	-94.09	33000	39200	40° 14' 34.16" N	70° 13' 54.69" W	-60.398	-7.848
6:48:38.095	-81.905	33000	N/A	40° 15' 22.5" N	70° 12' 2.33" W	-59.594	-6.416
6:48:50.01	-69.99	33000	37600	40° 15' 31.33" N	70° 9' 55.5" W	-59.449	-4.800
6:49:1.98	-58.02	33000	N/A	40° 15' 59.95" N	70° 8' 0.85" W	-58.973	-3.340
6:49:14.04	-45.96	33000	38800	40° 17' 10.07" N	70° 6' 11.34" W	-57.803	-1.945
6:49:26.09	-33.91	33000	N/A	40° 17' 40.16" N	70° 4' 7.13" W	-57.302	-0.364
6:49:49.985	-10.015	33000	42400	40° 19' 21.72" N	70° 0' 23.93" W	-55.607	2.475
6:50:2.01	2.01	32000	N/A	40° 19' 31.73" N	69° 58' 16.39" W	-55.437	4.097

Table 4a. All Gibbsboro (GIB) ARSR-4 Secondary Returns for Beacon Code 1712 starting 200 seconds before accident.

UTC Time HH:MM:SS	Elapsed Time Seconds	ARSR4 Measured Altitude feet	Latitude DD:MM:SS	Longitude DD:MM:SS	Distance E of ACK Nautical Miles	Distance N of ACK Nautical Miles
6:49:37.985	-22.015	45200	40° 17' 6.34" N	70° 2' 14.41" W	1.070	-57.820
6:51:38.015	98.015	53600	40° 20' 4.27" N	69° 46' 29.16" W	13.082	-54.833

Table 4b. Selected Gibbsboro (GIB) ARSR-4 Primary Returns.

UTC Time HH:MM:SS	Elapsed Time Seconds	Mode C Altitude feet	ARSR4 Measured Altitude feet	Latitude DD:MM:SS	Longitude DD:MM:SS	Distance N of ACK Nautical Miles	Distance E of ACK Nautical Miles
6:46:40.415	-199.585	33000	34800	40° 9' 15.1" N	70° 30' 50.88" W	-65.675	-20.818
6:46:52.37	-187.630	33000	34400	40° 9' 46.63" N	70° 29' 6.09" W	-65.155	-19.479
6:47:4.425	-175.575	33000	34400	40° 10' 23.21" N	70° 26' 54" W	-64.553	-17.792
6:47:16.37	-163.630	33000	33600	40° 10' 55.3" N	70° 24' 58.21" W	-64.024	-16.314
6:47:28.3	-151.700	33000	34400	40° 11' 29.89" N	70° 23' 16.89" W	-63.452	-15.020
6:47:40.265	-139.735	33000	34400	40° 12' 2.86" N	70° 21' 10.25" W	-62.907	-13.404
6:47:52.3	-127.700	33000	34000	40° 12' 37.2" N	70° 19' 4.99" W	-62.339	-11.806
6:48:4.25	-115.750	33000	34000	40° 13' 13.85" N	70° 17' 14.2" W	-61.732	-10.393
6:48:16.185	-103.815	33000	34000	40° 13' 51.55" N	70° 15' 24.68" W	-61.106	-8.996
6:48:28.145	-91.855	33000	33600	40° 14' 22.1" N	70° 13' 24.23" W	-60.600	-7.461
6:48:40.2	-79.800	33000	34000	40° 14' 54.48" N	70° 11' 37.86" W	-60.062	-6.105
6:48:52.145	-67.855	33000	34000	40° 15' 26.98" N	70° 9' 26.97" W	-59.521	-4.437
6:49:4.2	-55.800	33000	33600	40° 16' 1.28" N	70° 7' 30.2" W	-58.951	-2.950
6:49:15.92	-44.080	33000	33600	40° 16' 36.79" N	70° 5' 34.7" W	-58.359	-1.479
6:49:27.985	-32.015	33000	34000	40° 17' 13.5" N	70° 3' 40.5" W	-57.747	-0.025
6:49:40.025	-19.975	33000	33600	40° 17' 43.97" N	70° 1' 34.97" W	-57.238	1.572
6:49:51.995	-8.005	32900	34000	40° 18' 23.05" N	69° 59' 43.36" W	-56.585	2.992
6:50:3.925	3.925	31600	32400	40° 18' 55.36" N	69° 57' 40.28" W	-56.043	4.557
6:50:15.88	15.880	25500	26800	40° 19' 32.75" N	69° 56' 3.4" W	-55.409	5.788
6:50:27.915	27.915	18400	18800	40° 20' 4.86" N	69° 54' 2.5" W	-54.862	7.324

Table 5a. All North Truro (NOR) ARSR-4 Secondary Returns for Beacon Code 1712 starting 200 seconds before accident.

UTC Time HH:MM:SS	Elapsed Time Seconds	ARSR4 Measured Altitude feet	Latitude DD:MM:SS	Longitude DD:MM:SS	Distance N of ACK Nautical Miles	Distance E of ACK Nautical Miles
6:50:40.185	40.185	17200	40° 20' 44.49" N	69° 51' 14.29" W	-54.173	9.457
6:50:52.25	52.25	19200	40° 21' 16.69" N	69° 49' 15.63" W	-53.632	10.963
6:51:3.86	63.86	24800	40° 21' 28.65" N	69° 47' 26.98" W	-53.428	12.343
6:51:15.93	75.93	24000	40° 21' 6.96" N	69° 47' 11.34" W	-53.789	12.543
6:51:27.865	87.865	23200	40° 20' 48.72" N	69° 46' 19.06" W	-54.091	13.208
6:51:39.81	99.81	18400	40° 20' 55.07" N	69° 46' 7.74" W	-53.985	13.351
6:51:51.86	111.86	14400	40° 20' 59.52" N	69° 45' 6.64" W	-53.908	14.128
6:52:3.915	123.915	8000	40° 20' 56.24" N	69° 45' 18.45" W	-53.963	13.978

Table 5b. Selected North Truro (NOR) ARSR-4 Primary Returns.

UTC Time HH:MM:SS	Elapsed Time Seconds	Mode C Altitude feet	ARSR4 Measured Altitude feet	Latitude DD:MM:SS	Longitude DD:MM:SS	Distance N of ACK Nautical Miles	Distance E of ACK Nautical Miles
6:46:50.53	-189.47	33000	33600	40° 9' 45.58" N	70° 29' 26.56" W	-65.172	-19.740
6:47:2.585	-177.415	33000	33600	40° 10' 32.85" N	70° 27' 23.71" W	-64.390	-18.170
6:47:14.27	-165.73	33000	33200	40° 11' 22" N	70° 25' 21.15" W	-63.577	-16.604
6:47:26.355	-153.645	33000	33200	40° 11' 50.96" N	70° 23' 19.95" W	-63.100	-15.058
6:47:38.3	-141.7	33000	33200	40° 12' 24.14" N	70° 21' 27.84" W	-62.551	-13.627
6:47:50.35	-129.65	33000	33600	40° 12' 55.97" N	70° 19' 26.67" W	-62.025	-12.081
6:48:2.295	-117.705	33000	33600	40° 13' 21.85" N	70° 17' 39.61" W	-61.597	-10.716
6:48:14.265	-105.735	33000	33200	40° 13' 56.41" N	70° 15' 38.5" W	-61.025	-9.172
6:48:26.27	-93.73	33000	33600	40° 14' 34.94" N	70° 13' 46.72" W	-60.385	-7.747
6:48:38.32	-81.68	33000	34000	40° 15' 12.37" N	70° 11' 45.83" W	-59.763	-6.206
6:48:50.26	-69.74	33000	34400	40° 15' 51.27" N	70° 9' 45.07" W	-59.116	-4.667
6:49:2.31	-57.69	33000	33600	40° 16' 10.21" N	70° 7' 53.61" W	-58.801	-3.248
6:49:14.31	-45.69	33000	34800	40° 16' 51.78" N	70° 5' 53.02" W	-58.109	-1.712
6:49:26.35	-33.65	33000	36000	40° 17' 12.84" N	70° 4' 1.55" W	-57.758	-0.293
6:49:38.1	-21.9	33000	34400	40° 17' 57.07" N	70° 2' 1.21" W	-57.020	1.238
6:49:50.135	-9.865	33000	33600	40° 18' 42.77" N	70° 0' 1.11" W	-56.256	2.766
6:50:2.1	2.1	32000	33200	40° 19' 29.78" N	69° 58' 0.52" W	-55.469	4.299
6:50:14.09	14.09	26800	28400	40° 19' 31.54" N	69° 56' 14.08" W	-55.431	5.653
6:50:26.18	26.18	19100	22400	40° 20' 20.19" N	69° 54' 9.92" W	-54.607	7.229

Table 6a. All Riverhead (RIV) ARSR-4 Secondary Returns for Beacon Code 1712 starting 200 seconds before accident.

UTC Time HH:MM:SS	Elapsed Time Seconds	ARSR4 Measured Altitude feet	Latitude DD:MM:SS	Longitude DD:MM:SS	Distance N of ACK Nautical Miles	Distance E of ACK Nautical Miles
6:50:38.125	38.125	16000	40:21:28.963 N	69:51:32.515 W	-53.432	9.223
6:50:50.16	50.16	18800	40:21:56.482 N	69:49:33.439 W	-52.969	10.735
6:51:2.05	62.05	22000	40° 21' 26.35" N	69° 48' 4.08" W	-53.468	11.872
6:51:14.1	74.1	24800	40:22:6.043 N	69:47:2.239 W	-52.804	12.655
6:51:26.135	86.135	24000	40:21:46.512 N	69:46:27.629 W	-53.128	13.096
6:51:38.1	98.1	17600	40° 21' 14.05" N	69° 45' 54.05" W	-53.668	13.524
6:52:2.045	122.045	12800	40° 21' 24.03" N	69° 45' 38.23" W	-53.501	13.725
6:52:14.1	134.1	12400	40:22:0.808 N	69:45:26.065 W	-52.887	13.877
6:52:26.05	146.05	10800	40° 21' 22.04" N	69° 45' 27.87" W	-53.534	13.856
6:52:38.1	158.1	N/A	40° 18' 32.07" N	69° 55' 30.13" W	-56.387	6.209
6:53:38.1	218.1	N/A	40° 19' 17.88" N	69° 54' 11.99" W	-55.621	7.201
6:53:50.115	230.115	N/A	40° 18' 53.84" N	69° 58' 5.3" W	-56.026	4.236

Table 6b. Selected Riverhead (RIV) ARSR-4 Primary Returns.

Pressure millibars	Temp deg. C	Dew Point deg. C	Wind Dir degrees	Wind Speed knots	Height feet	Pressure Alt. feet	Height - P. Alt. feet
1025.0	14.0	14.0	240	4.9	66	-319	385
1000.0	13.2	13.2	245	19.8	750	364	386
991.1	12.9	12.9	245	26.8	997	610	387
984.0	12.6	12.6	246	27.2	1196	808	388
971.0	14.8	12.7	248	28.0	1565	1174	391
955.9	13.7	12.2	250	28.9	1998	1604	394
925.0	11.4	11.1	255	30.9	2908	2500	408
922.0	11.3	10.6	255	30.9	2999	2588	410
908.0	10.6	8.5	253	31.7	3418	3004	414
888.9	10.4	5.1	250	32.8	3999	3579	421
867.0	10.2	1.2	247	34.3	4682	4250	432
857.0	10.6	-2.0	245	35.0	5000	4562	438
850.0	10.8	-4.2	250	33.8	5223	4781	442
826.2	10.6	-4.4	255	31.9	6001	5539	461
812.0	10.4	-4.6	255	30.0	6473	6000	473
796.2	9.2	-5.1	255	28.0	7001	6520	481
767.1	7.0	-6.1	255	24.9	8002	7501	501
739.2	4.8	-7.0	260	25.8	8999	8470	529
700.0	1.6	-8.4	260	28.9	10464	9883	581
688.0	0.6	-11.4	259	29.2	10920	10328	592
659.9	-1.5	-14.7	255	29.9	12001	11396	605
610.9	-5.5	-20.9	255	32.8	14003	13349	653
580.0	-8.1	-25.1	258	33.5	15347	14647	700
565.2	-8.7	-29.7	260	33.8	16004	15289	715
540.0	-9.7	-37.7	264	34.2	17163	16414	749
505.0	-12.9	-30.9	269	34.9	18850	18048	802
500.0	-13.5	-30.5	270	35.0	19099	18289	810
487.0	-15.3	-26.3	270	37.1	19755	18925	829
482.0	-16.0	-26.7	270	37.9	20003	19173	830
444.0	-21.5	-29.9	270	49.9	22005	21131	874
422.0	-24.9	-31.9	275	47.9	23241	22327	914
411.0	-26.5	-36.5	277	46.9	23870	22944	925
400.0	-27.5	-47.5	280	45.8	24512	23575	937
391.7	-28.1	-49.8	280	42.9	25003	24060	943
375.3	-29.4	-54.6	285	37.9	26004	25044	960
354.0	-31.1	-61.1	282	37.2	27376	26375	1001
315.4	-37.8	-56.6	275	35.9	30007	28962	1045
300.0	-40.7	-54.7	275	35.9	31151	30066	1084
251.4	-51.2	-60.3	275	42.9	35007	33882	1125
250.0	-51.5	-60.5	275	42.0	35130	34000	1130

Table 7a. Radiosonde Data from Upton, NY, for 1200 UTC (0700 EST) 10/31/1999.

Pressure millibars	Temp deg. C	Dew Point deg. C	Wind Dir degrees	Wind Speed knots	Height feet	Pressure Alt. feet	Height - P. Alt. feet
1026.0	13.2	8.7	210	15.0	53	-346	399
1007.0	15.6	13.3	217	20.8	572	171	401
1000.0	15.4	12.9	220	22.9	767	364	403
991.7	14.8	12.6	225	26.8	997	594	404
956.4	12.0	11.2	230	24.9	1998	1589	409
936.0	10.4	10.4	237	27.5	2595	2178	417
927.0	11.2	11.2	239	28.7	2860	2441	419
925.0	11.4	9.2	240	28.9	2920	2500	420
922.3	11.6	8.1	240	28.9	2999	2579	419
917.0	12.0	6.0	240	29.7	3159	2736	422
915.0	12.2	-0.8	240	30.0	3219	2795	423
902.0	12.4	1.4	240	31.9	3612	3183	429
889.3	11.7	1.2	240	33.8	3999	3566	433
850.0	9.4	0.4	235	33.8	5238	4781	457
826.5	8.9	-6.5	235	32.8	6001	5530	471
810.0	8.6	-11.4	241	32.3	6548	6065	483
798.0	8.0	-10.0	245	31.9	6953	6461	492
796.6	7.9	-10.6	245	31.9	7001	6507	494
786.0	7.2	-14.8	247	31.5	7362	6861	501
778.0	6.4	-4.6	248	31.2	7638	7130	507
767.5	5.6	-5.2	250	30.9	8002	7487	515
739.4	3.6	-6.7	260	28.9	8999	8463	536
724.0	2.4	-7.6	262	27.0	9561	9010	551
710.0	2.8	-14.2	264	25.2	10079	9516	563
700.0	2.0	-13.0	265	23.9	10456	9883	573
659.8	-2.0	-15.9	270	28.0	12001	11400	602
630.0	-5.1	-18.1	270	29.7	13209	12573	636
610.9	-6.0	-24.1	270	30.9	14003	13349	653
604.0	-6.3	-26.3	272	30.9	14294	13634	659
564.8	-9.0	-28.3	285	30.9	16004	15307	697
549.0	-10.1	-29.1	284	33.0	16726	16007	719
501.3	-15.4	-30.5	280	39.8	19003	18226	776
500.0	-15.5	-30.5	280	38.9	19067	18289	778
490.0	-16.9	-30.9	280	38.9	19566	18777	789
481.2	-17.8	-32.9	280	38.9	20003	19213	790
400.0	-26.5	-53.5	265	26.8	24473	23575	898
391.1	-27.7	-55.1	260	24.9	25003	24096	908
377.0	-29.7	-57.7	262	26.8	25868	24940	928
314.3	-40.2	-53.1	270	35.9	30007	29040	967
300.0	-42.9	-51.9	275	36.9	31070	30066	1004
255.0	-51.7	-56.5	280	39.5	34599	33579	1020
250.1	-52.8	-57.5	280	39.8	35007	33992	1015
250.0	-52.8	-57.5	280	39.8	35017	34000	1017

Table 7b. Radiosonde Data from Chatham, MA, for 1200 UTC (0700 EST) 10/31/1999.

North Truro (NOR)			
Actual MSL Altitude (feet)	**Sample Size (number of returns)**	**Error in Sensed Altitude Data (feet)**	**Standard Deviation of Altitude Error (feet)**
100 - 5,000	379	3,851	3,383
5,000 - 10,000	767	-450	1,423
10,000 - 15,000	1,003	-1,211	1,724
15,000 - 20,000	1,619	-1,039	1,867
20,000 - 25,000	2,121	-360	1,374
25,000 - 30,000	4,091	-74	770
30,000 - 35,000	10,019	-307	772

Riverhead (RIV)			
Actual MSL Altitude (feet)	**Sample Size (number of returns)**	**Error in Sensed Altitude Data (feet)**	**Standard Deviation of Altitude Error (feet)**
100 - 5,000	1,511	9,384	2,699
5,000 - 10,000	201	1,015	2,634
10,000 - 15,000	267	-158	1,530
15,000 - 20,000	1,032	-459	1,550
20,000 - 25,000	2,398	-187	1,400
25,000 - 30,000	4,570	-157	1,118
30,000 - 35,000	10,018	-81	1,108

Table 8. NOR and RIV sensed altitude errors due to ducting effects as provided by the 84 RADES.

EST Time	ET, sec.	Source	Comment	Plot Code
1:48:18.55	-101.45	cam	[sound similar to cockpit door operating]	C:1
1:48:30.69	-89.31	cam-?	[unintelligible phrase]	C?:1
1:48:39.92	-80.08	cam-2b	I rely on God. [heard faintly]	C2B:1
1:48:57.93	-62.07	cam	[series of thumps and clicks starts]	C:2
1:49:14.93	-45.07	cam	[series of thumps and clicks ends]	C:3
1:49:18.37	-41.63	cam	[sound similar to electric seat motor]	C:4
1:49:30.16	-29.84	cam	[sound of 2 faint thumps and one louder thump]	C:5
1:49:47.54	-12.46	cam	[sound of 2 clicks and 2 thumps]	C:6
1:49:48.42	-11.58	cam-2b	I rely on God.	C2B:2
1:49:53.32	-6.68	cam	[sound of 1 loud thump and 3 faint thumps]	C:7
1:49:57.33	-2.67	cam-2b	I rely on God.	C2B:3
1:49:58.75	-1.25	cam-2b	I rely on God.	C2B:4
1:49:58.78	-1.22	cam	[4 tones similar to Master Caution aural beeper]	C:8
1:50:00.15	0.15	cam-2b	I rely on God.	C2B:5
1:50:01.60	1.60	cam-2b	I rely on God.	C2B:6
1:50:02.93	2.93	cam-2b	I rely on God.	C2B:7
1:50:04.42	4.42	cam-2b	I rely on God.	C2B:8
1:50:04.72	4.72	cam	[sound of loud thump]	C:9
1:50:05.89	5.89	cam-2b	I rely on God.	C2B:9
1:50:06.37	6.37	cam-1a	what's happening? what's happening?	C1A:1
1:50:07.07	7.07	cam-2b	I rely on God.	C2B:10
1:50:07.11	7.11	cam	[sound of numerous thumps and clinks starts]	C:10
1:50:08.20	8.20	cam	[repeating hi-low tone similar to Master Warning aural starts and continues to end of recording]	C:11
1:50:08.48	8.48	cam-2b	I rely on God.	C2B:11
1:50:08.53	8.53	cam-1a	what's happening?	C1A:2
1:50:15.15	15.15	cam-1a	what's happening, Gamil? what's happening?	C1A:3
1:50:19.51	19.51	cam	[4 tones similar to Master Caution aural beeper]	C:12
1:50:21.10	21.10	cam	[sound of numerous thumps and clinks stops]	C:13
1:50:24.92	24.92	cam-1a	what is this? what is this? did you shut the engine(s)?	C1A:4
1:50:26.55	26.55	cam-1a	get away in the engines. [translated as said]	C1A:5
1:50:28.85	28.85	cam-1a	shut the engines.	C1A:6
1:50:29.66	29.66	cam-2b	it's shut.	C2B:12
1:50:31.25	31.25	cam-1a	pull.	C1A:7
1:50:32.75	32.75	cam-1a	pull with me.	C1A:8
1:50:34.78	34.78	cam-1a	pull with me.	C1A:9
1:50:36.84	36.84	cam-1a	pull with me.	C1A:10
1:50:38.47	38.47	END OF RECORDING		END

Table 9. Selected CVR sounds and comments.

This page intentionally left blank

This page intentionally left blank

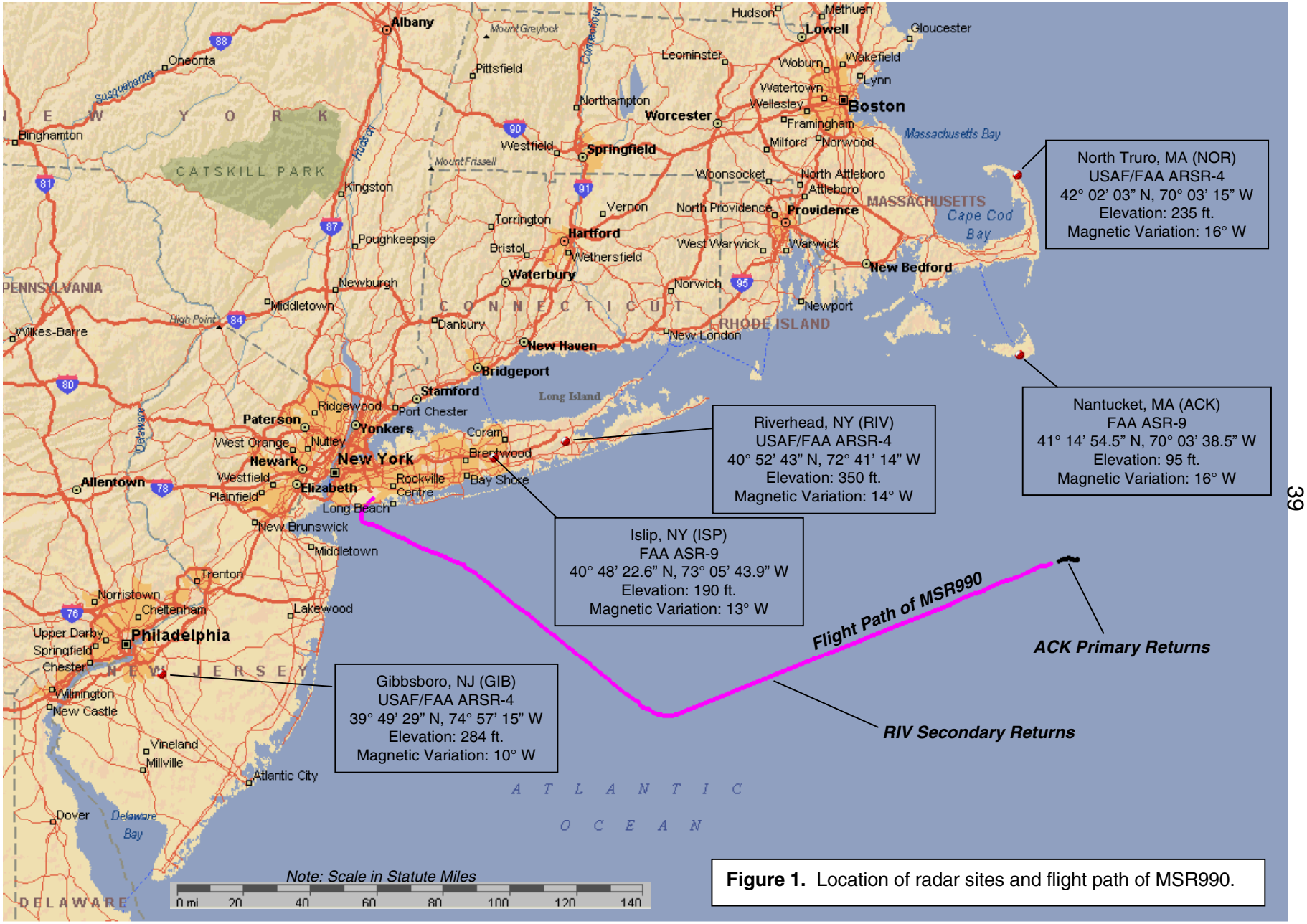

Figure 1. Location of radar sites and flight path of MSR990.

Egypt Air Flight 990: Boston NTAP & Nantucket ASR9 Data

Plan View: Latitude vs. Longitude, Full Scale

ASR9 Primary Data Corrected for Slant Range using 84 RADES Altitude Measurement Derived From ARSR4

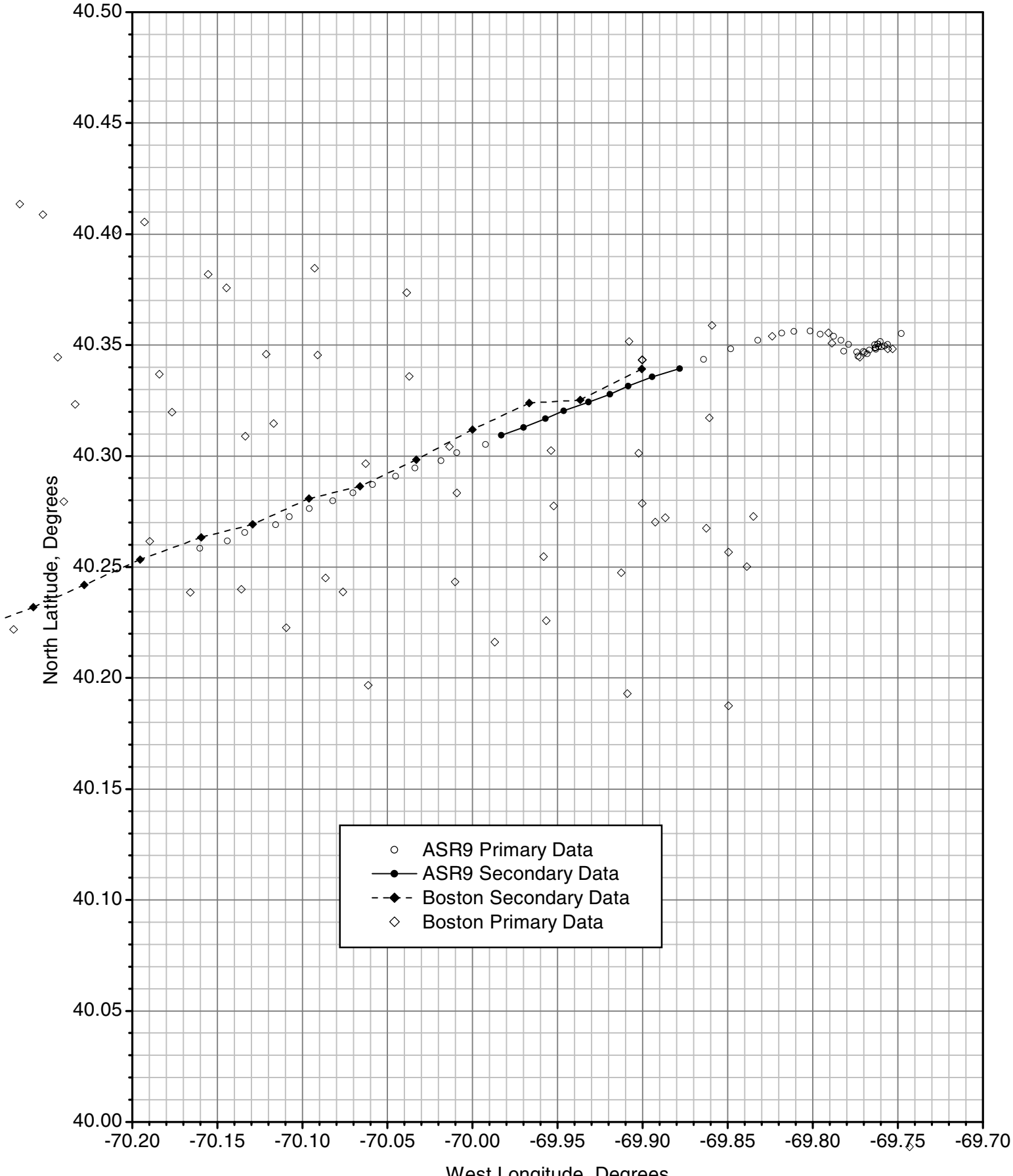

Figure 2a

Egypt Air Flight 990: Boston NTAP & Nantucket ASR9 Data

Plan View: Latitude vs. Longitude, Compressed Scale
ASR9 Primary Data Corrected for Slant Range using 84 RADES Altitude Measurement Derived From ARSR4

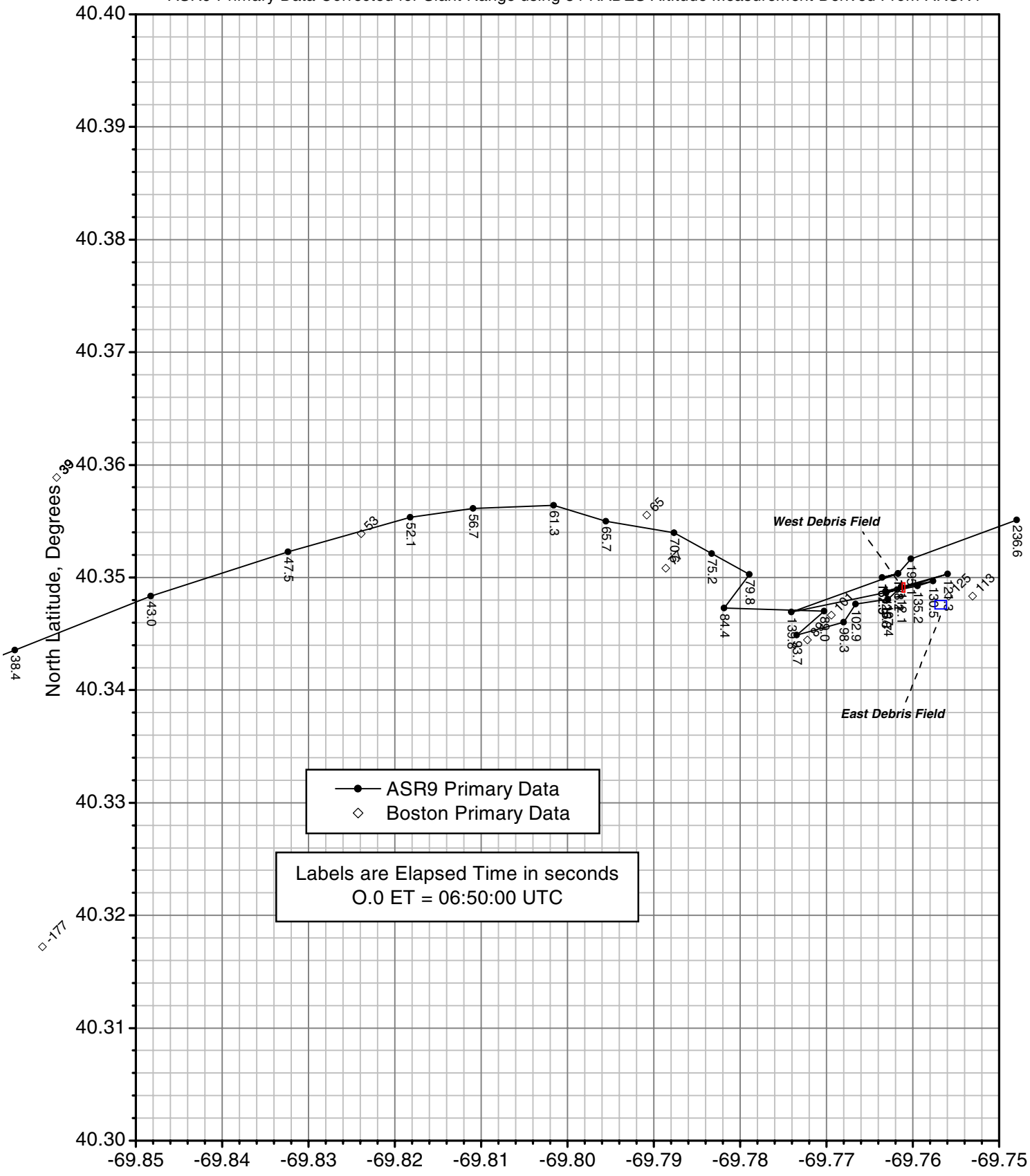

Figure 2b

Egypt Air Flight 990: Boston NTAP & Nantucket ASR9 Data

Time History: Latitude, Longitude, & Altitude, Full Scale

ASR9 Primary Data Corrected for Slant Range using 84 RADES Altitude Measurement Derived From ARSR4

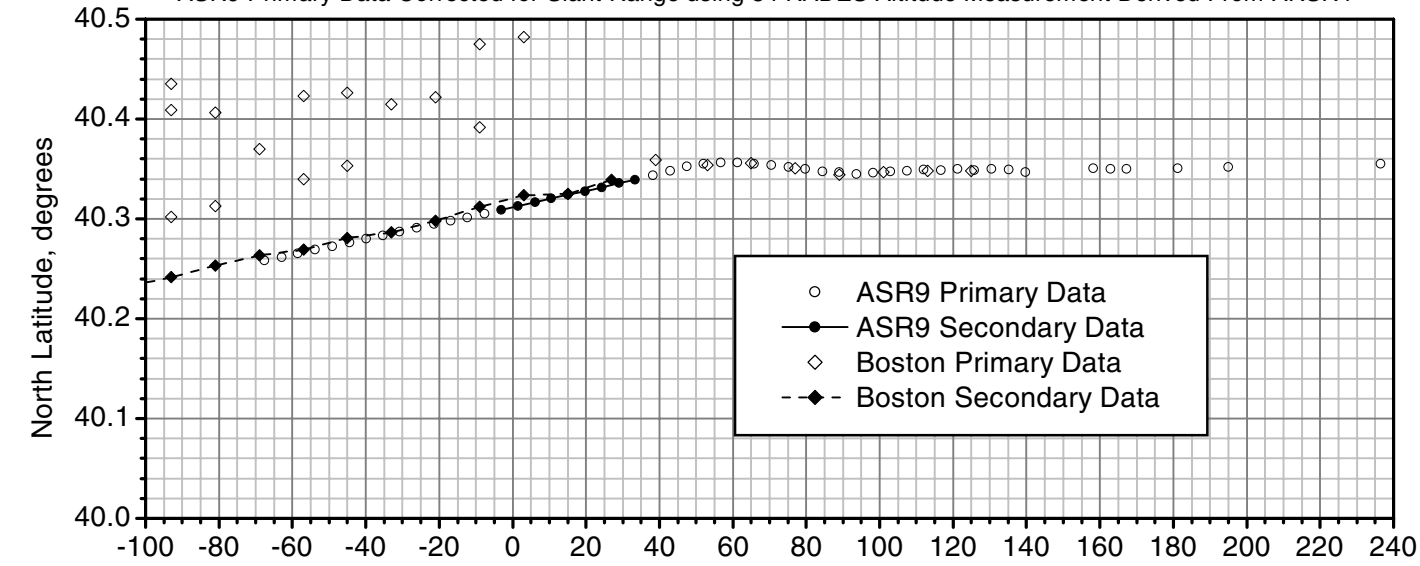

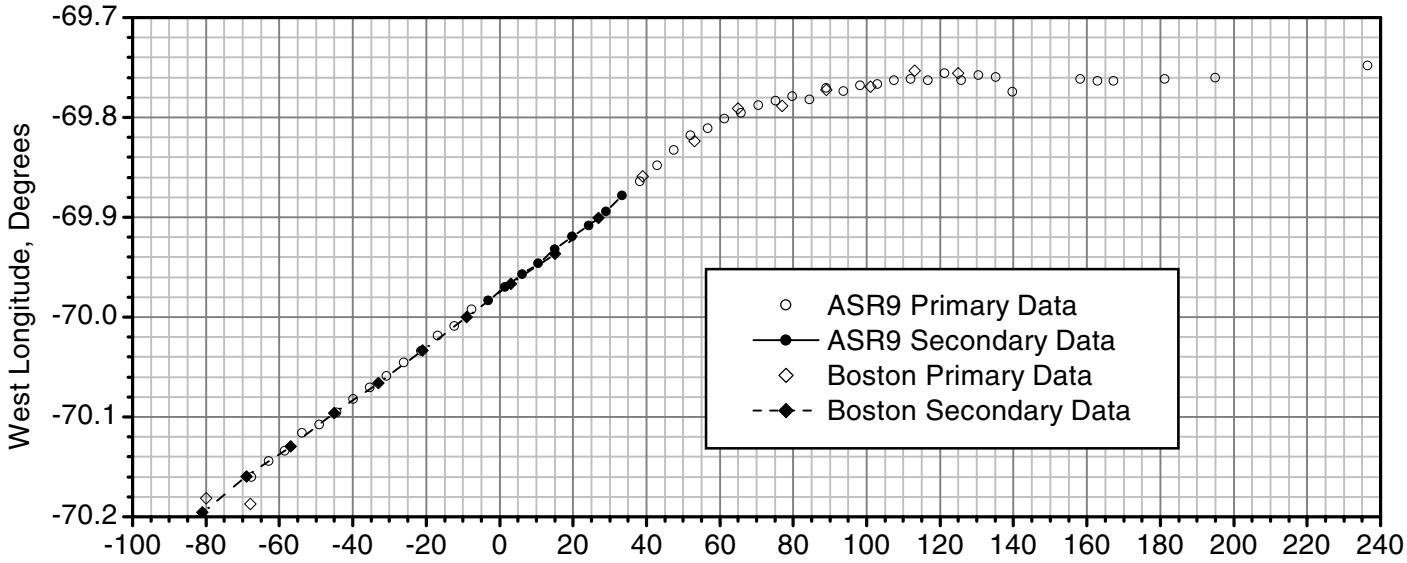

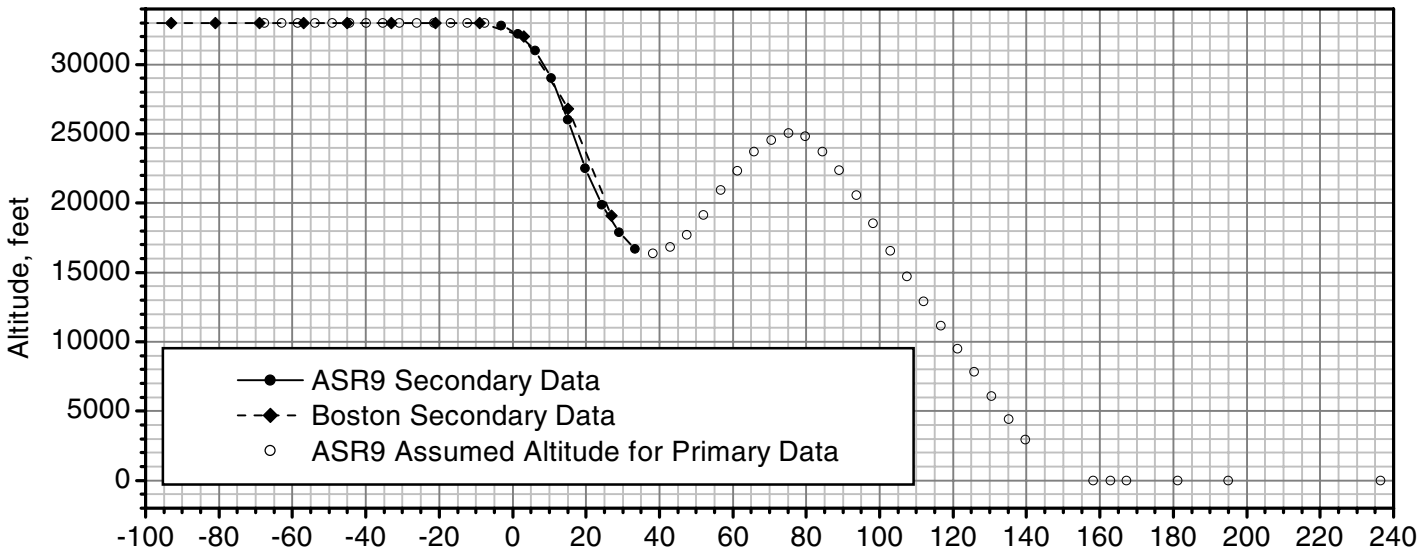

-100 -80 -60 -40 -20 0 20 40 60 80 100 120 140 160 180 200 220 240

Elapsed Time, Seconds

0.0 ET = 06:50:00 UTC

Figure 3a

Egypt Air Flight 990: Boston NTAP & Nantucket ASR9 Data

Time History: Latitude, Longitude, & Altitude, Compressed Scale
ASR9 Primary Data Corrected for Slant Range using 84 RADES Altitude Measurement Derived From ARSR4

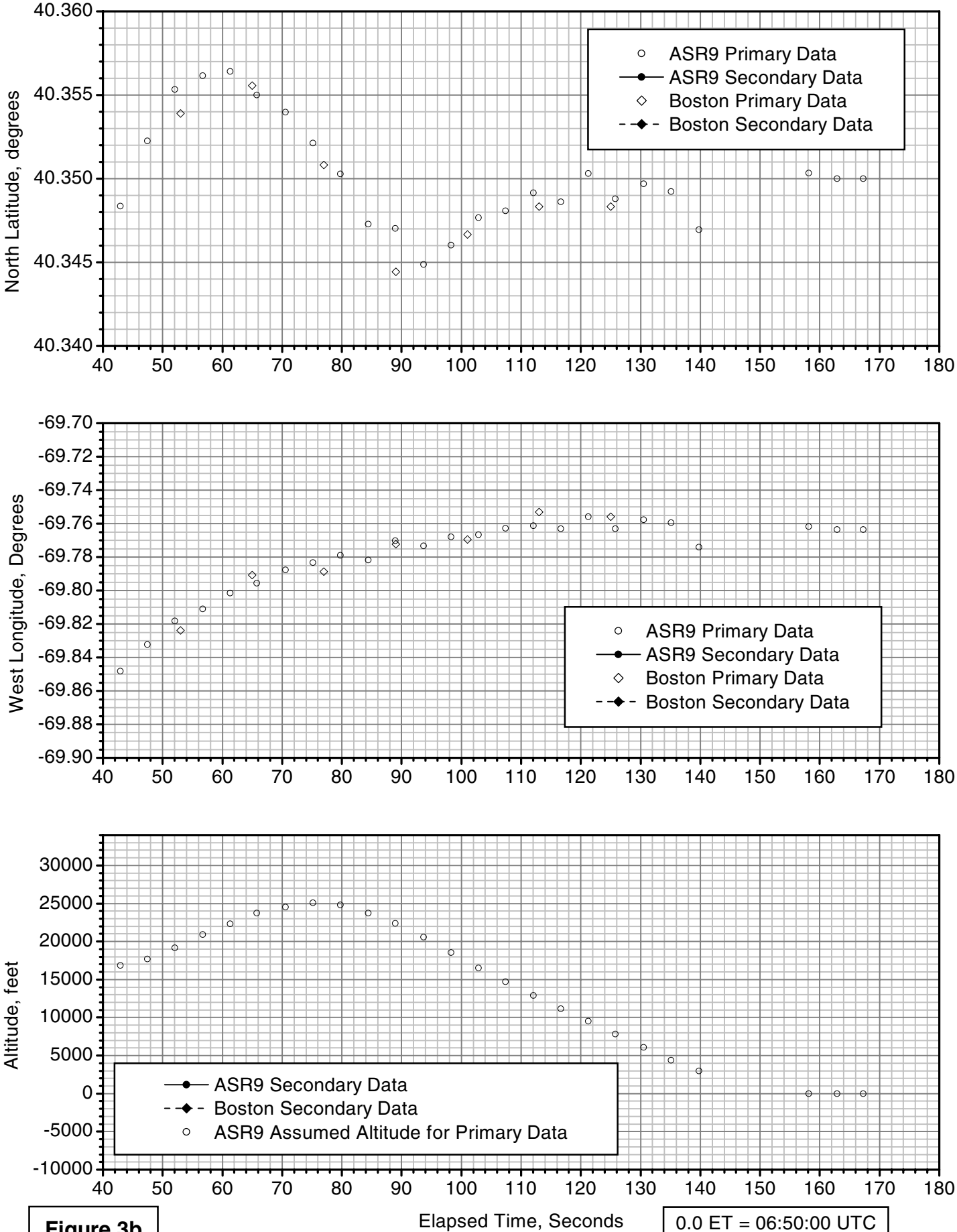

Figure 3b

Egypt Air Flight 990: Boston NTAP & Nantucket ASR9 Data

Plan View: North vs. East, Full Scale

ASR9 Primary Data Corrected for Slant Range using 84 RADES Altitude Measurement Derived From ARSR4

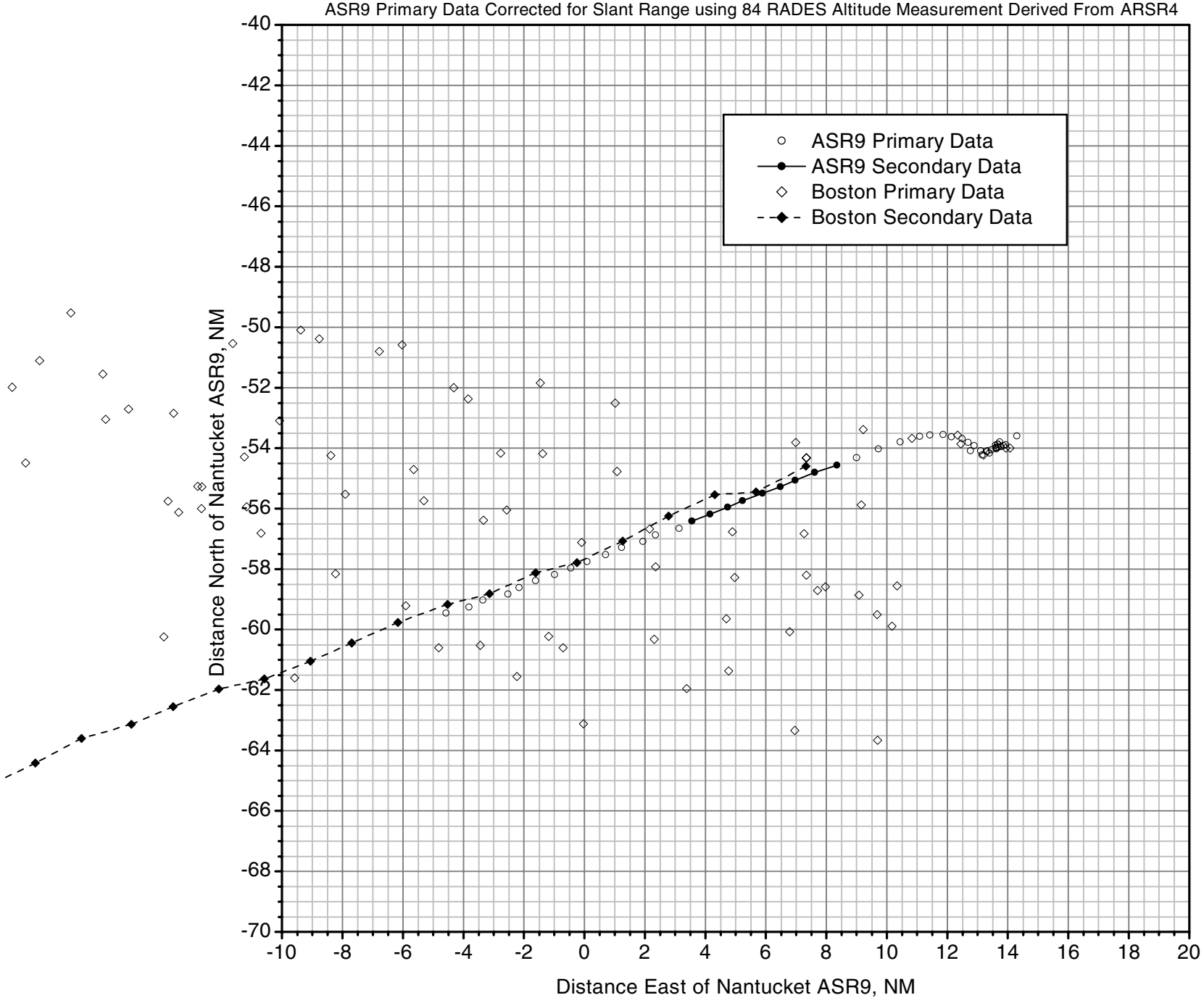

Figure 4a

Egypt Air Flight 990: Boston NTAP & Nantucket ASR9 Data

Plan View: North vs. East, Compressed Scale

ASR9 Primary Data Corrected for Slant Range using 84 RADES Altitude Measurement Derived From ARSR4

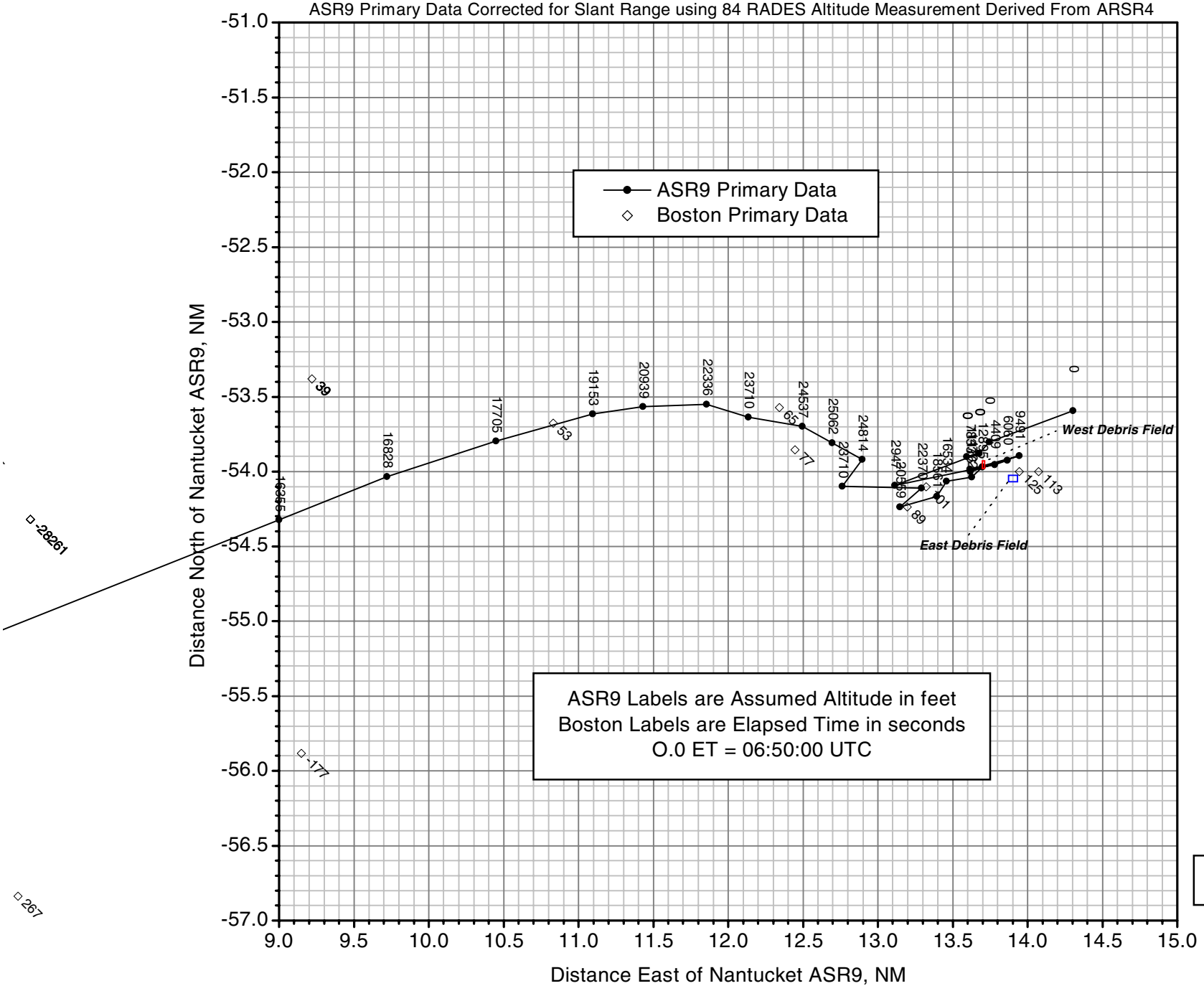

Figure 4b

Egypt Air Flight 990: Boston NTAP & Nantucket ASR9 Data

Time History: North, East, & Rate of Climb, Full Scale

ASR9 Primary Data Corrected for Slant Range using 84 RADES Altitude Measurement Derived From ARSR4

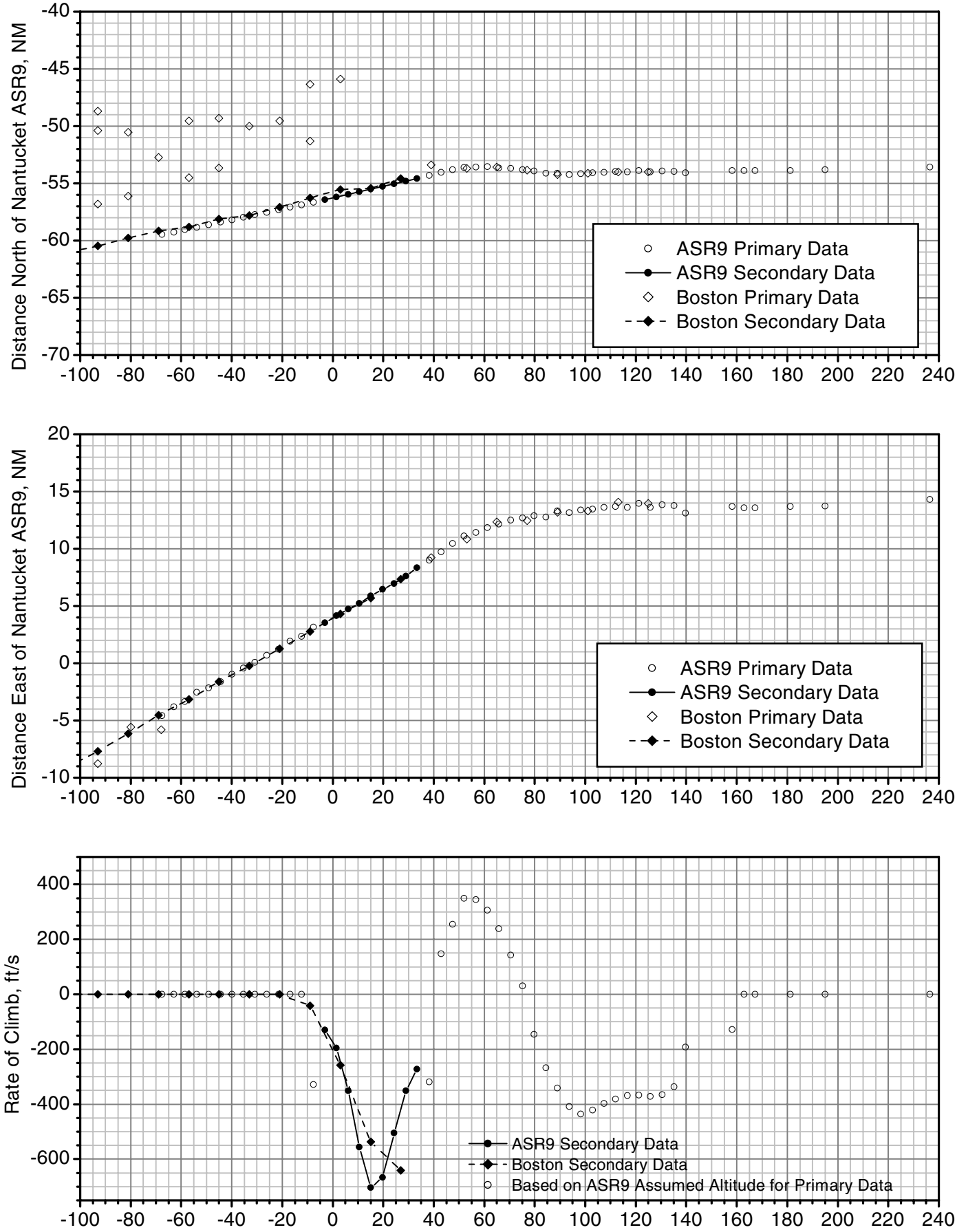

Figure 5a

Egypt Air Flight 990: Boston NTAP & Nantucket ASR9 Data

Time History: North, East, & Rate of Climb, Compressed Scale

ASR9 Primary Data Corrected for Slant Range using 84 RADES Altitude Measurement Derived From ARSR4

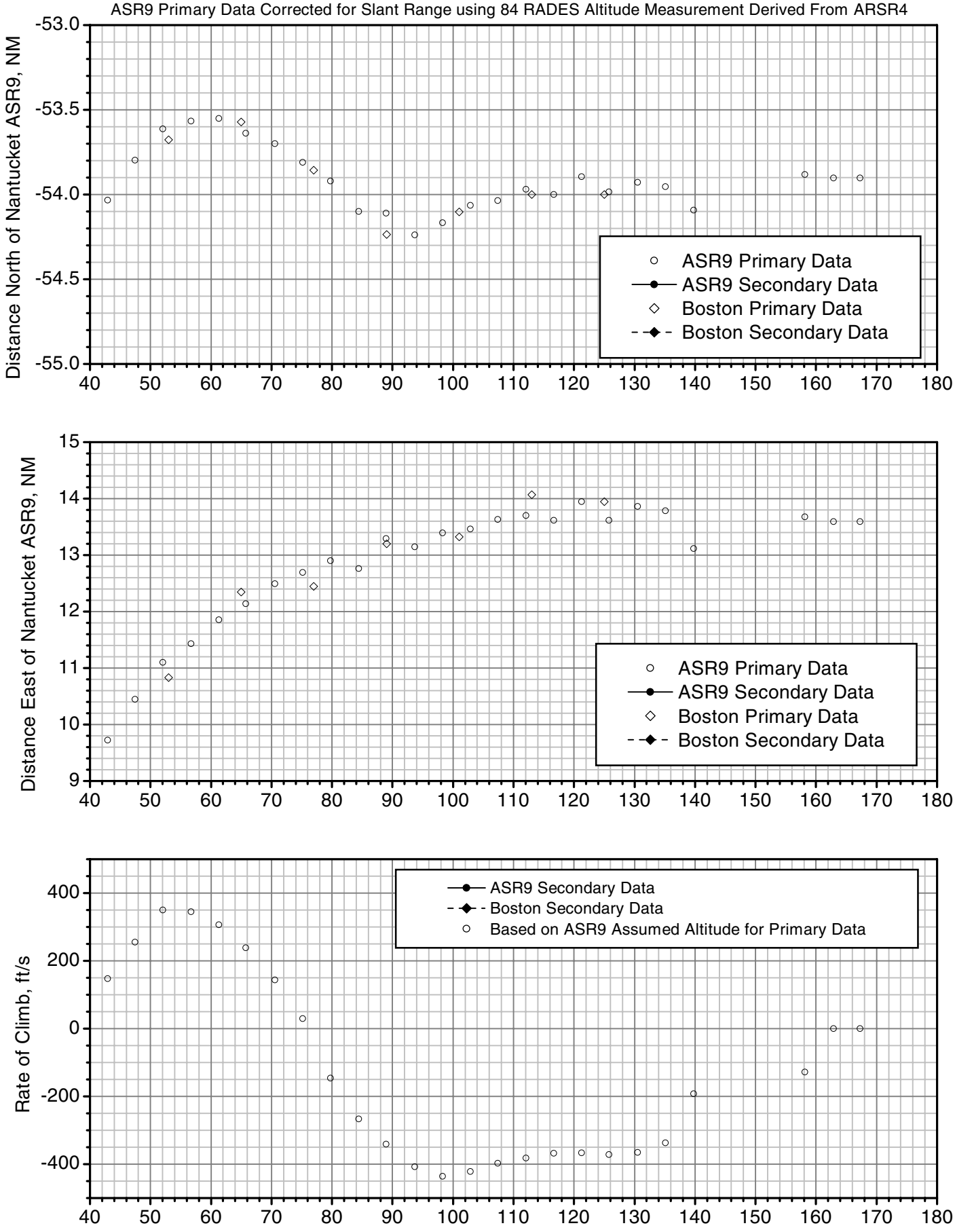

Figure 5b

Figure 6a. Primary and Secondary Returns from GIB, RIV, & NOR ARSR-4 Radars - Plan View
(Full Scale)

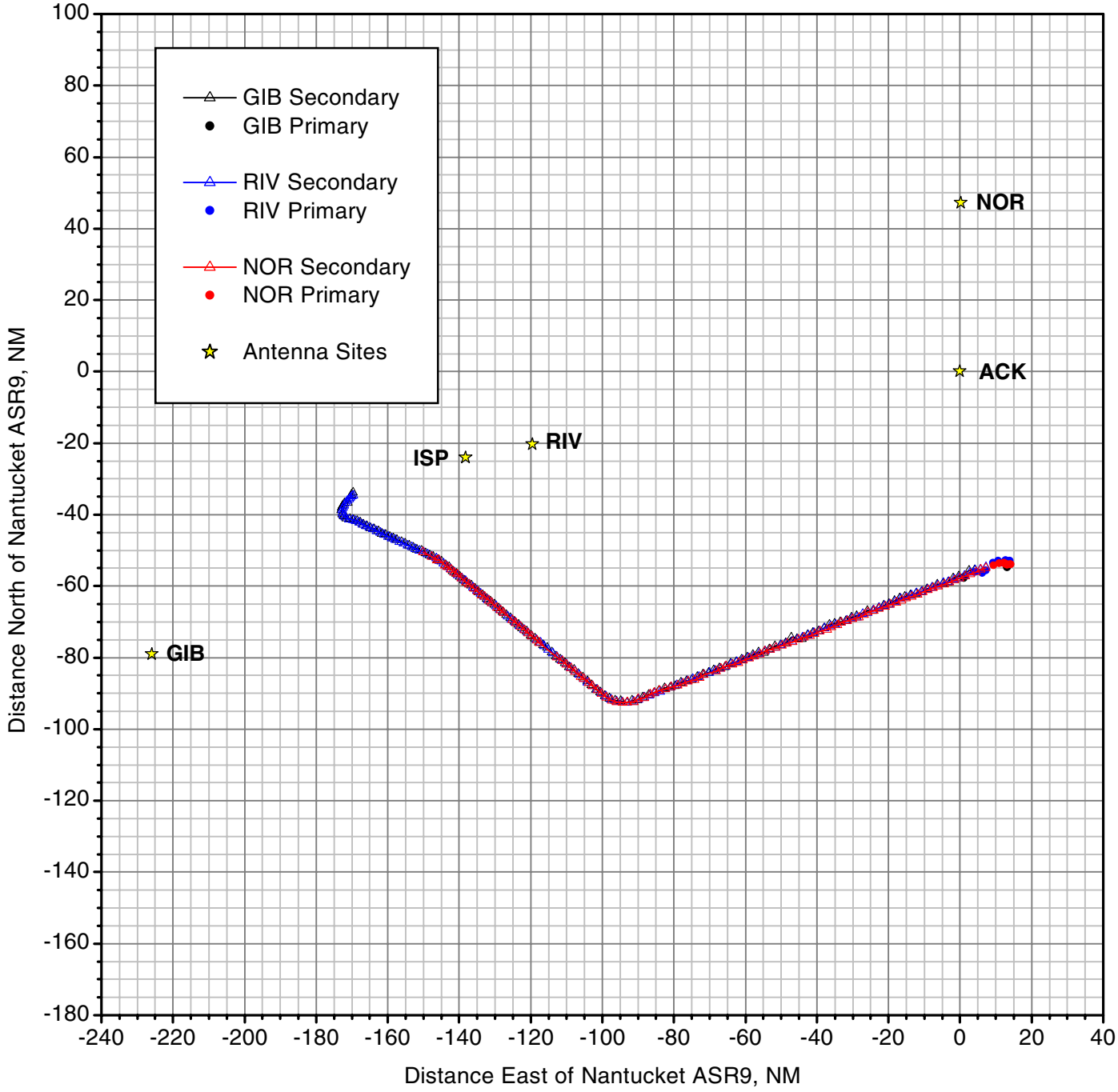

Figure 6b. Primary and Secondary Returns from GIB, RIV, & NOR ARSR-4 Radars - Plan View

(Compressed Scale)

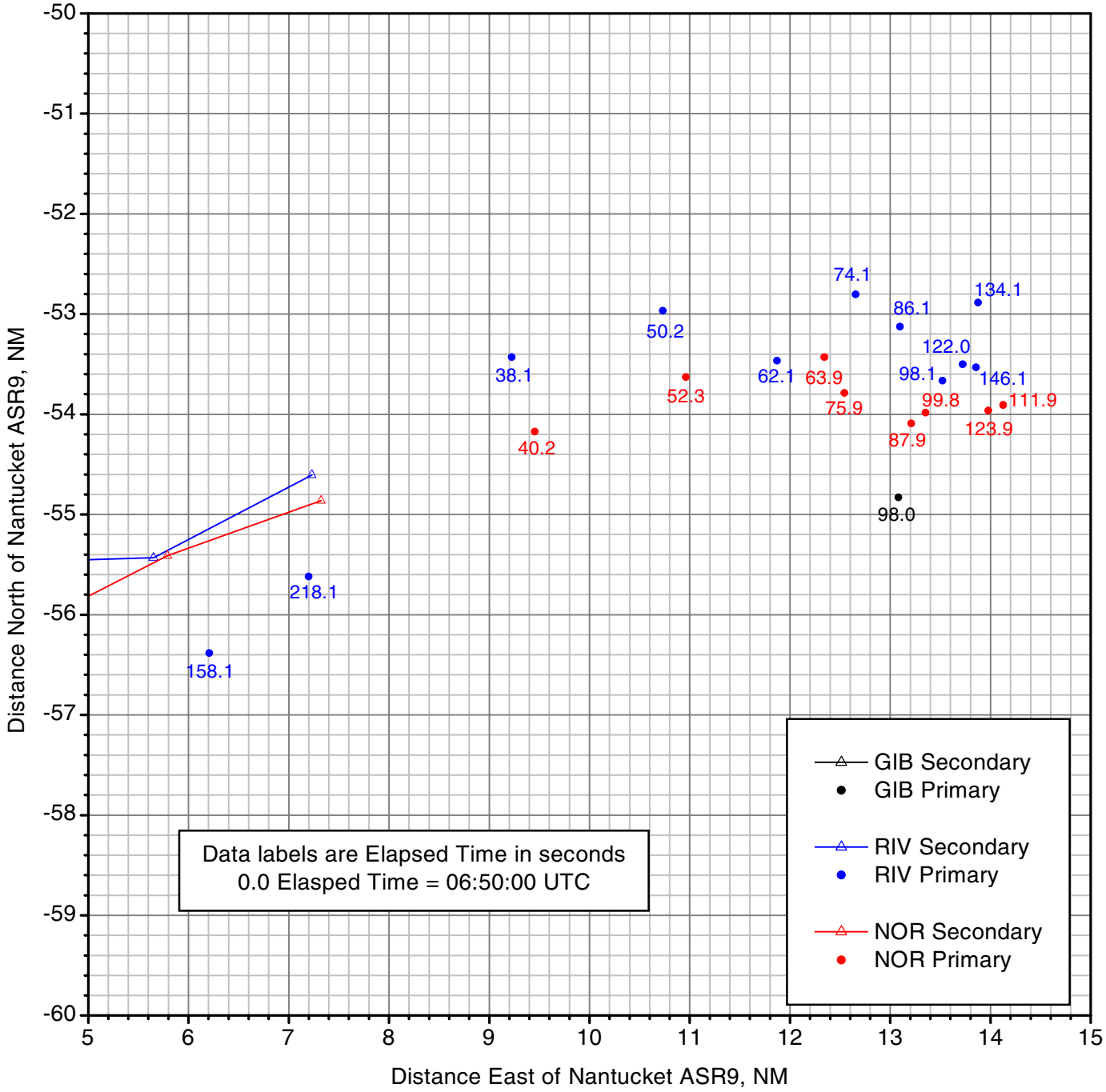

Figure 7a: Altitude Data from Air Force 84th Radar Evaluation Squadron (Full Scale)

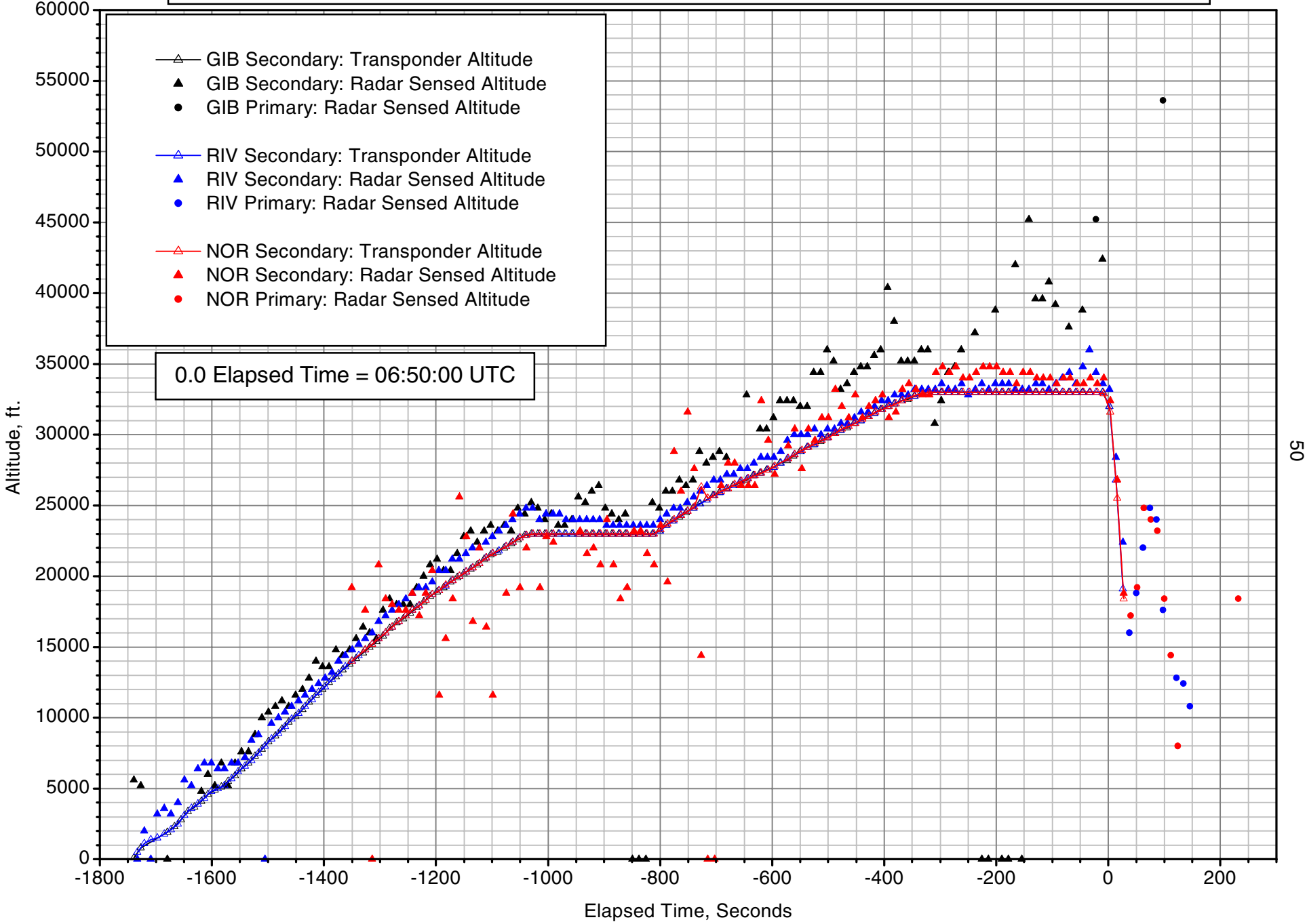

Figure 7b: Altitude Data from Air Force 84th Radar Evaluation Squadron (Compressed Scale)

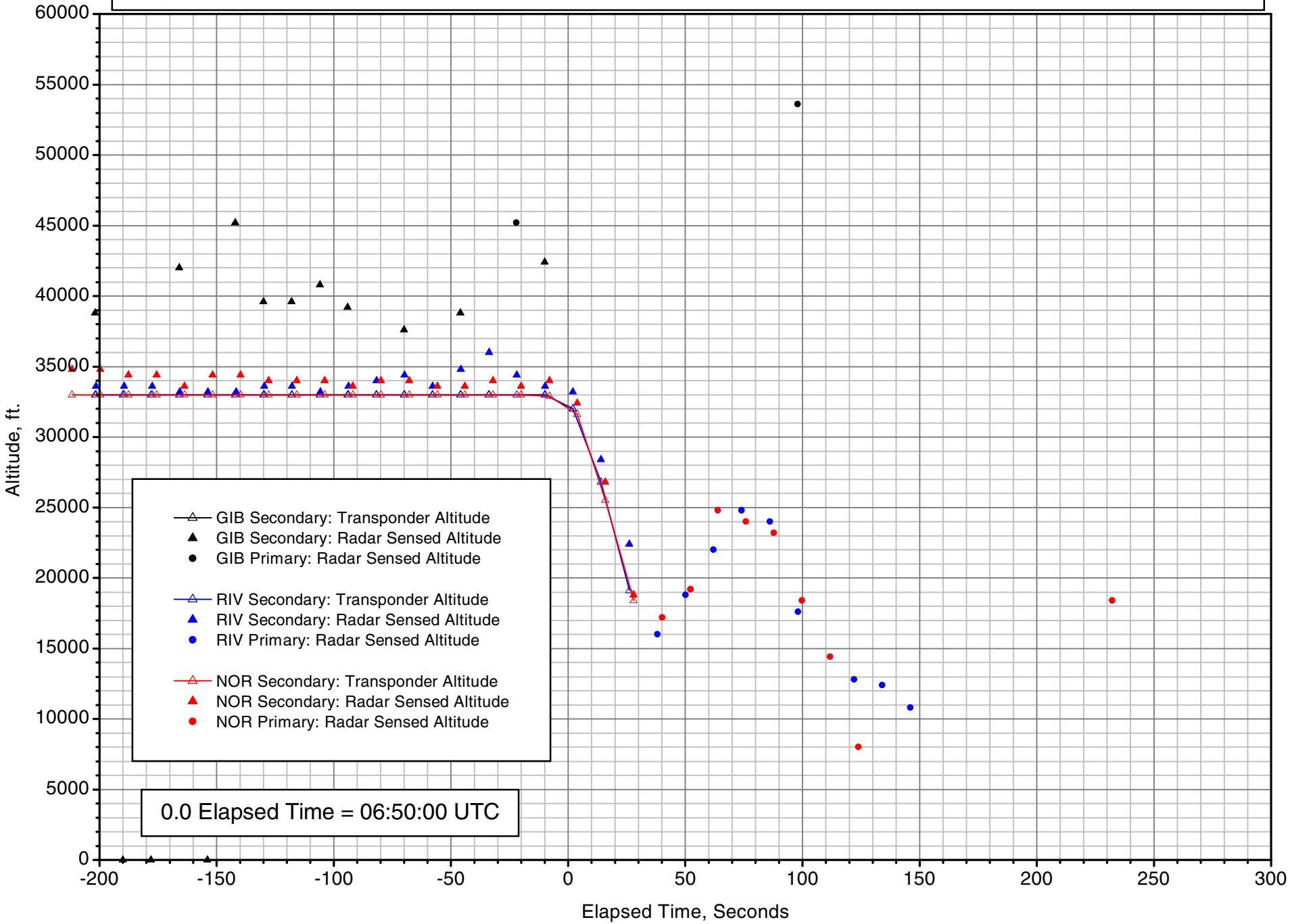

Figure 8a. Primary Returns from GIB from 0630-0700 UTC

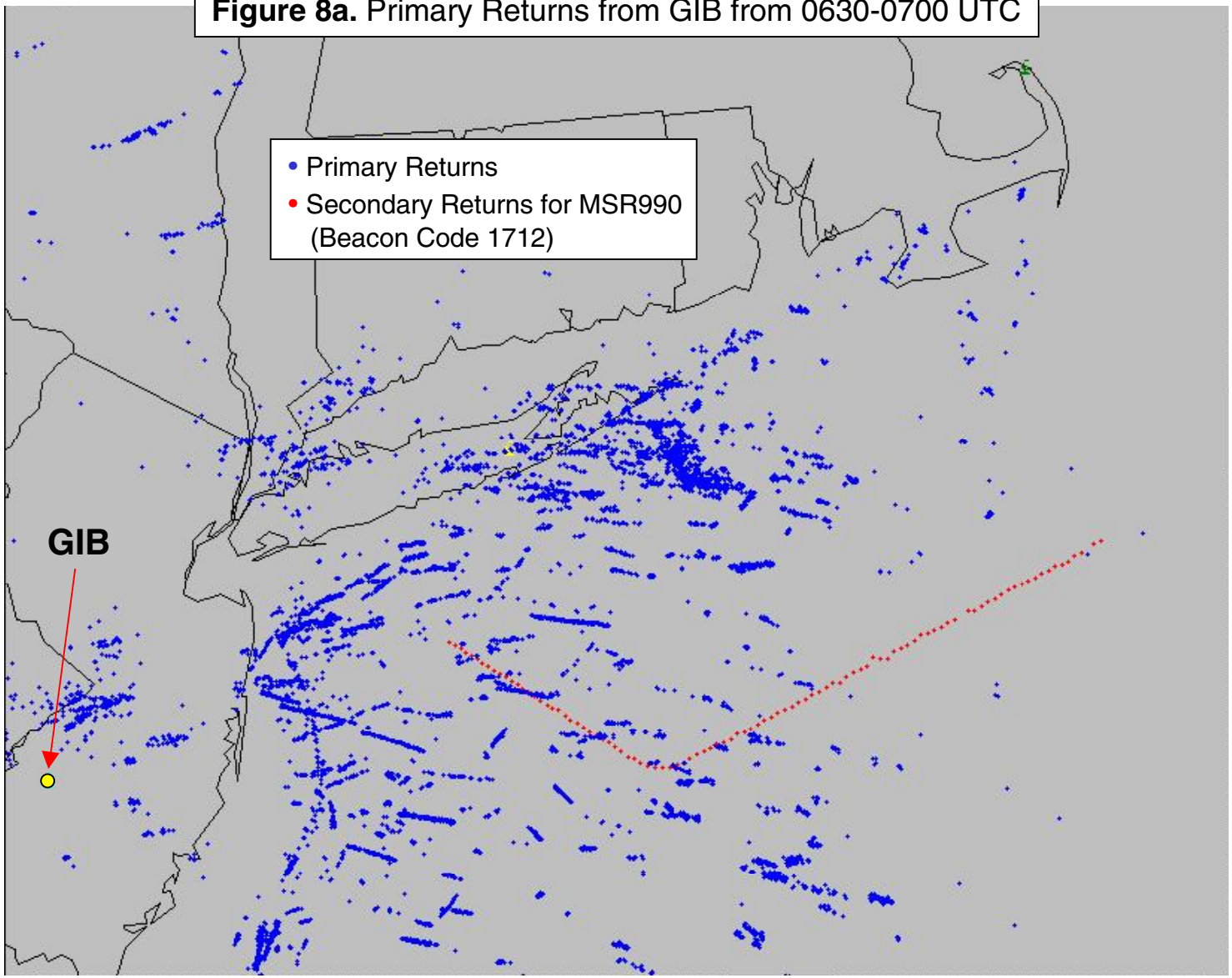

Figure 8b. Primary Returns from NOR from 0630-0700 UTC

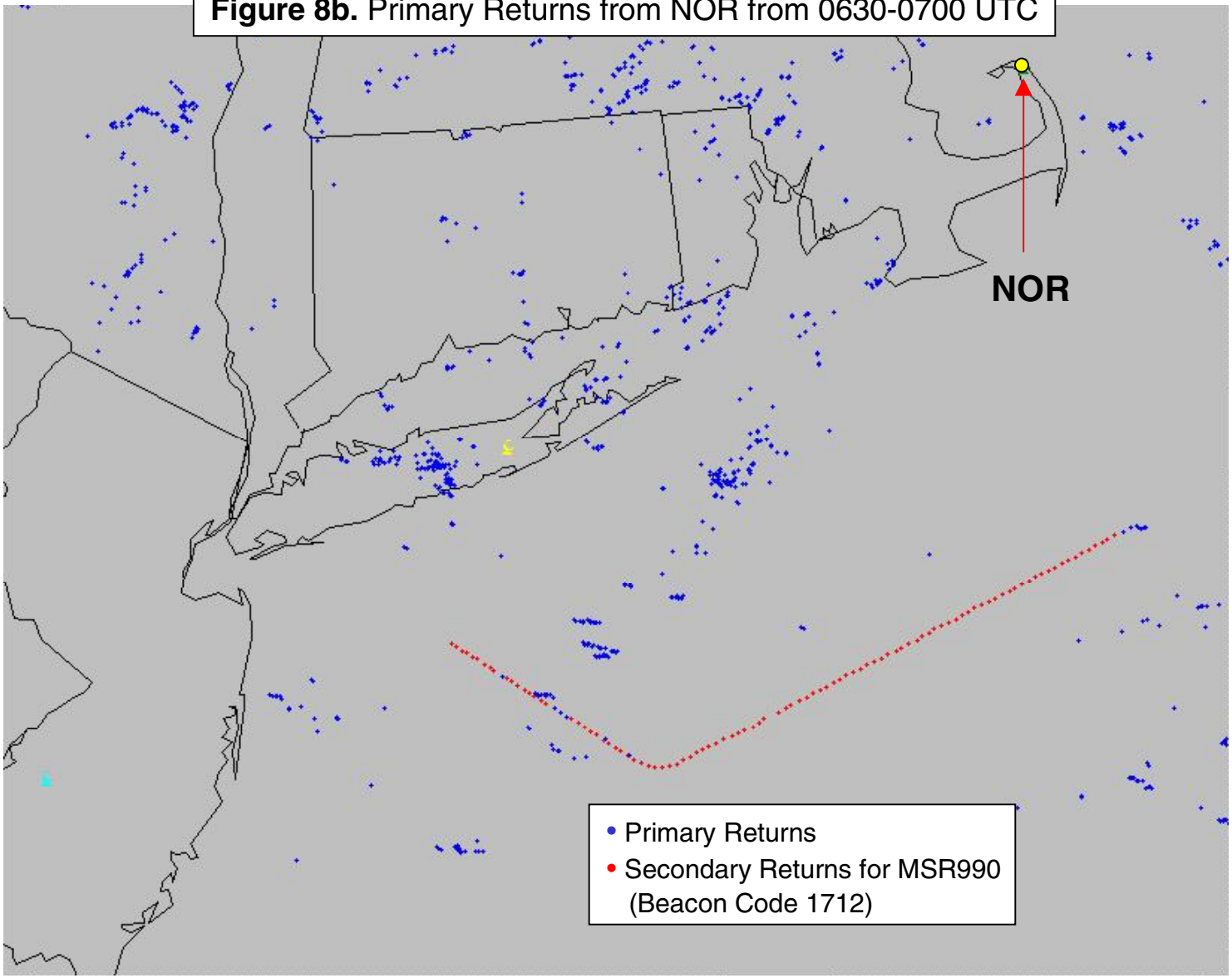

Figure 8c. Primary Returns from RIV from 0630-0700 UTC

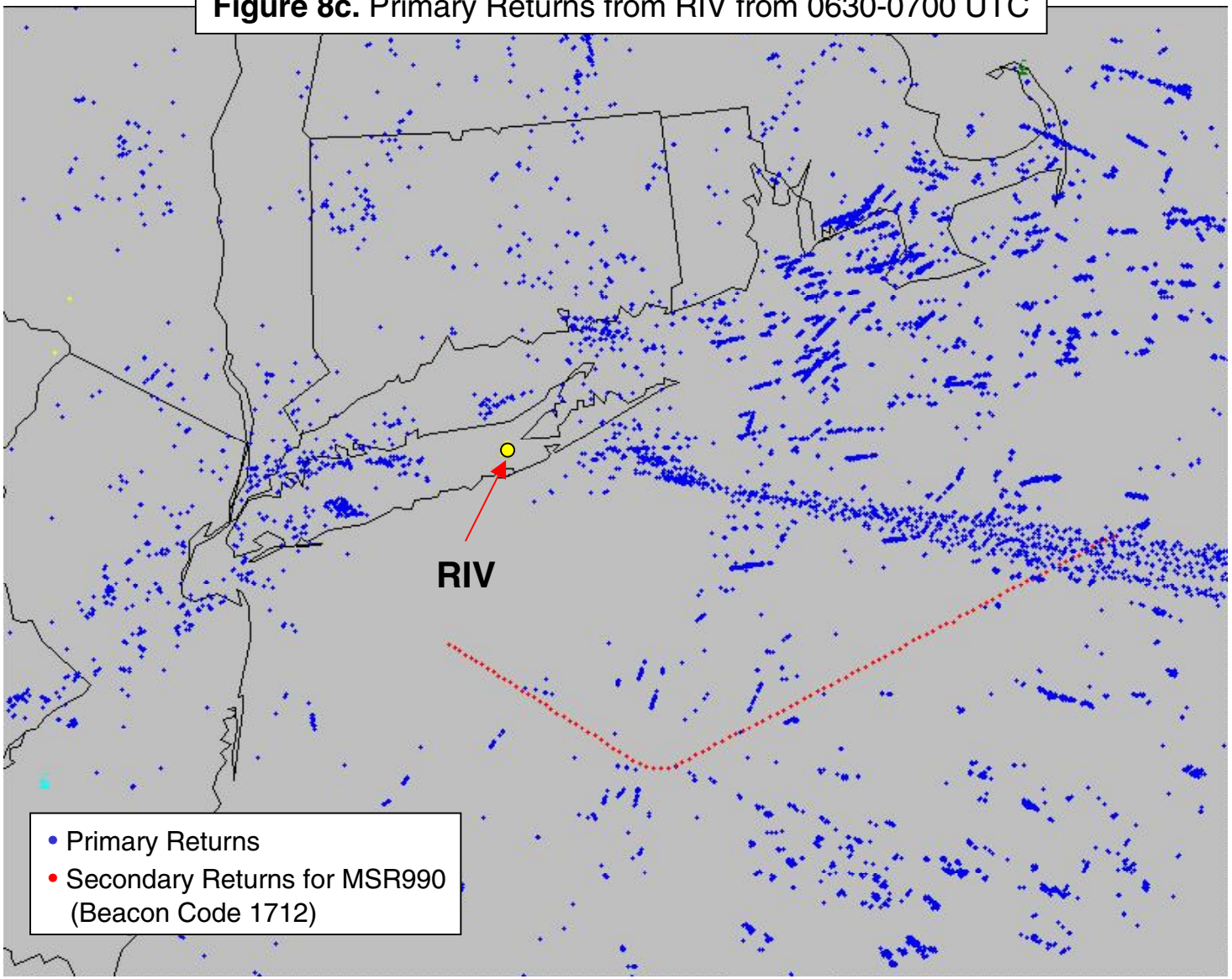

Figure 9a: Curve Fits of Radar Data for Performance Calculations

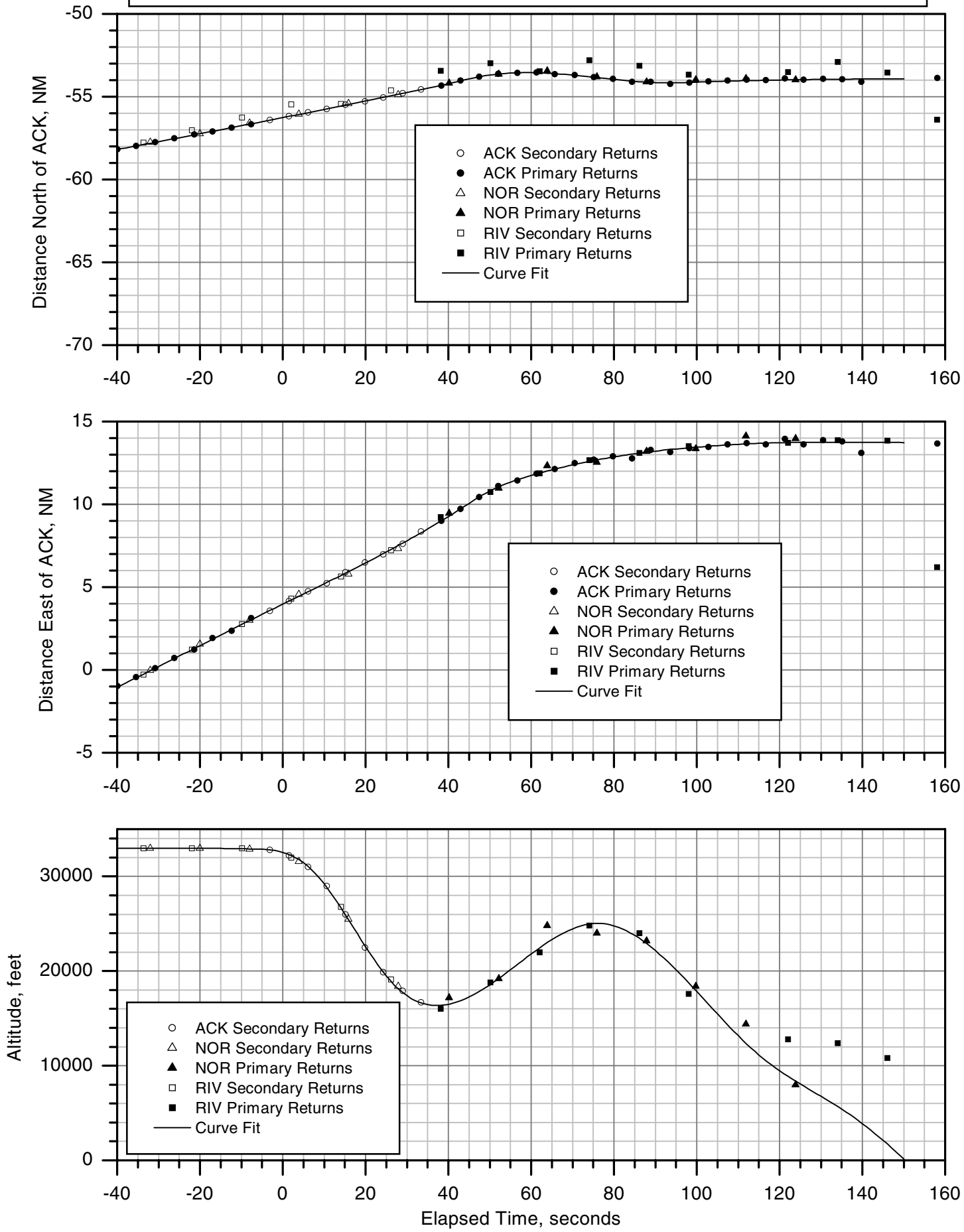

Figure 9b: Curve Fits of Radar Data for Performance Calculations - Plan View

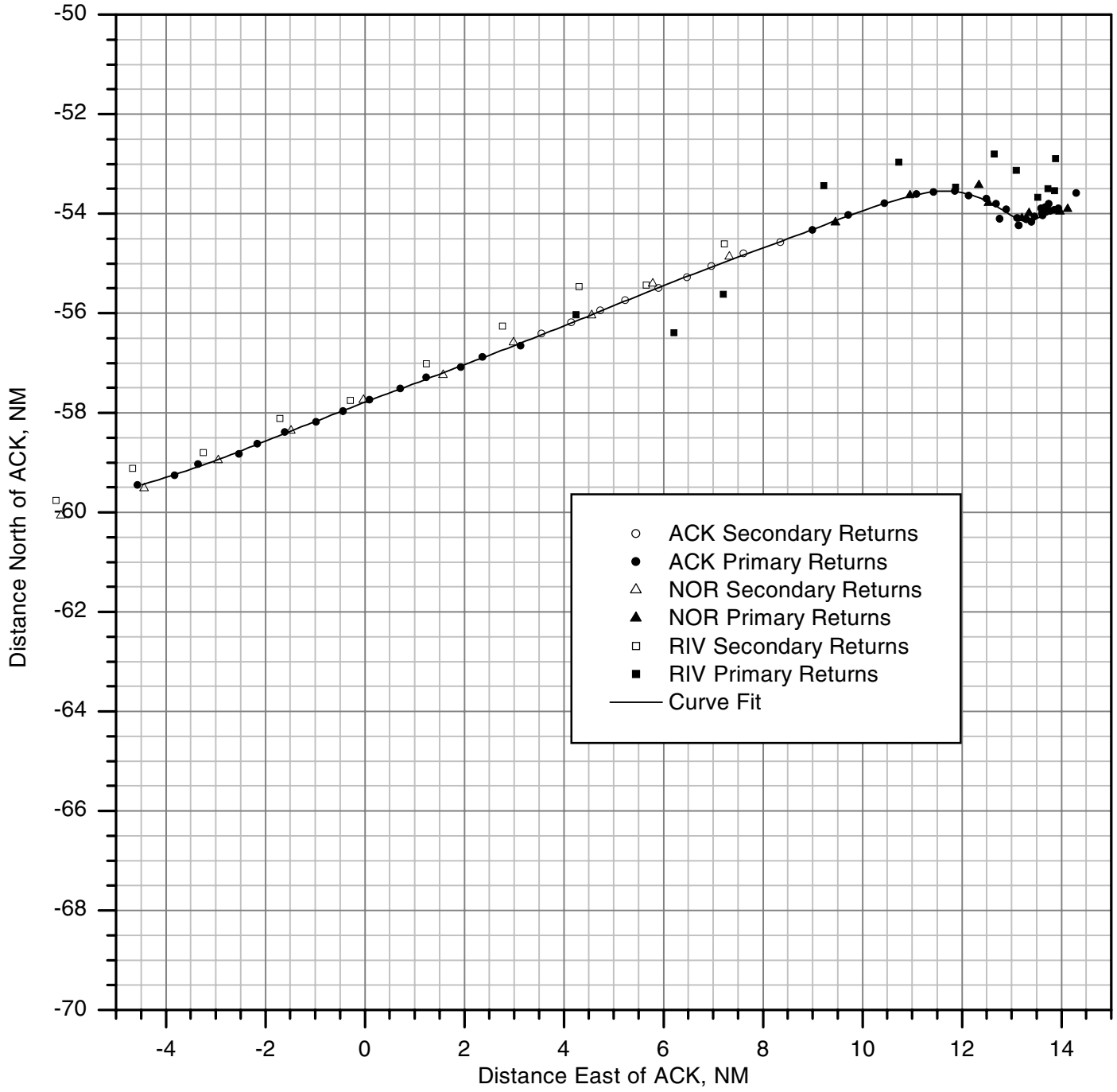

Figure 10a. EgyptAir 990 - Altitudes

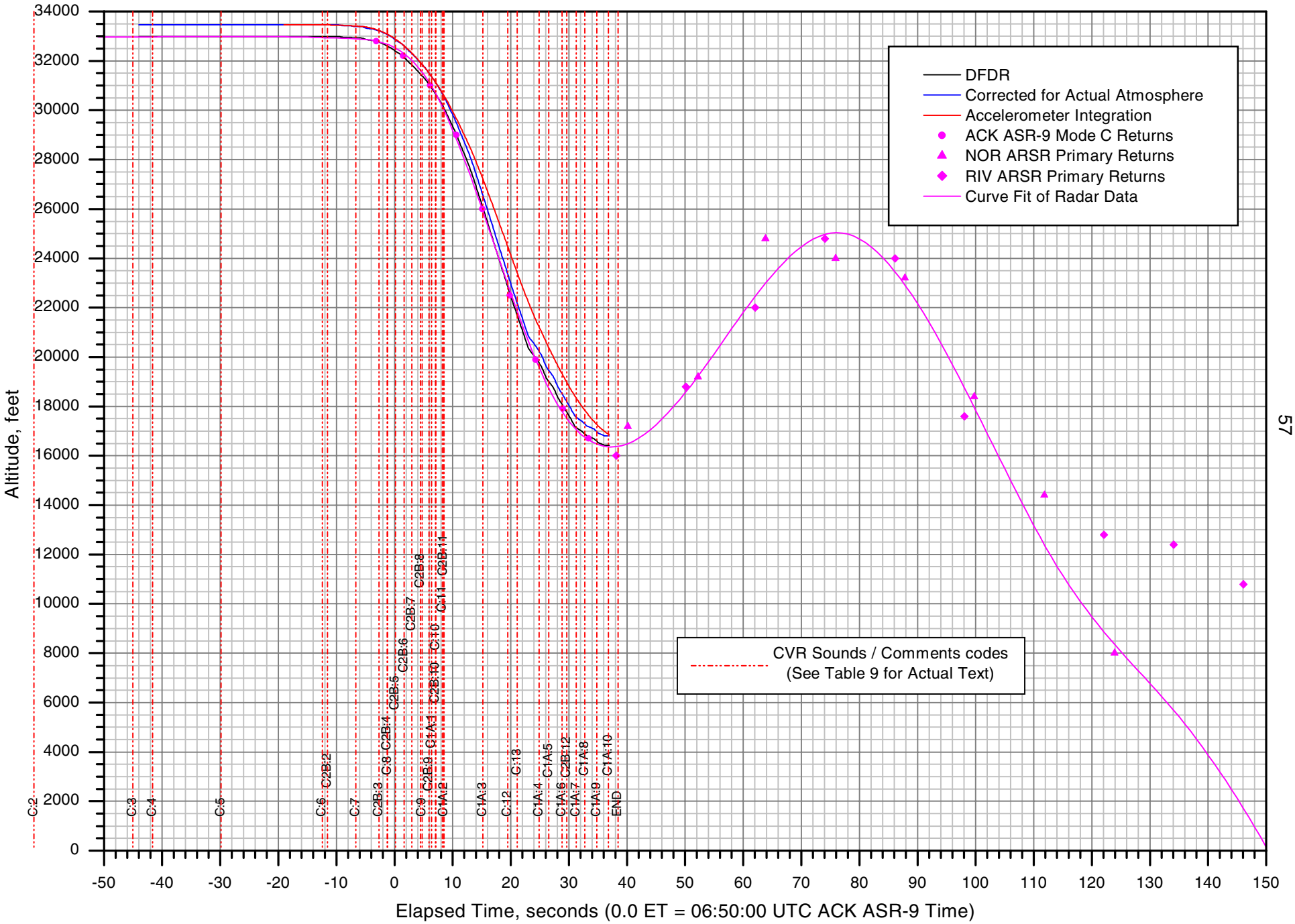

Figure 10b. EgyptAir 990 - Altitudes (Compressed Scale)

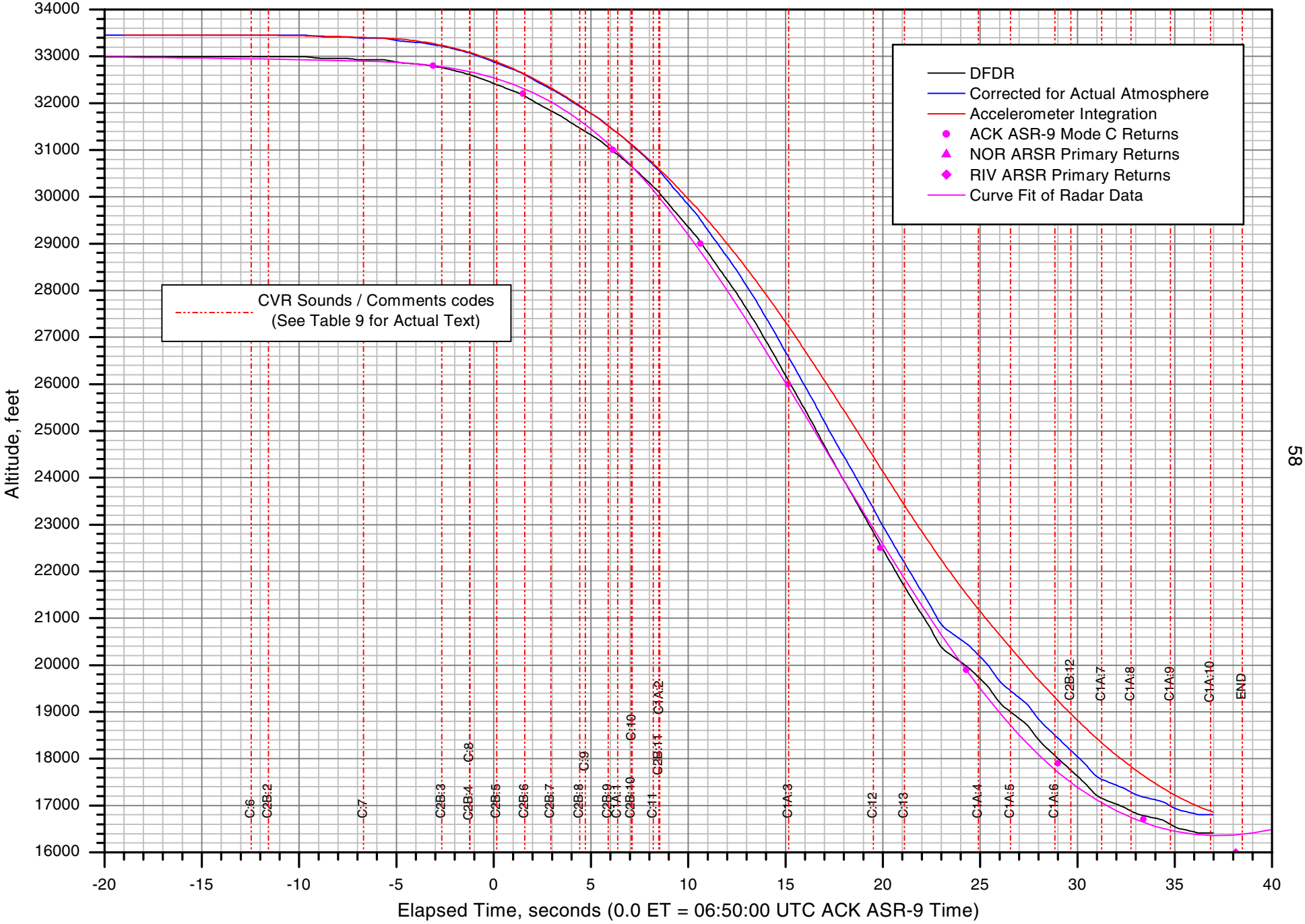

Figure 11a. EgyptAir 990 - Speeds

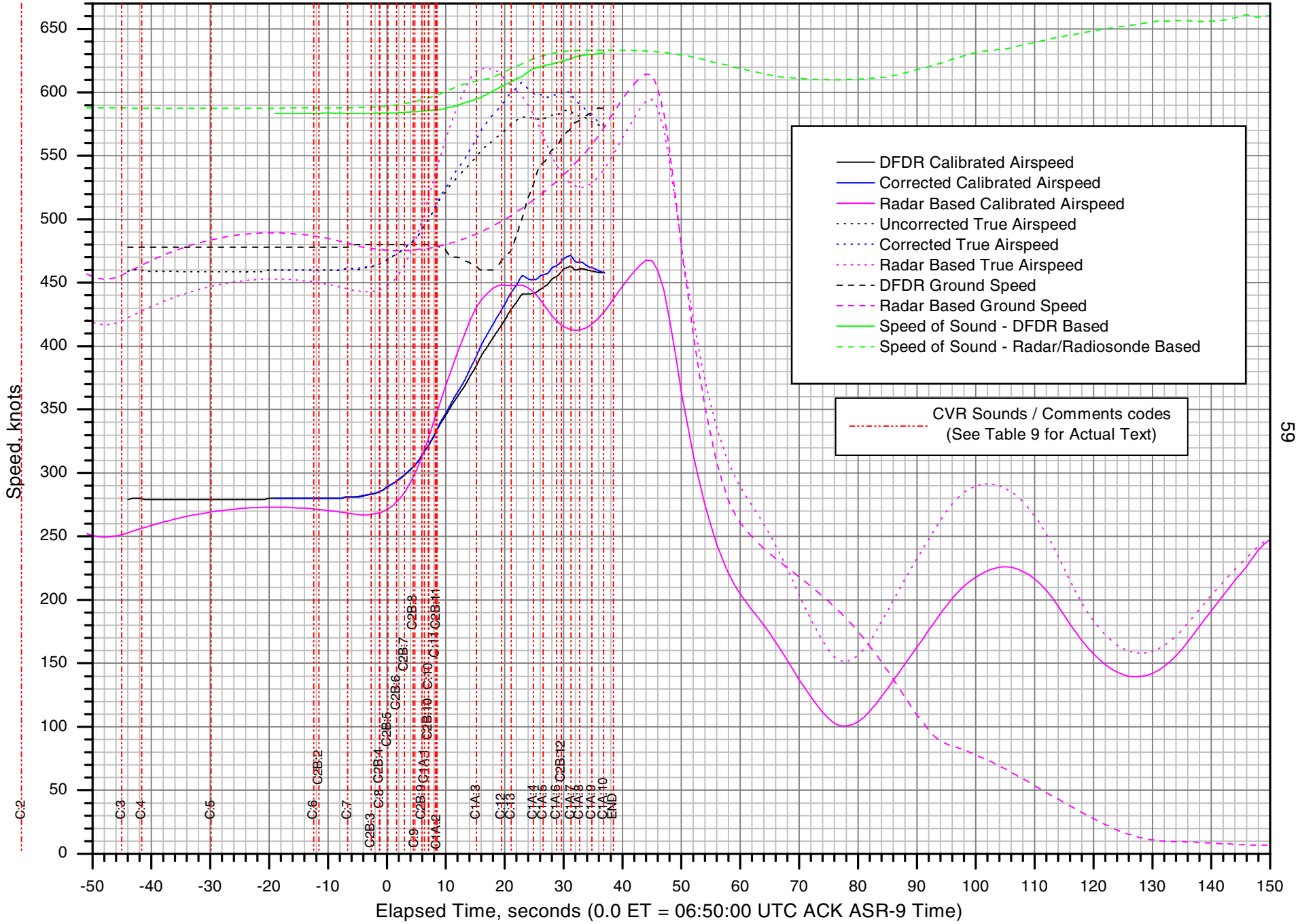

Figure 11b. EgyptAir 990 - Speeds (Compressed Scale)

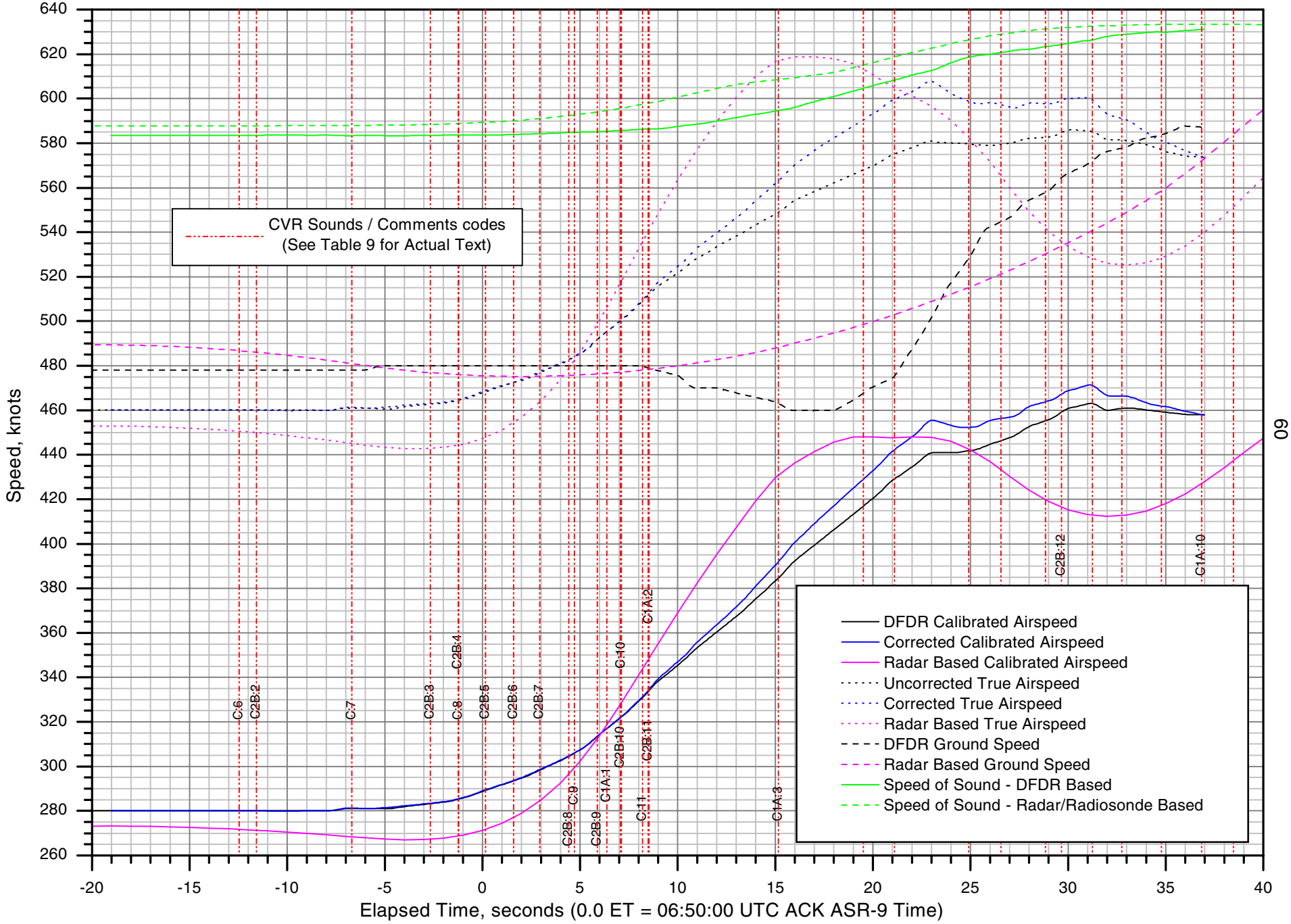

Figure 12a. EgyptAir 990 - Vertical Speed

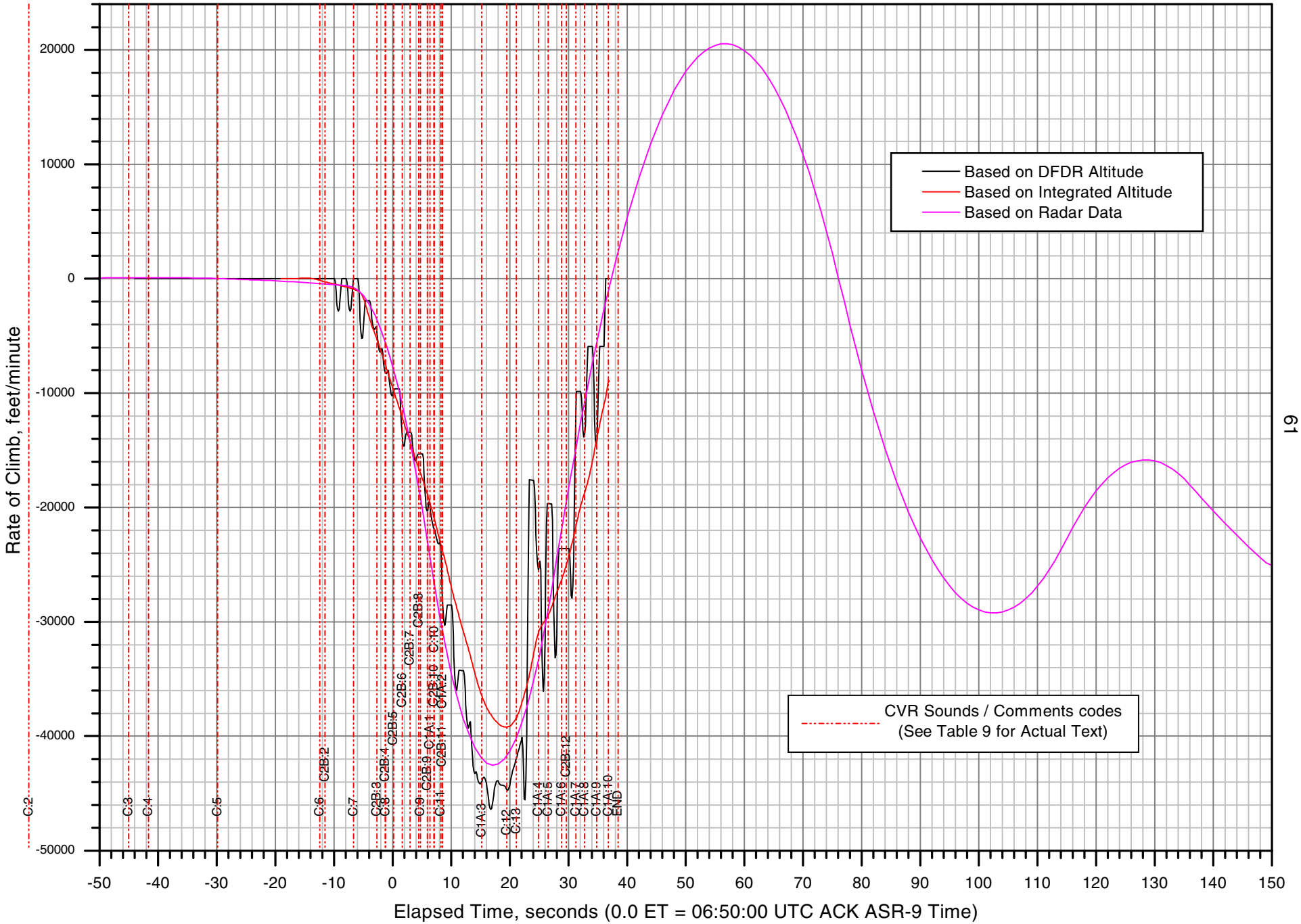

Figure 12b. EgyptAir 990 - Vertical Speed (Compressed Scale)

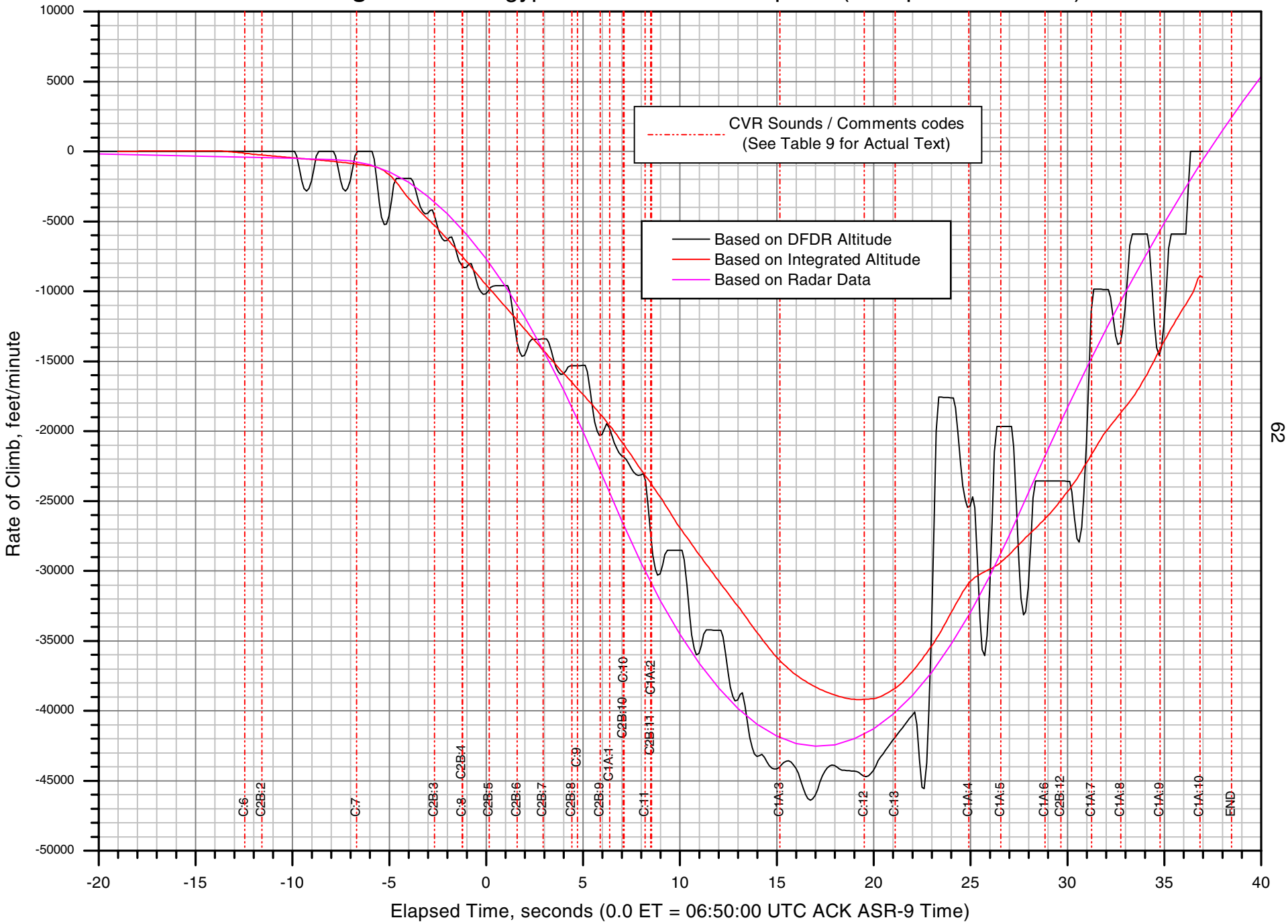

Figure 13a. EgyptAir 990 - Mach Number and Dynamic Pressure

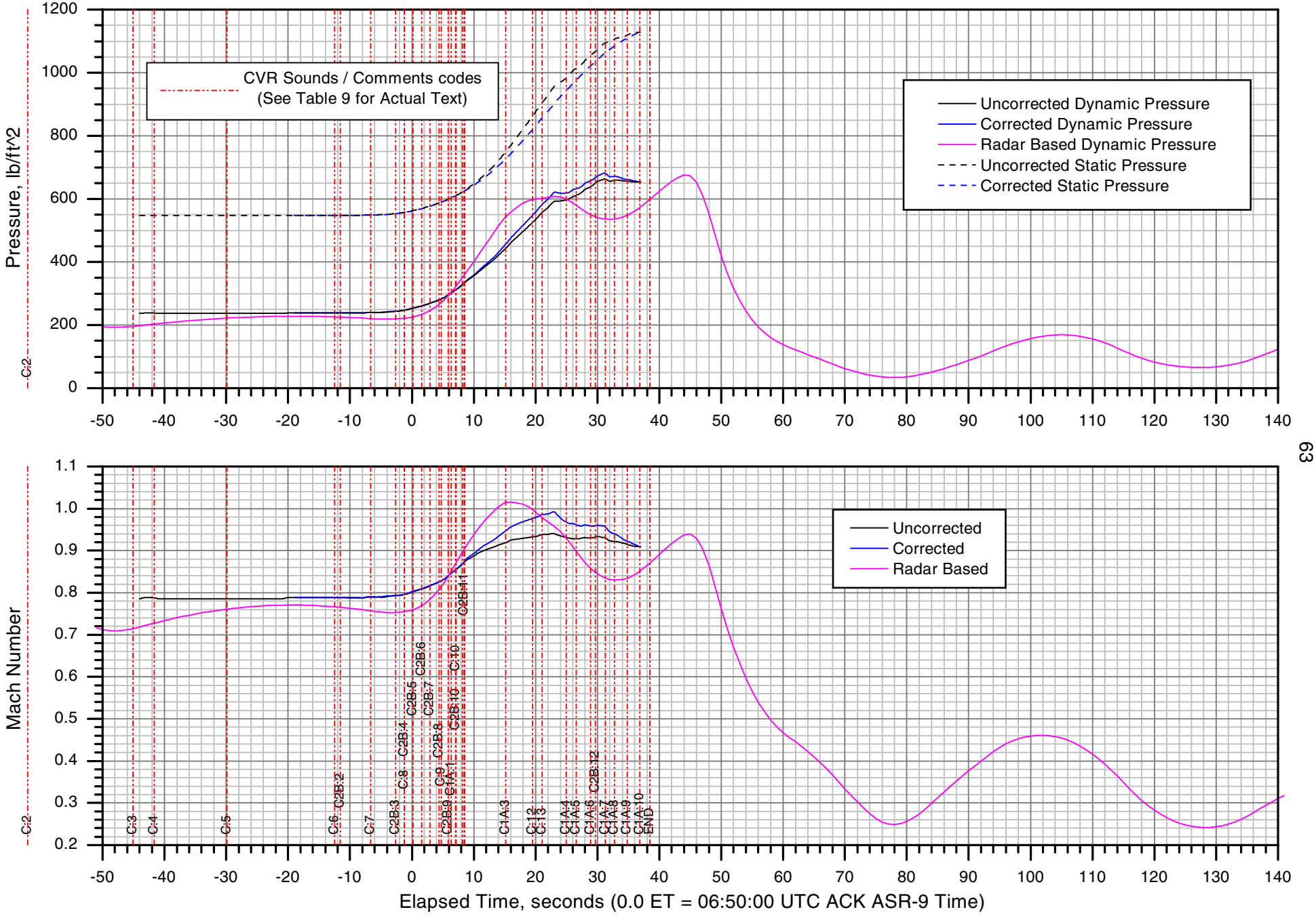

Figure 13b. EgyptAir 990 - Mach Number and Dynamic Pressure (Compressed Scale)

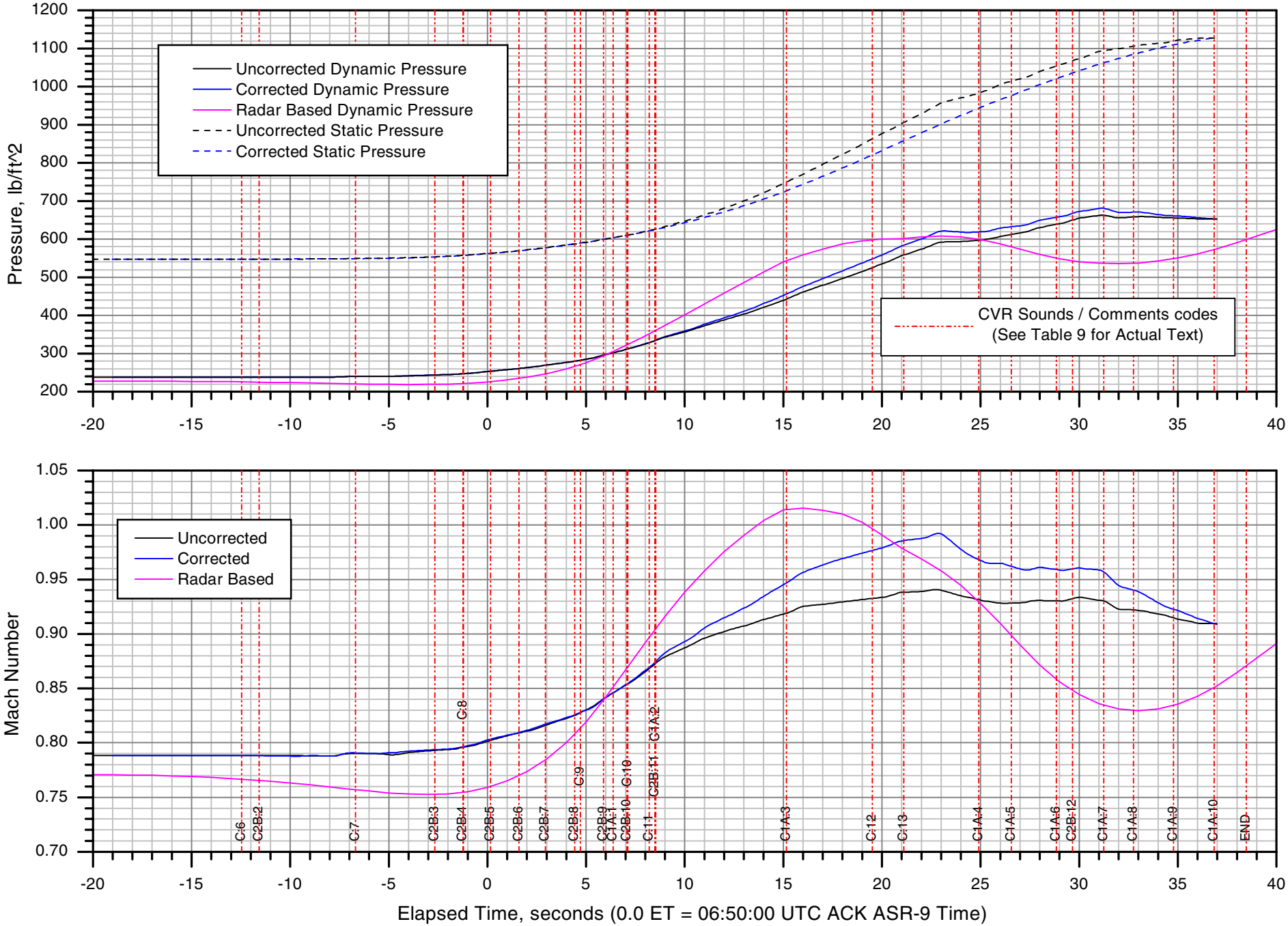

Figure 14a. EgyptAir 990 - Longitudinal Flight Angles

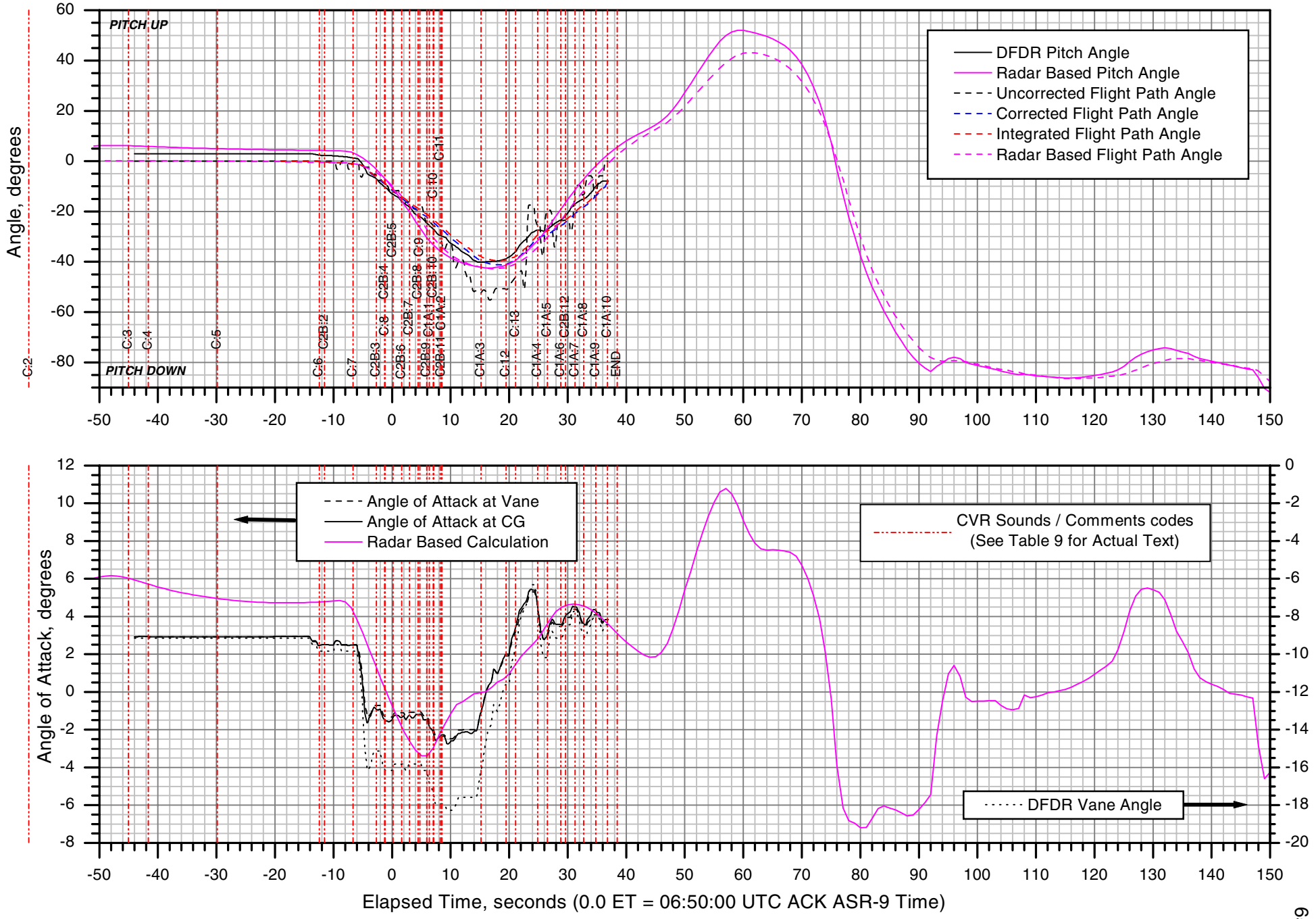

Figure 14b. EgyptAir 990 - Longitudinal Flight Angles (Compressed Scale)

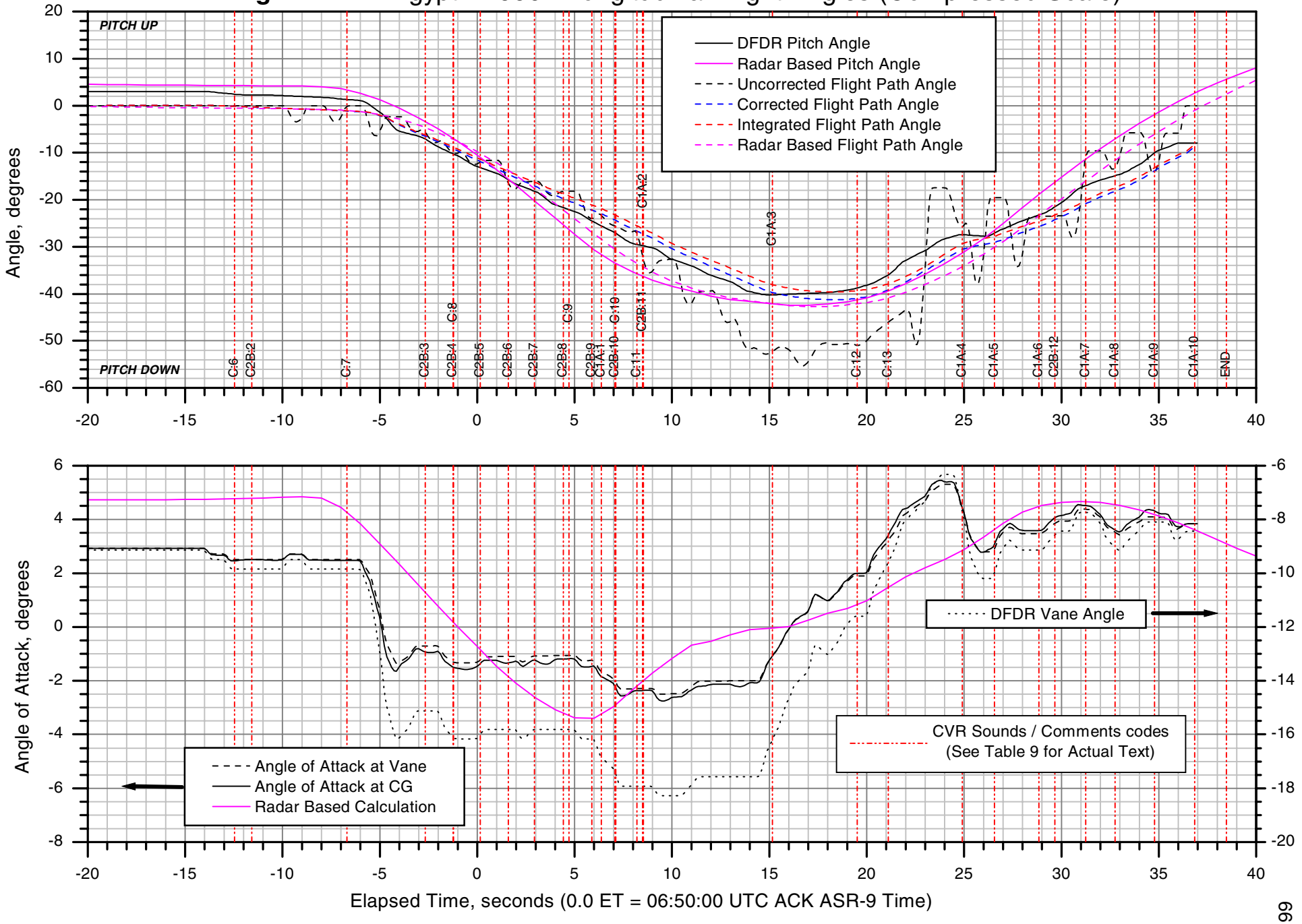

Figure 15a. EgyptAir 990 - Lateral/Directional Flight Angles

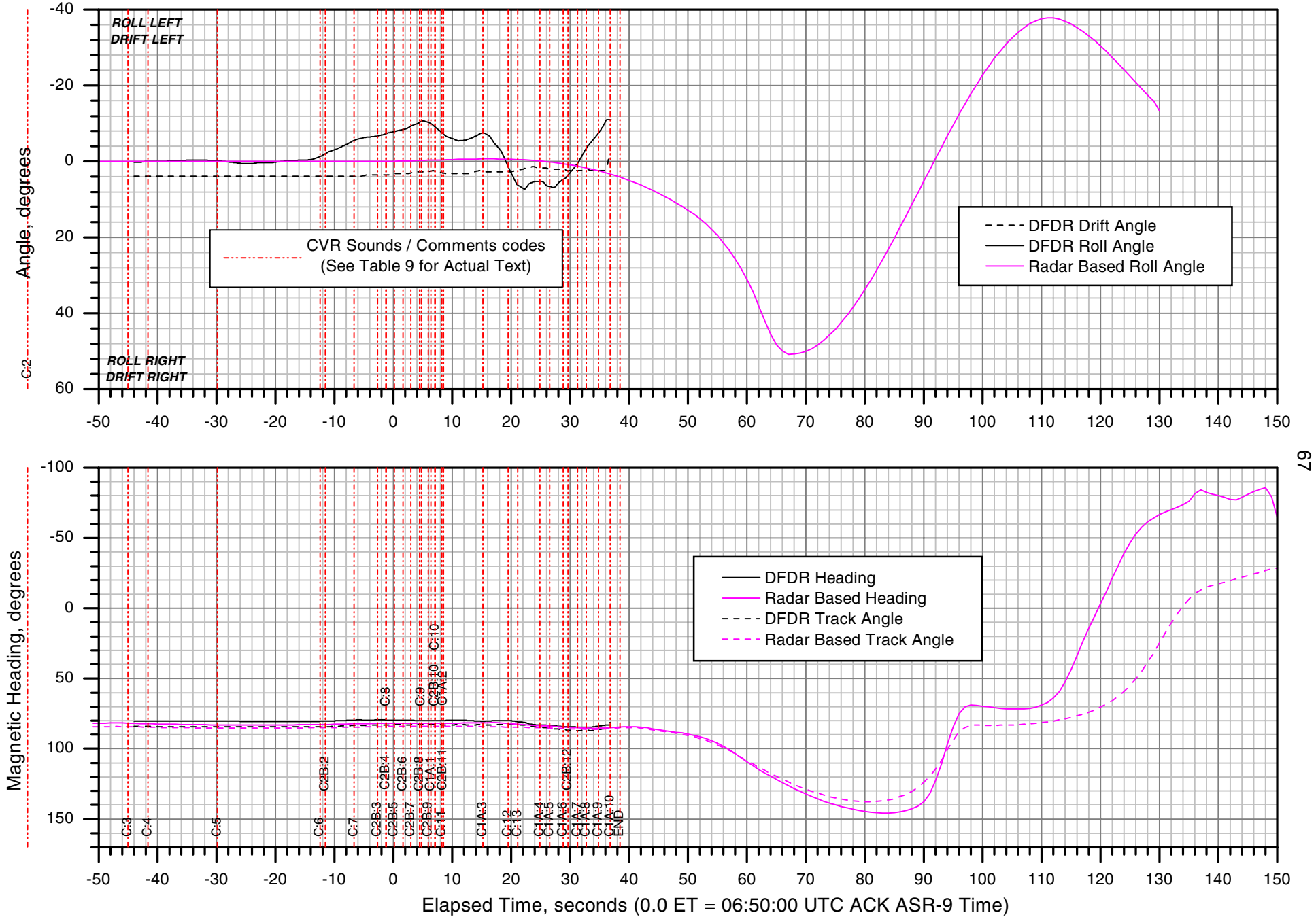

Figure 15b. EgyptAir 990 - Lateral/Directional Flight Angles (Compressed Scale)

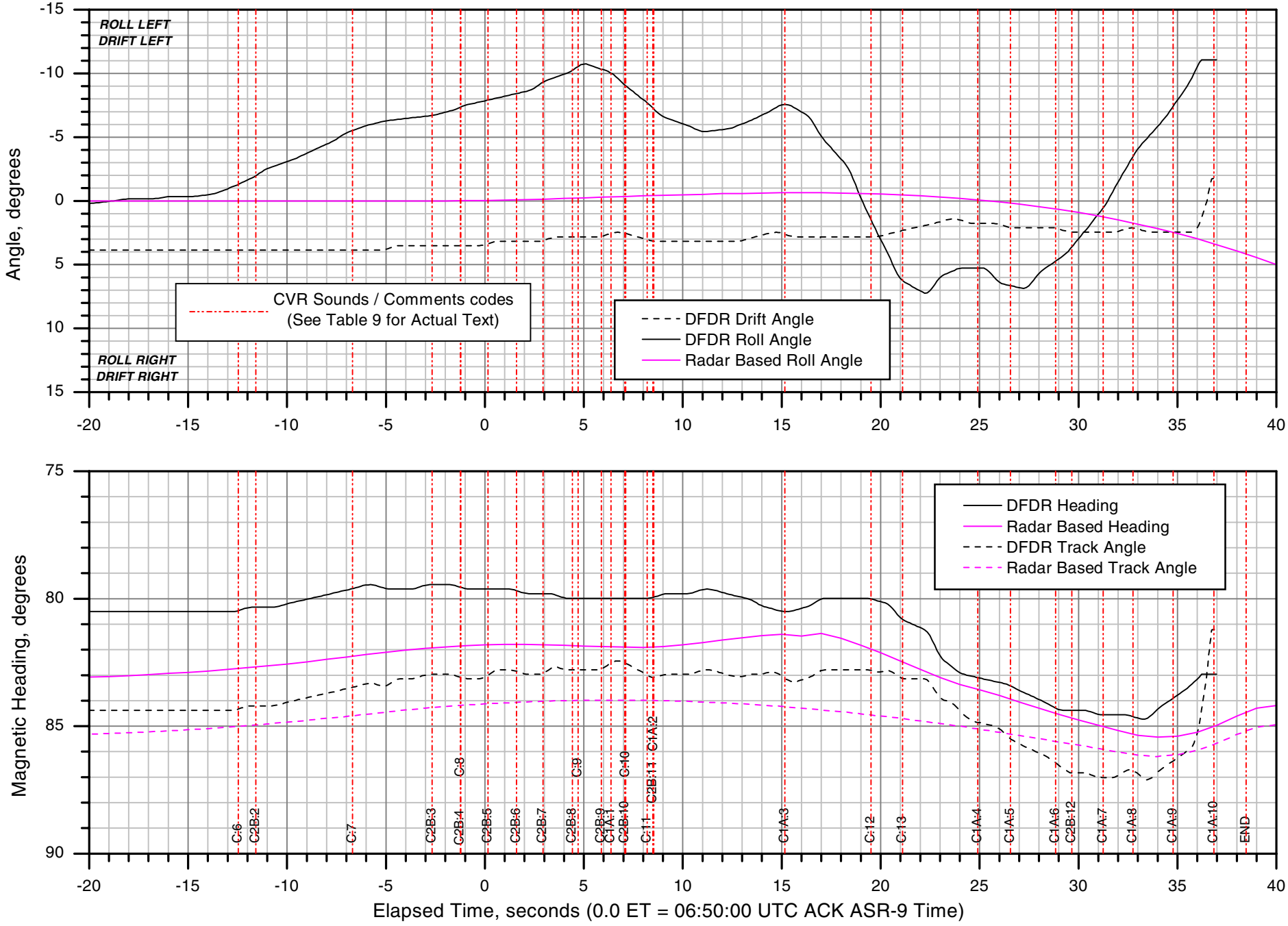

Figure 16. EgyptAir 990 - Load Factors

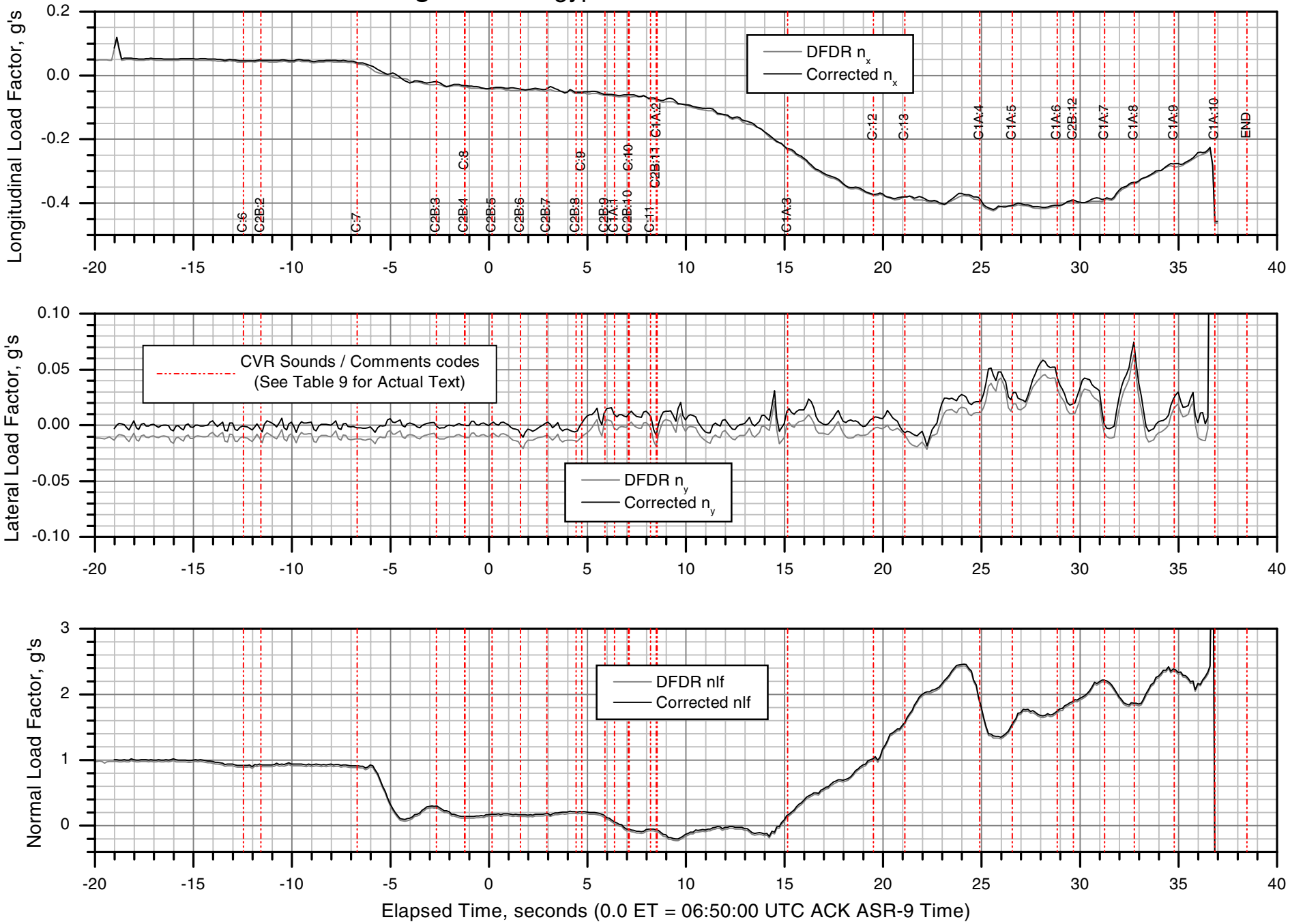

Figure 17. EgyptAir 990 - Longitudinal & Directional Flight Controls

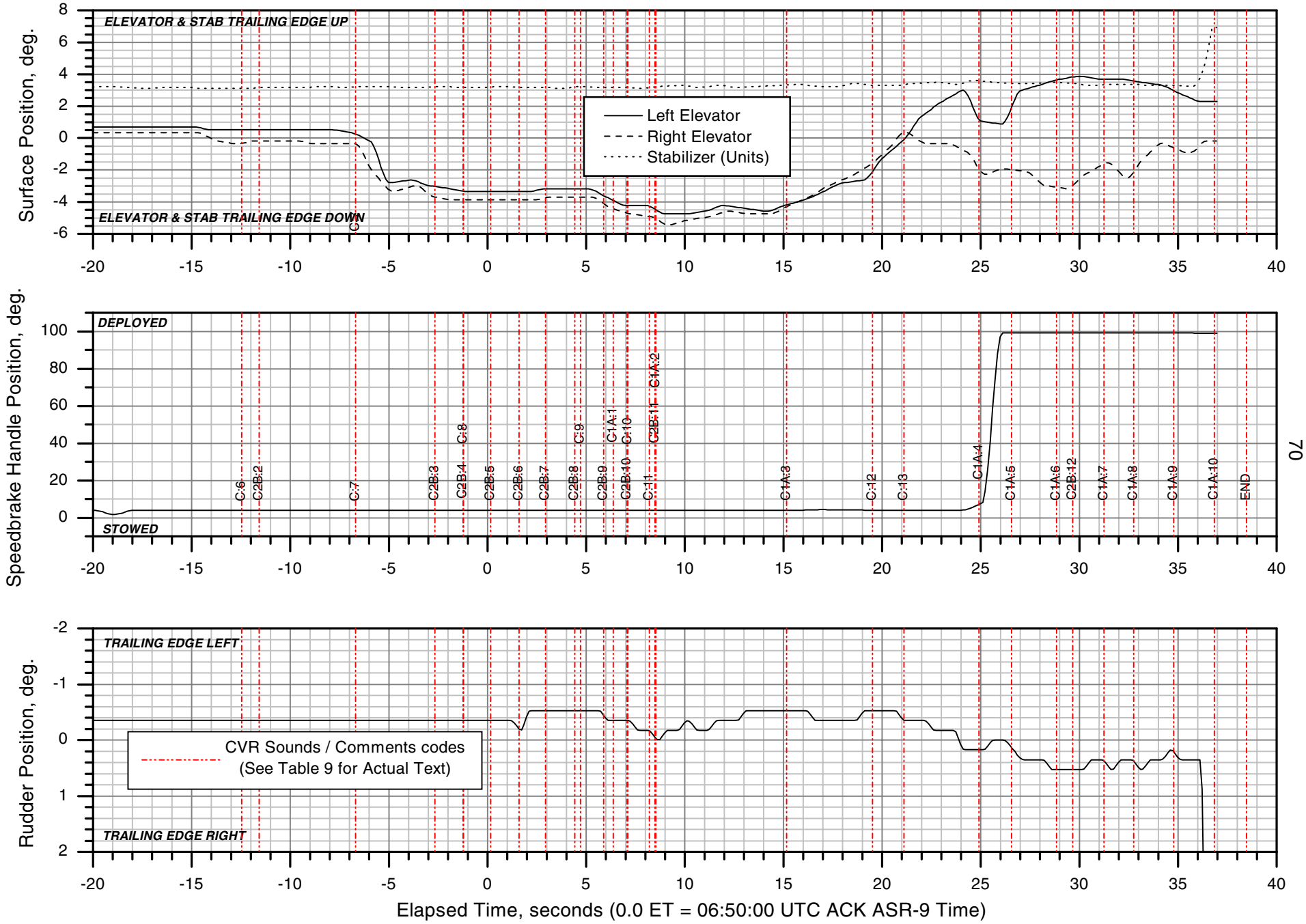

Figure 18. EgyptAir 990 - Ailerons

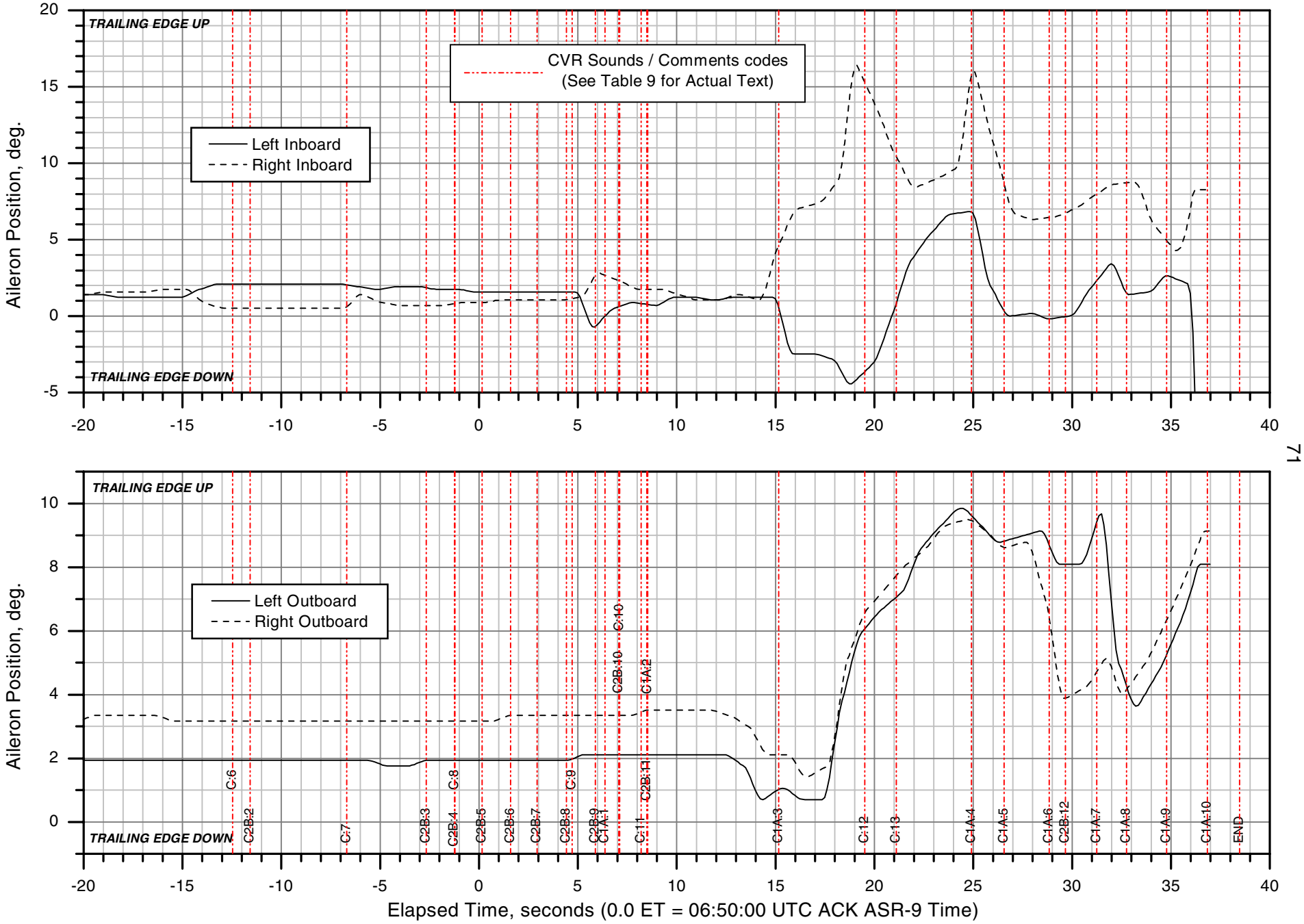

Figure 19. EgyptAir 990 - Engine Parameters

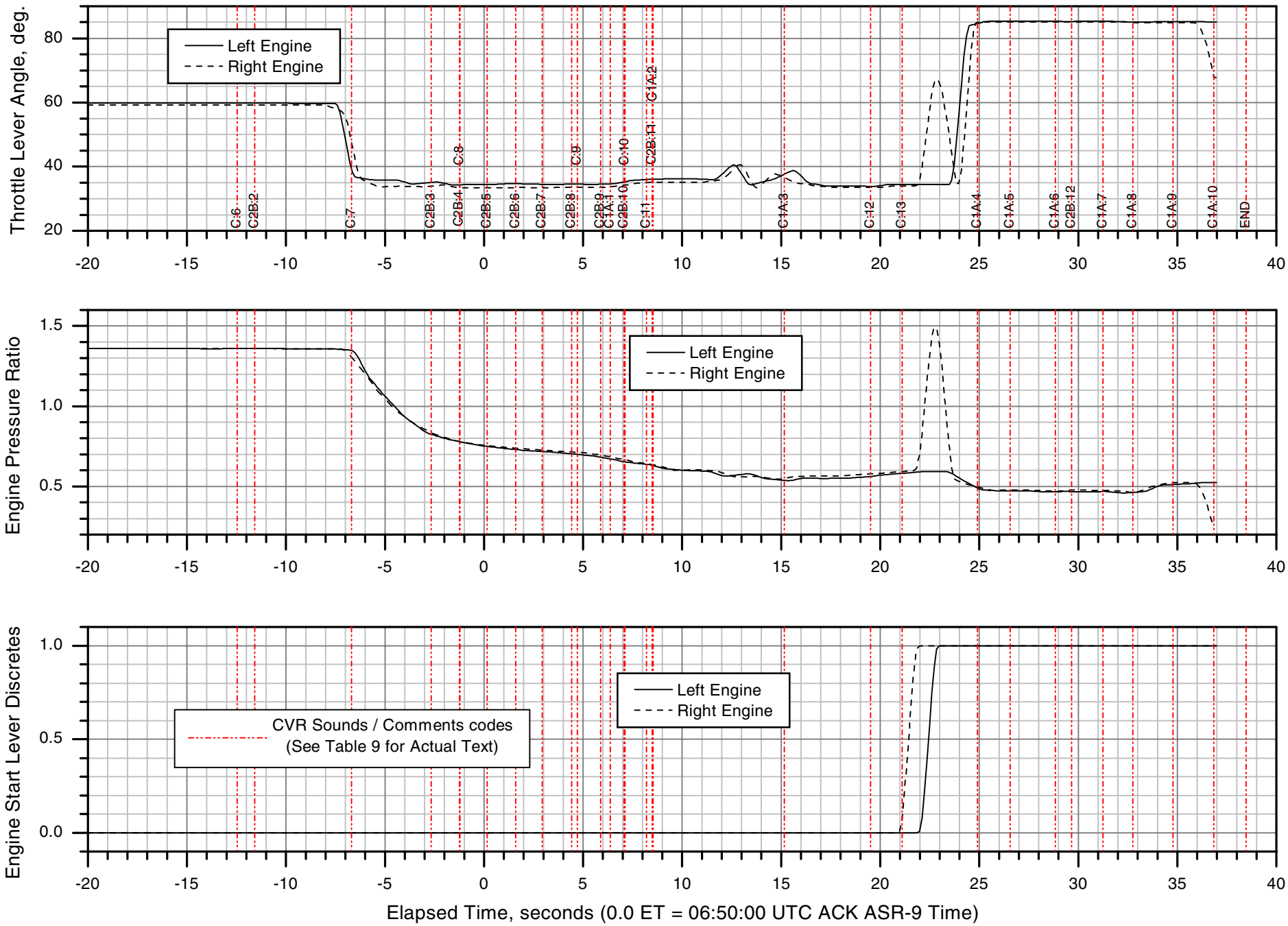

Figure 20. EgyptAir 990 - Miscellaneous Discretes

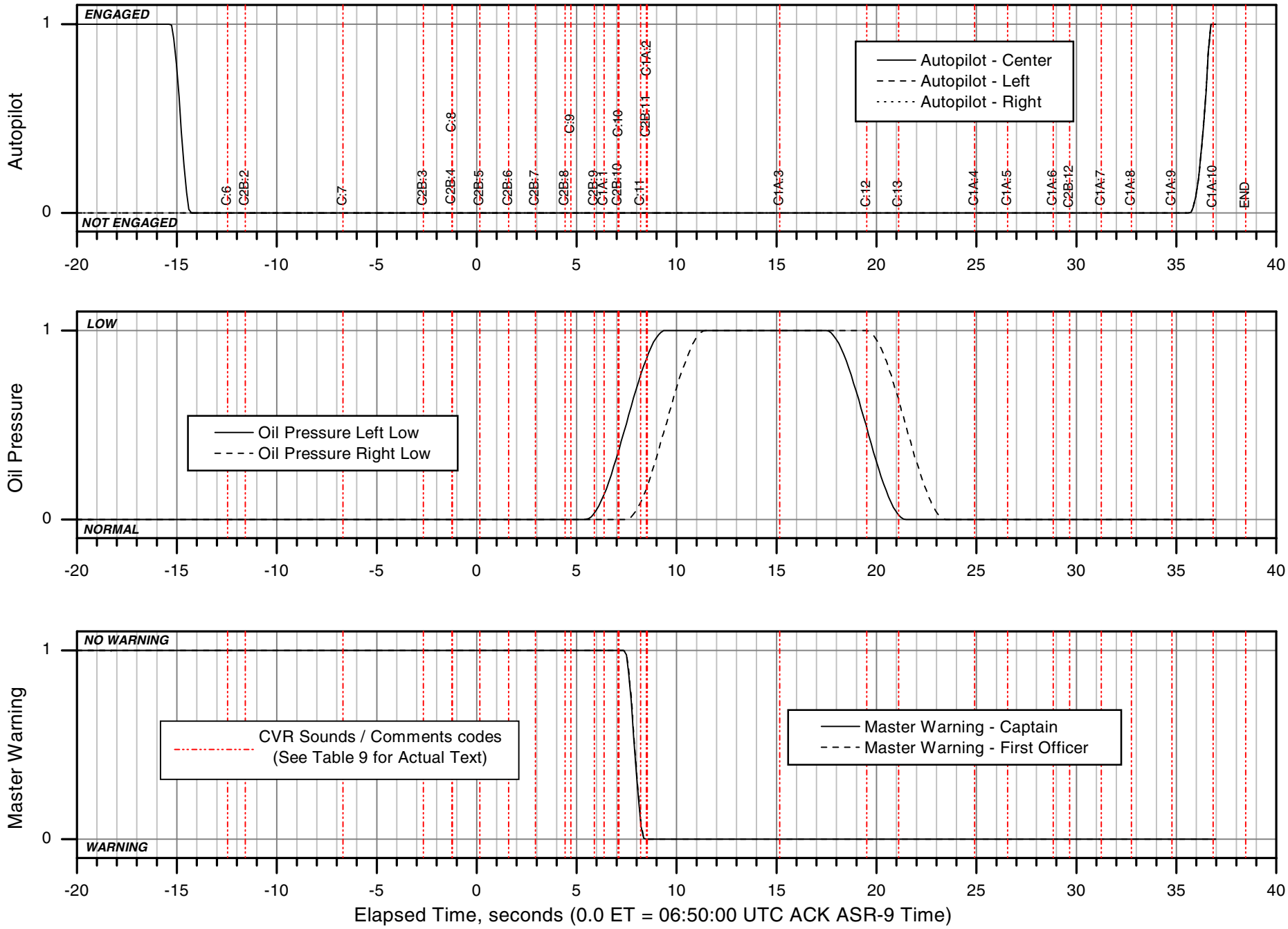

Figure 21a. EgyptAir 990 - Atmosphere

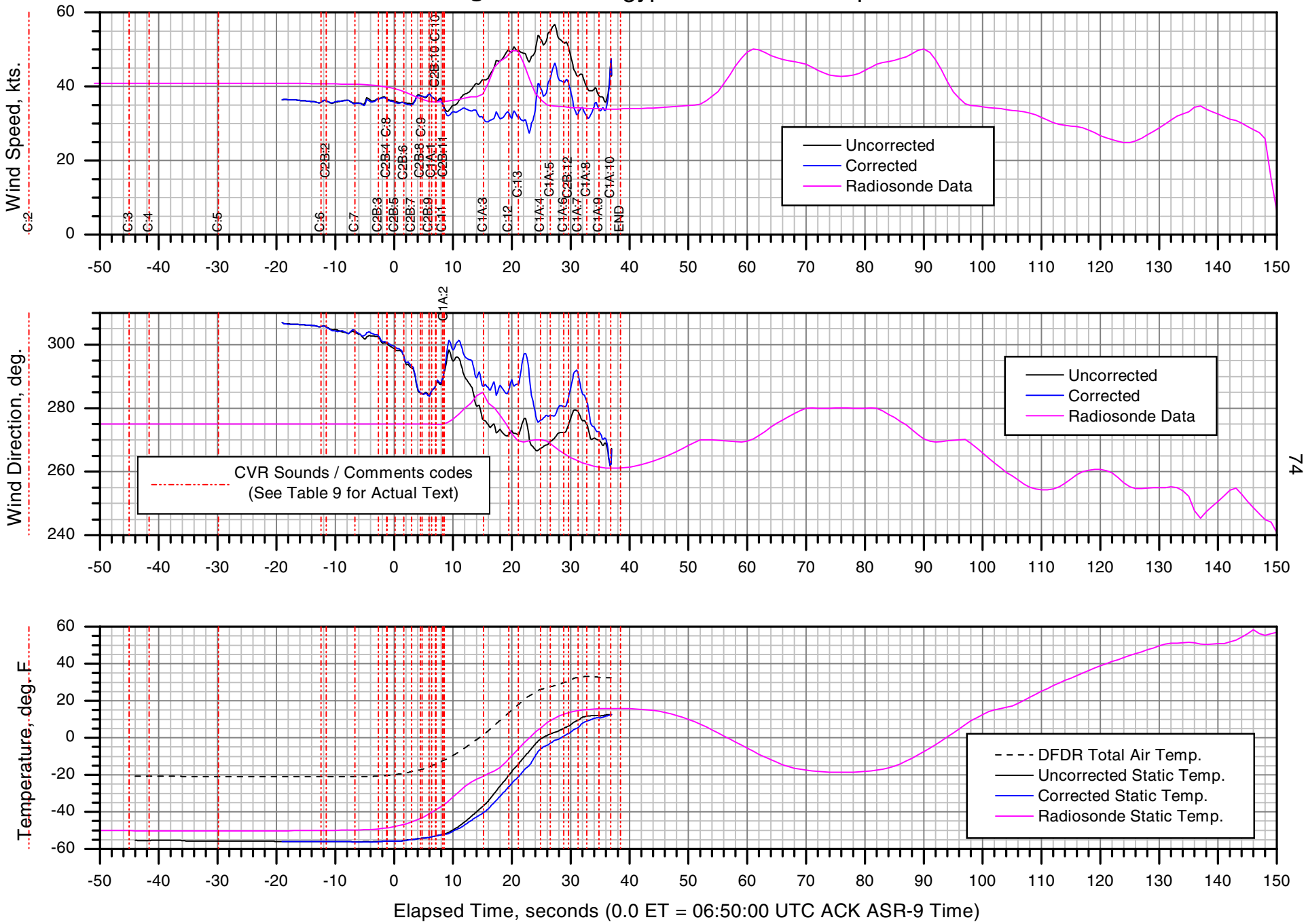

Figure 21b. EgyptAir 990 - Atmosphere (Compressed Scale)

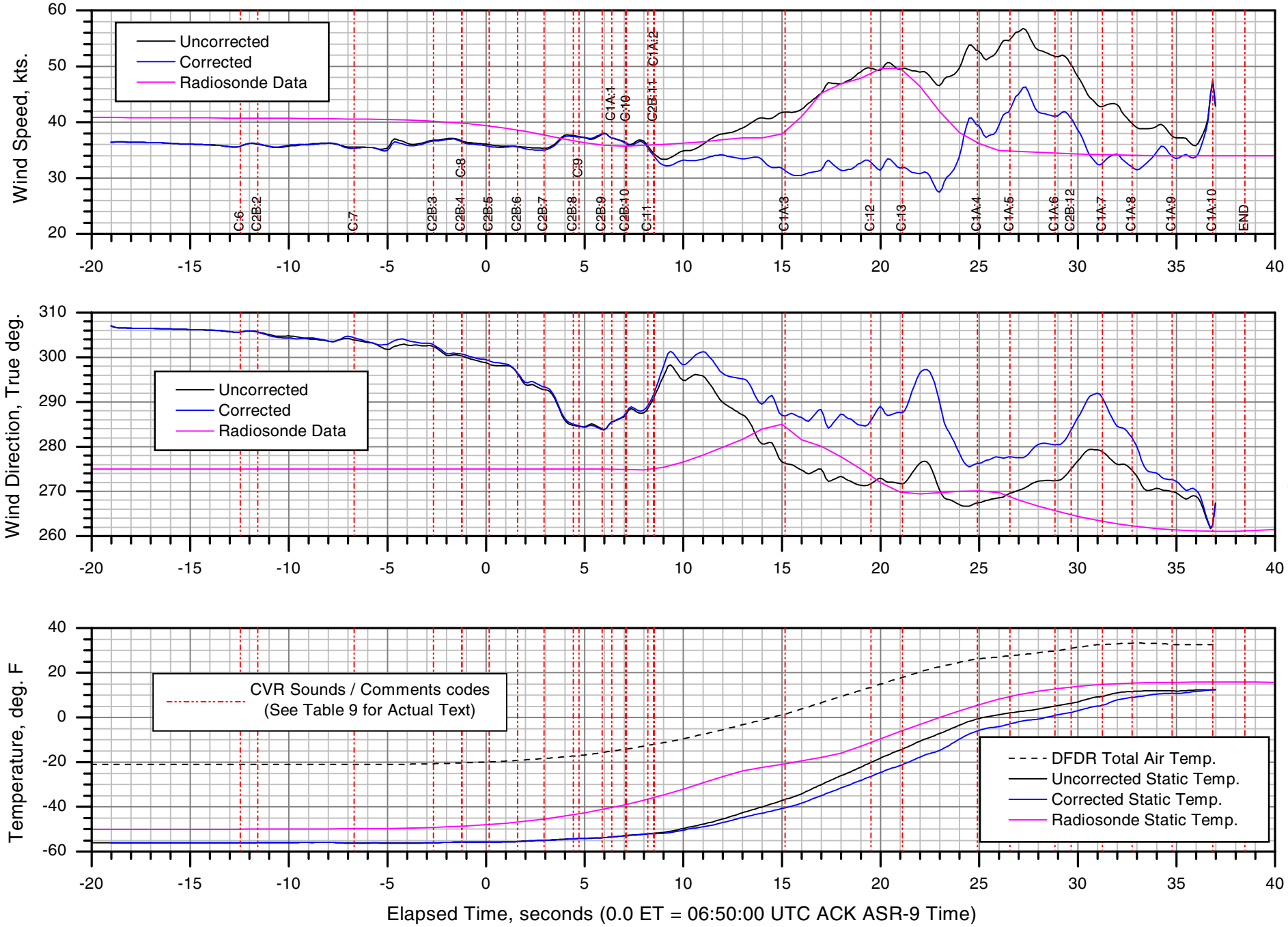

Figure 22. EgyptAir 990 - Radiosonde Data for Radar Based Performance Calculations

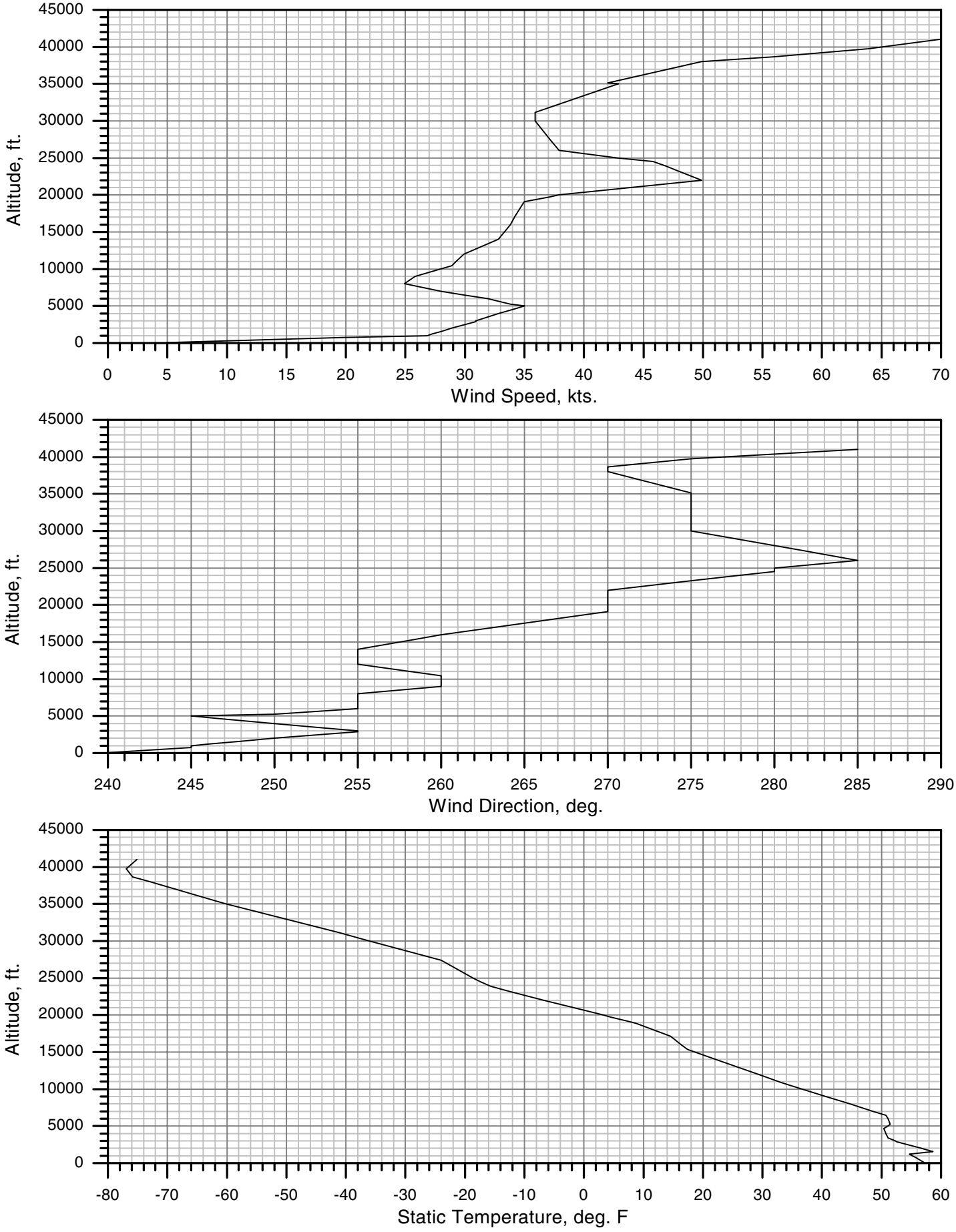
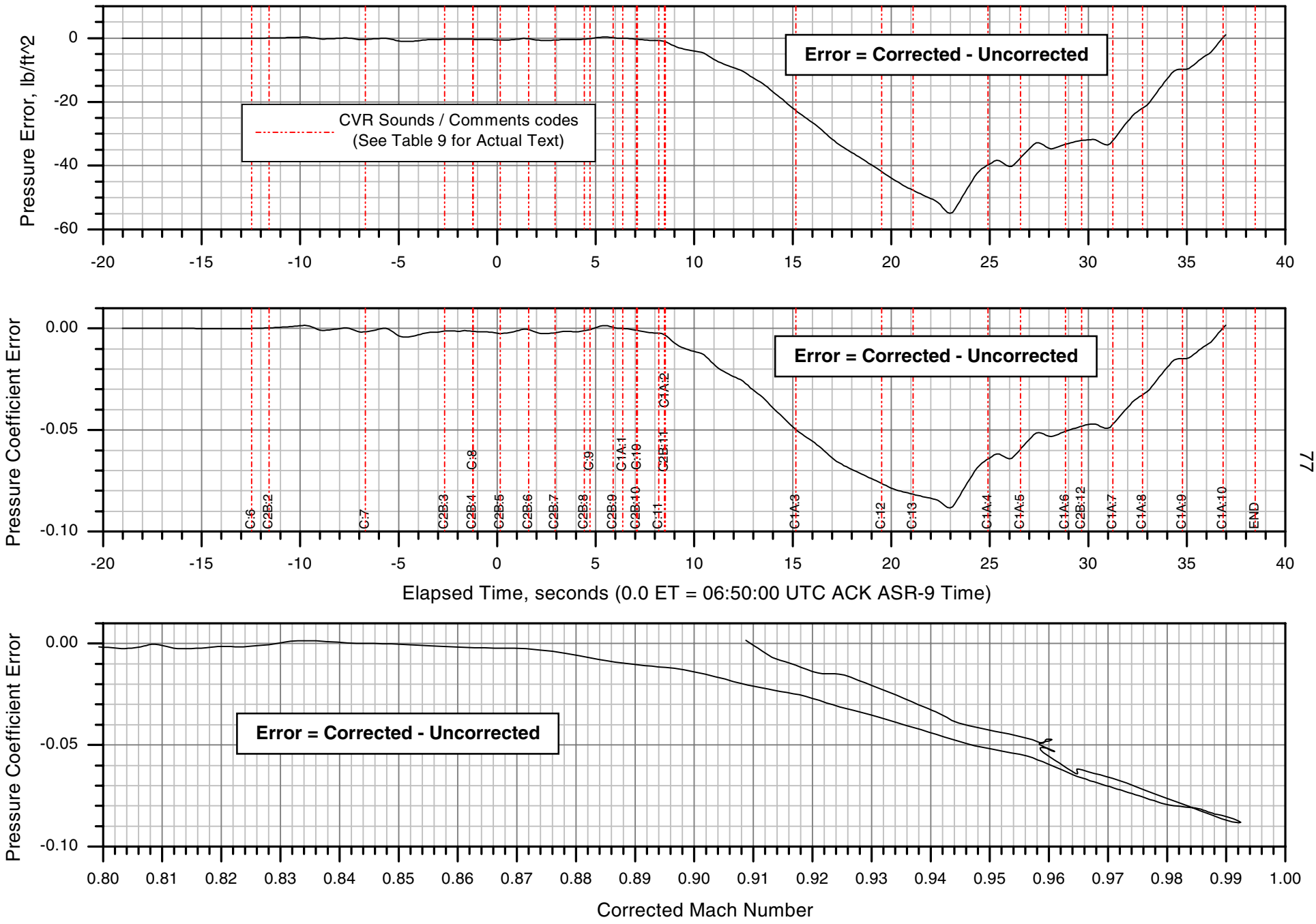
Figure 23. EgyptAir 990 - Static Pressure Measurement Errors